BOOKLET

PhD STUDENT CONGRESS

19, 20 & 21 June 2024

Chambery – Le-Bourget-du-Lac

ISTerre
Institut des Sciences de la Terre

LIST OF ED STEP PHD STUDENTS AT ISTERRE

DISTRIBUTION

Team distribution

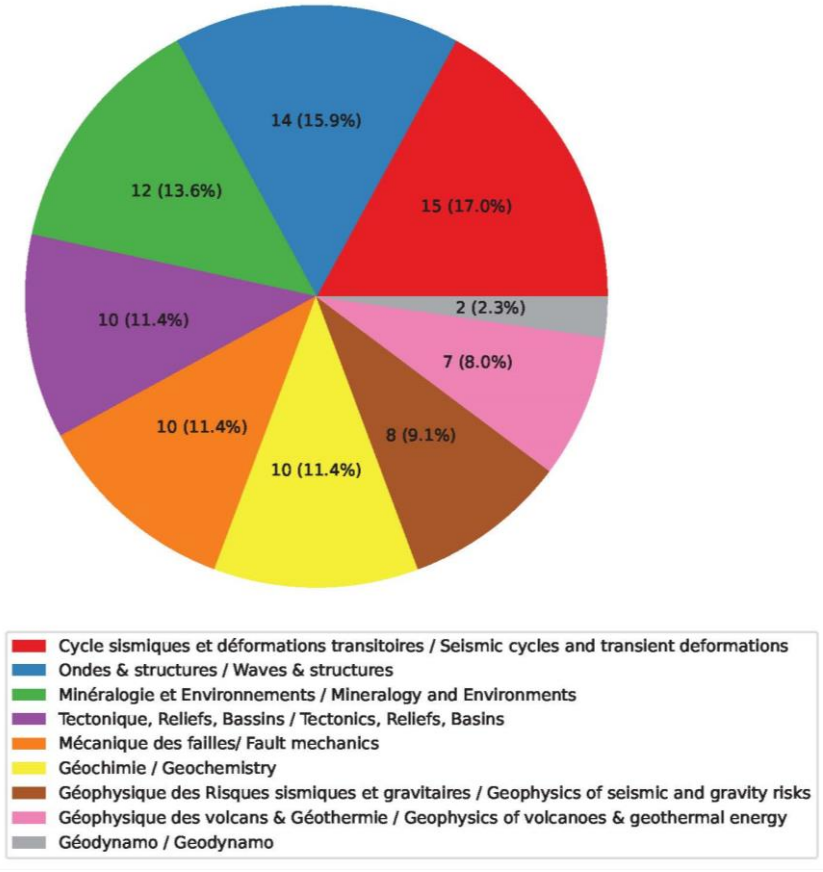

Distribution of doctoral students' years of thesis

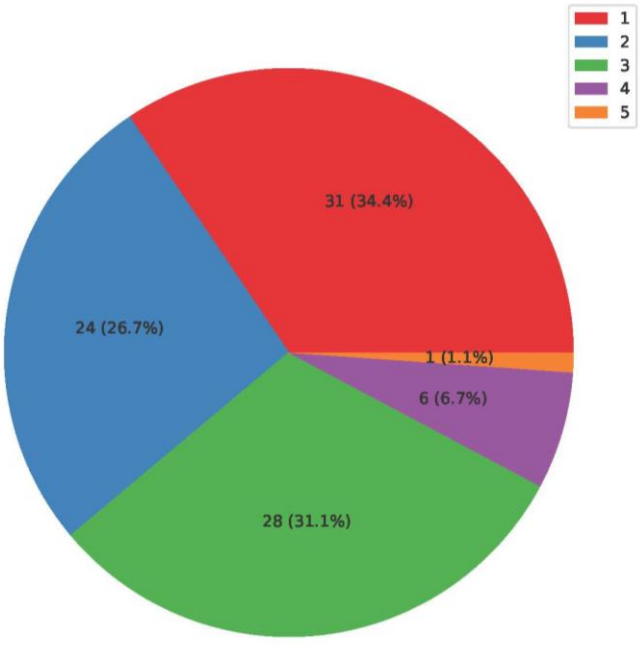

PhD Students' Thesis Abstracts

This booklet is a compilation of the ISTerre PhD students' thesis abstract for the year 2024.
Its purpose is to have a state of advancement of the thesis ongoing at ISTerre laboratories and to keep a trace of every thesis subject done in the institute.
This document is made on the occasion of the PhD Congress of 2024 hold at ISTerre Chambéry, where some of the following subjects were presented. Each student is the authors of its thesis abstract and figure.

Mohamed Amine ABDELLAZIZ

Optimal Experimental Design for Seismic Imaging

Year 3

Supervisors: Ludovic Métivier, Romain Brossier, Édouard Oudet (LJK)

Ondes & structures / Waves & structures

We propose a novel method for the optimal design of acquisition geometry in terms of imaging quality by improving the distribution of the wavenumber content of the approximate full waveform inversion gradient at a specified target. A study through diffraction tomography shows that for a regular layout of the acquisition, the distribution of the wavenumbers is not regular and for a fixed maximum offset those points will vary inside an envelope which can be approximated in 3D by a spherical dome. We are interested in finding the positions of sources and receivers that give a regular wavenumbers sampling inside this envelope.

Inside the envelope we can generate from the wavenumbers a Voronoi Tessellation, which is a partition of the space into Voronoi cells. Each cell is generated by a wavenumber, called seed, and contains all the points of the domain that are closer to this point than any of the other seeds. A Centroidal Voronoi Tessellation is a special instance of Voronoi Tessellation where the seeds coincide with the center of masses of the cells. To find such a tessellation we can search for seeds that are minimizers of an energy function defined in the Computational Geometry literature. This function describes the homogeneity in size of the Voronoi cells. The smaller in value the function is, the more similar in size are the cells and the more regular the sampling inside the envelope is.

What we propose is to define a new objective function that links the acquisition to the Voronoi tessellation generated by the wavenumbers and measure the homogeneity through the previous energy function. By minimizing this newly designed objective function we can find acquisition geometries that improve our regularity criterion. It is also possible to add constraints on the deployment area (by considering polygonal bounds on the surface and exclusion zones) and take into account the effects on the illumination from the heterogeneity of the initial model (by supposing the velocity model is 1D for example).

The method achieves to generate acquisition geometries that provide a better sampling than one where the sources and receivers are regularly spaced. This has the effect of improving the quality of the full waveform inversion gradient and producing inversions with improved quality around the target. We believe that those new developments open up new perspectives for target-oriented full waveform inversion and optimal post acquisition data selection.

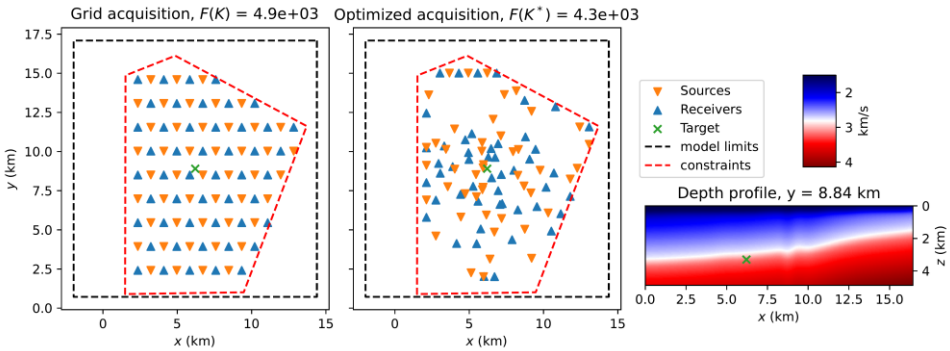

Example of two acquisitions: 1) on the left an acquisition with regularly spaced sources and receivers and 2) an acquisition in the center panel with the same number of devices that has been optimized with regards to a target in the center. The deployment area is defined by a red polygon, so no sources or receiver can be positioned outside it. The optimization has been carried out by considering the complex initial velocity model on the right panel. We notice that the method attempts to concentrate sources and receivers above the target while positioning some at the boundary of the deployment area so that we have access to far-offsets. The constraint has been respected since the acquisition is confined inside the area of deployment and we notice a decrease in the objective function F.

Ricardo AGUILERA CORTÉS

Impact of climate change on the dynamics of the Magallanes-Fagnano Fault (Tierra del Fuego, Chile)

Year 1

Supervisors: Joseph Martinod, Riccardo Vassallo

Tectonique, Reliefs, Bassins / Tectonics, Reliefs, Basins

My doctoral research focuses on the active tectonics of the Magallanes-Fagnano Fault (MFF) located in the region of Tierra del Fuego, Chile. This major transform fault separates the Scotia and South America tectonic plates. This study is conducted in a region that offers a unique natural laboratory for studying the interplay of geological forces with tectonics and their implications on seismic hazards in the region, as well as paleoseismologic studies. My research has allowed me to find evidence of ruptures related to recent co-seismic activity of the MFF in Chilean territory, which to date had not yet been described. This represents an important contribution and an advance for the development of paleoseismology in this area. My research aims to deeply understand the paleoseismic history and tectonic evolution of the MFF and to unravel the temporal and spatial patterns of past seismic events along the fault in Chilean territory, such as the last earthquake occurred in 1949.

The MFF in the Southern Andes accommodates left-lateral motion between the South American and Scotia plates. Historical earthquakes in Tierra del Fuego, notably in 1879 and 1949, underscore its seismic activity. Several studies already described surface ruptures associated to the 1949 earthquake in Eastern Tierra del Fuego (Argentina). This work presents first evidence historical co-seismic rupture in Chilean territory. Morphotectonic evidence, including non-degraded scarps, fractures in quaternary cover, tilted trees, supports the very recent activity for the fault. Dendrochronological analysis aims to corroborate these findings. Oblique fractures and pop-up structures along fault scarps indicate a complex fault behaviour. Understanding fault behaviour in the Chilean sector contributes to seismic hazard assessment in the region. First results of this research will be presented in this congress under the title “Evidence of 1949 earthquake co-seismic ruptures in western Tierra del Fuego, Chile”.

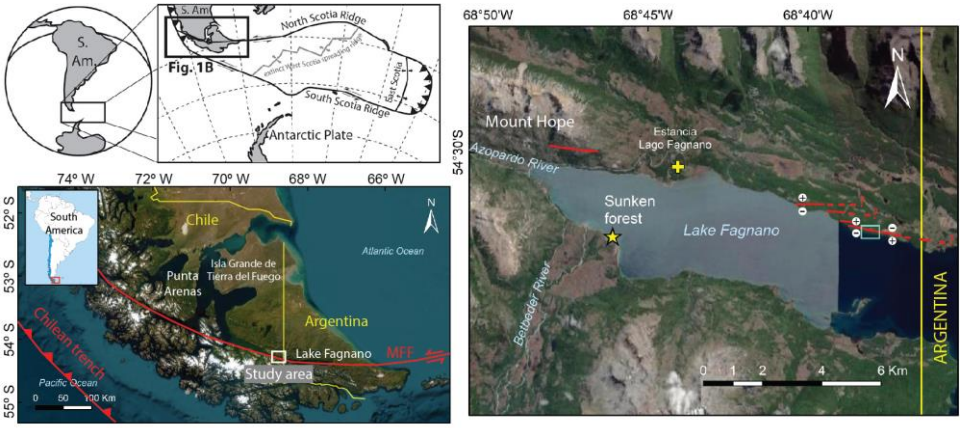

Top-left: Geodynamic setting of the study area.
Bottom-left: Regional tectonic setting showing the boundary of the MFF. White rectangle shows the location of our study area around Lake Fagnano in Chilean territory (Right).
Right: Map showing the location of recent ruptures (red lines) identified on the northern part of Lake Fagnano in Chile. The plus and minus symbology represents positive and negative topography of the scarp, respectively. The reported sunken forest location is shown in this map.

Houssam AL JAMAL

Comprehensive seismic damage predictions at building scale in Beirut for a large magnitude earthquake on the Mount Lebanon fault

Year 1

Supervisors: **Cécile Cornou, Mathieu Causse**

Géophysique des Risques sismiques et gravitaires / Geophysics of seismic and gravity risks

Ground motion simulation is crucial for seismic risk assessment in cities with limited recorded strong ground motion data. Lebanon is prone to a high seismicity given its location along the Dead Sea Transform fault system, but has recently experienced only low to moderate instrumental seismicity. Beirut, the capital of Lebanon, was destroyed in 551 AD due to a large magnitude earthquake ($M_s \sim 7.3$) offshore Lebanon that was attributed to the Mount Lebanon Thrust (MLT) fault. In addition, Beirut is densely populated nowadays, and seismic design requirements were only recently introduced in Lebanon. Thus, the 551 AD historical earthquake underscores the need for ground motion simulation from the MLT source for analyzing the seismic risk in Beirut. The objective of this study is to perform a comprehensive seismic damage prediction in Beirut for a large magnitude earthquake on the Mount Lebanon Thrust fault. After identifying the scenarios of interest, we will develop either new or improved models of the MLT source, the ground motion simulation for Lebanon, the soil and site amplification, and the built environment of Beirut. The new and improved models will be then used to estimate the seismic damages in Beirut for the selected scenarios. Finally, sensitivity analysis and machine learning methods will be used to assess the influence of the various analysis parameters on the simulated damages. This work is expected to lead to an improved evaluation of the seismic risk in Beirut.

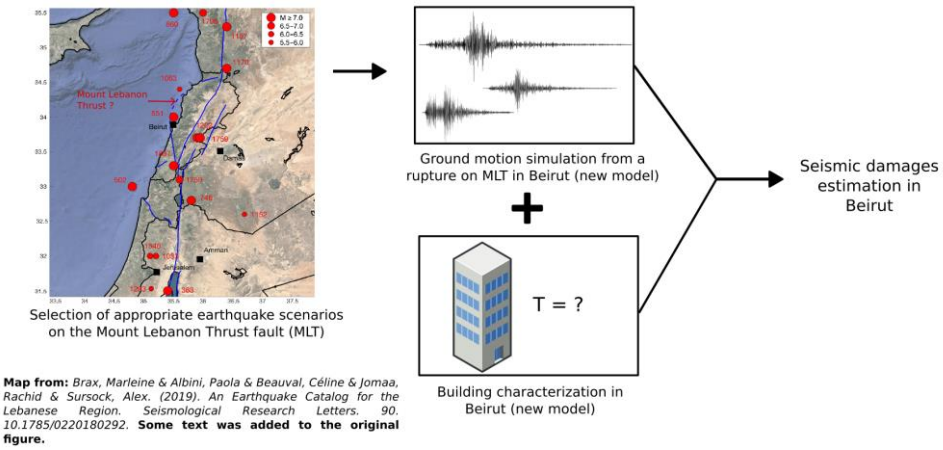

Overview of the methodology for the seismic damage prediction in Beirut.

Anne-Sarah AMBLARD

Mechanical modelling of sea ice

Year 1

Supervisors: **Jérôme Weiss**

Mécanique des failles/ Fault mechanics

Sea ice is a complex material that plays a key role in the climate system by strongly regulating heat and momentum exchanges between the ocean and atmosphere. When and where it is dense - during the winter and in the central Arctic mostly - it behaves as a continuous and damageable solid that is well-simulated using a visco-elasto-brittle model of the Maxwell-type (MEB, Dansereau et al., 2016; 2017, Rampal et al., 2019). Where it is highly fragmented and loosened – during the summer and the peripheral Arctic Ocean - it behaves like a granular media. Its mechanical resistance is then dominated by frictional contacts, a behavior that is not well-accounted for in current mechanical sea ice models and harder to quantify using observations

In this context, this work aims to improve the existing MEB model for sea ice by incorporating in it a parameterization of the effects of friction. To do so, we replicate with the model an annular Couette flow laboratory experiment that has investigated the frictional properties of a fault in floating ice and that, thereby enabling comparisons of the simulations with experimental findings.

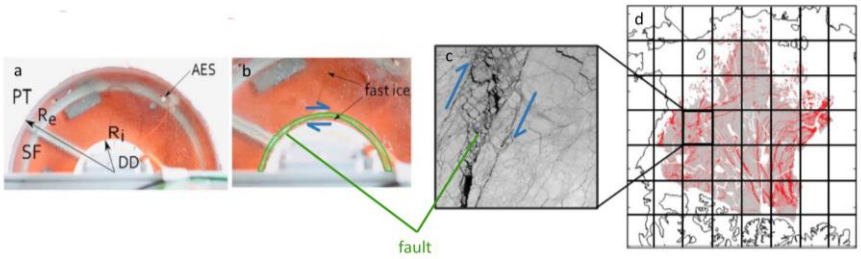

a) photograph taken from above of the annular Couette flow experiment before fracturating. Crédit V. Pelissier b) Zoom on the fault zone of the annular Couette flow after the creation of the fault. Credit V. Pelissier c) Satellite observation of sea ice covering an area of 50 by 50 km. Different zones can be distinguished: compact ice with elastic behavior around the fault zone exhibiting a higher damage and lower ice concentration. d) deformation rate of the entire Artic sea ice from RGPS dataset. (Credit S. Bouillon)

Duong Binh AU

Nucleation and the growth rates of $CaCO_3$ in cement pores and surfaces.

Year 1

Supervisors: Alexander Van Driessche (IACT CSIC-UGR), Alejandro Fernandez-Martinez

Géochimie / Geochemistry

Cement is the most widely used material globally, with its production contributing to approximately 8% of total anthropogenic CO_2 emissions. Carbonation processes applied to cement materials and recycled concrete offer promising technologies to reduce the carbon footprint associated with cement production and utilization. However, several fundamental questions remain unresolved for the large-scale implementation of these technologies. Understanding the formation mechanisms, polymorph selection, and texture of the resulting carbonated materials are crucial factors that must be addressed for the successful adoption of carbonated cementitious materials. In this PhD project, the nucleation and growth pathways of $CaCO_3$ at solid-liquid-water interfaces will be studied. In situ experiments will be performed using a set of lab-based characterization instruments (FTIR, Raman, AFM, Quartz-Crystal microbalance, UV-vis). These will be complemented with surface-sensitive synchrotron X-ray scattering investigations to determine $CaCO_3$ nucleation pathways and rates. These studies will result in a comprehensive description of the properties of oxide surfaces that are most adequate to promote $CaCO_3$ formation, of the nucleation and growth rates, and of the polymorph of the final $CaCO_3$ phase formed. This information is pivotal for the effective implementation of carbonation solutions for the cement industry.

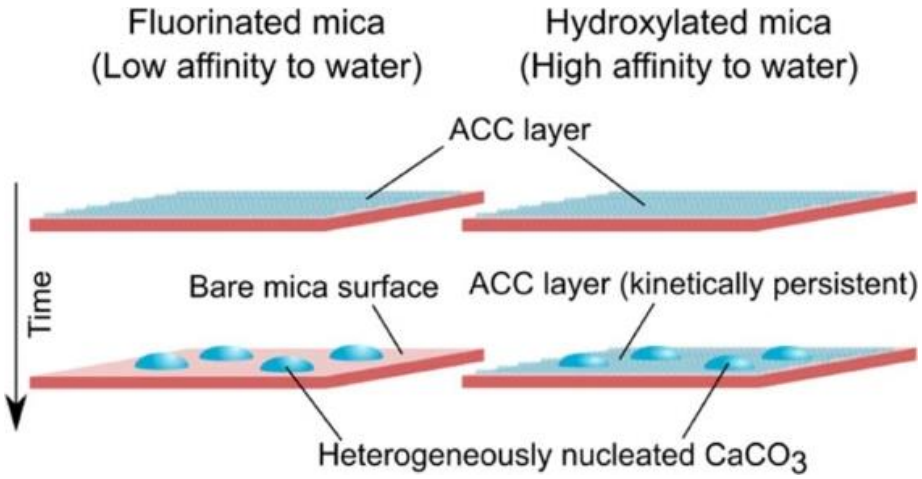

The image presents the formation of $CaCO_3$ on model substrates, particularly examining surface hydrophilicity. The upcoming research plan aims to expand this study to include other model substrates, such as variations in surface roughness, pH levels, and additional factors.

Annet BAKEN

Understanding how green additives control crystallization at the nanoscale

Year 3

Supervisors: Alexander Van Driessche (IACT CSIC-UGR), Alejandro Fernandez-Martinez, Marco Di Michiel (ESRF), Matthias Kellermeier (BASF SE)

Géochimie / Geochemistry

Additives – small amounts of (organic) molecules – are known to be able to control the outcome of a crystallization process, even when present in minor quantities. Outcomes of these additive-mineral interactions are ubiquitous. An example is the cement industry, which highly relies on additives to produce cement with tailored properties (e.g. approximately $20 billion/year are spent on cement additives). But, despite the pivotal role of organic molecules in the formation of industrial materials such as cement, surprisingly little is known about their modus operandi at the nanoscale during the early stages of nucleation and growth. We aim to correlate the physicochemical properties of model organic molecules with their functionality during the crystallization process of portlandite and gypsum. To achieve this, we employ in situ time-resolved Pair Distribution Function (PDF) analyses combined with potentiometric titration measurements, as well as complementary in situ Small-Angle X-ray Scattering (SAXS) experiments to monitor the mineralization process in the presence of different types of organic molecules. In particular, our newly devised method for PDF pushes the detection limit of what has been previously achieved in mineral nucleation studies from diluted solution. This study will contribute to a better fundamental understanding of nucleation with and without additives and hence, serve as a step forward in biomineralization research as well as offer new insights for the development of sustainable crystallization additives in industry.

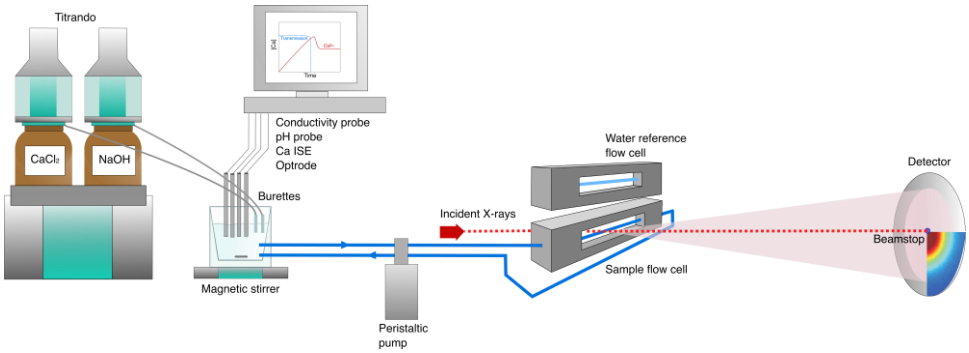

Titration set-up used to monitor the evolution of gypsum and portlandite nucleation with time. The experiments were repeated in beamline ID15A at the ESRF to observe nucleation at the nanoscale by employing synchrotron-based high energy X-ray scattering (HEXS).

Juliette BAS-LORILLOT

Mineral reactivity and microbial diversity associated with water-basalt interactions under subsurface conditions

Year 2

Supervisors: Damien Daval, Emmanuelle Gérard (IPGP)

Géochimie / Geochemistry

The purpose of my work is to assess the contribution of microorganisms to silicate weathering in basaltic subsurface environments. Although about 70% of microorganisms live in subsurface environments and have long been suspected to impact silicate weathering, the corresponding rates and mechanisms remain poorly constrained.

To study the microbial diversity in these environmental settings, field campaigns were carried out in Iceland targeting 22 basaltic aquifers with contrasted physicochemical properties (temperatures and pH ranging from 30 to 100°C and from 7 to 11). The biomass was collected by filtration using 0.22 µm filter. DNA was then extracted from the filters before Illumina MiSeq tag sequencing of the 16S rRNA-encoding gene. Bioinformatic analyses show that most of our samples are dominated by the phylum Nitrospirota, for the bacteria and the phylum Crenarchaeota and Hadarchaeota for the archaea. The microorganisms found in these analyses are consistent with what can be expected in deep aquifers and basaltic environments according to the literature.

In parallel, dissolution experiments were conducted in a range of pH and temperature relevant to the targeted basaltic aquifers to characterize the abiotic reactivity of basaltic glass and olivine using non-invasive techniques such as vertical scanning interferometry. At these conditions, our preliminary results show that the reactivity of olivine is lower than expected whereas the reactivity of basaltic glass is consistent with data reported in the literature.

During a final field campaign in Iceland, water and concentrate of micro-organisms from four targeted aquifers were collected in order to carry out new dissolution experiments. The wells were selected among the 22 studied for their diverse characteristics. Experiments were carried out under biotic and abiotic conditions using samples of basaltic glass and olivine. They are conducted in oxygen-tight bottles at a temperature relevant to the targeted aquifers (60 and 30°C). Preliminary results show that in the biotic experiments with basaltic glass, microorganisms seem to have been able to survive and develop. We are waiting for the results of further analyses (VSI) and future experiments to discuss their impact on silicate dissolution.

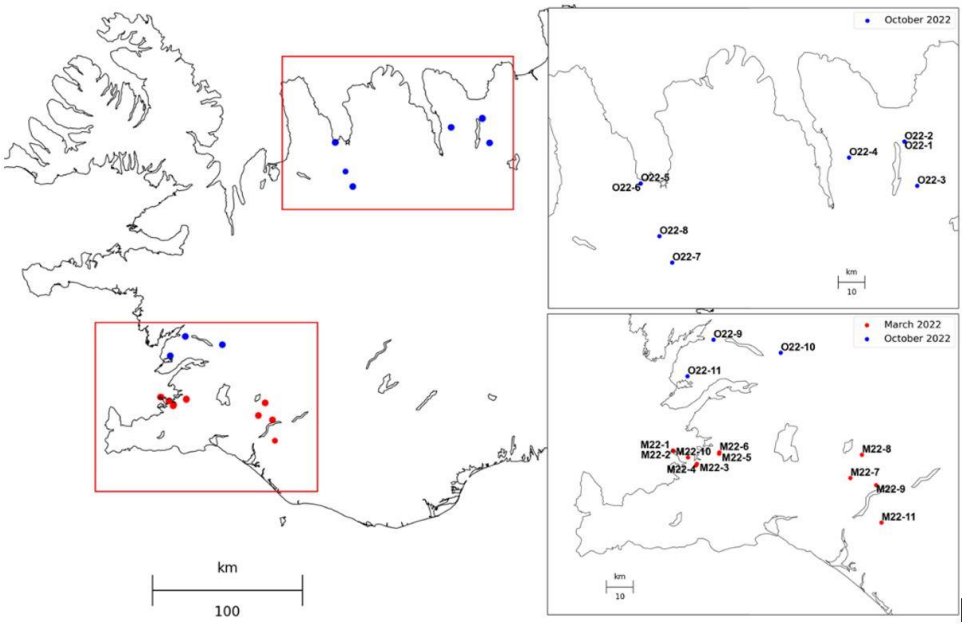

Location of the Icelandic aquifers sampled in March and October 2022 (red and blue dots respectively).

Lahcene BELLOUNIS

Spectral Element Modeling and joint inversion of magnetic, gravimetric and electric data

Year 1

Supervisors: Claire Bouligand

Géophysique des volcans & Géothermie / Geophysics of volcanoes & geothermal energy

Potential field data are frequently used to highlight geological features in geothermal areas (faults, lithological contacts, alteration zone). From 2021 to 2023, new gravity and high-resolution drone-borne magnetic data were collected over the Krafla geothermal area, located in the northern volcanic zone (NVZ) of Iceland, with the goal of imaging the geothermal system that lies beneath. As is often the case in volcanic and geothermal settings, the area is characterized by strong topographic variations which have a major influence on potential field data. To accurately account for topography with reasonable computational cost, we develop a numerical tool for the modeling and inversion of gravity and magnetic data using the integral equation (IE) method. The IE method allows to use deformable element cells and unstructured meshes, making the approach convenient and flexible for such purposes. We show that higher accuracy in the numerical integration is obtained when the method is combined with a local iterative octree refinement, allowing to reduce the effect of singularities close to observation points. We use a fifth order Gaussian quadrature on triquadratic elements to numerically evaluate the integrals. Another advantage to the method is that physical properties of the subsurface are defined on control points of hexahedral elements and discontinuities in the parameters (air-soil, faults, cavities) can be easily reproduced and accounted for. The method is used here to invert existing (Magnusson, ÍSOR-2016/013) and new gravity data to construct a density model of the Krafla geothermal area. The same code will ultimately be used to perform a joint inversion of gravity, magnetic and electromagnetic data (Arnason, 2020) to make use of their different lateral resolutions and sensitivities with depth.

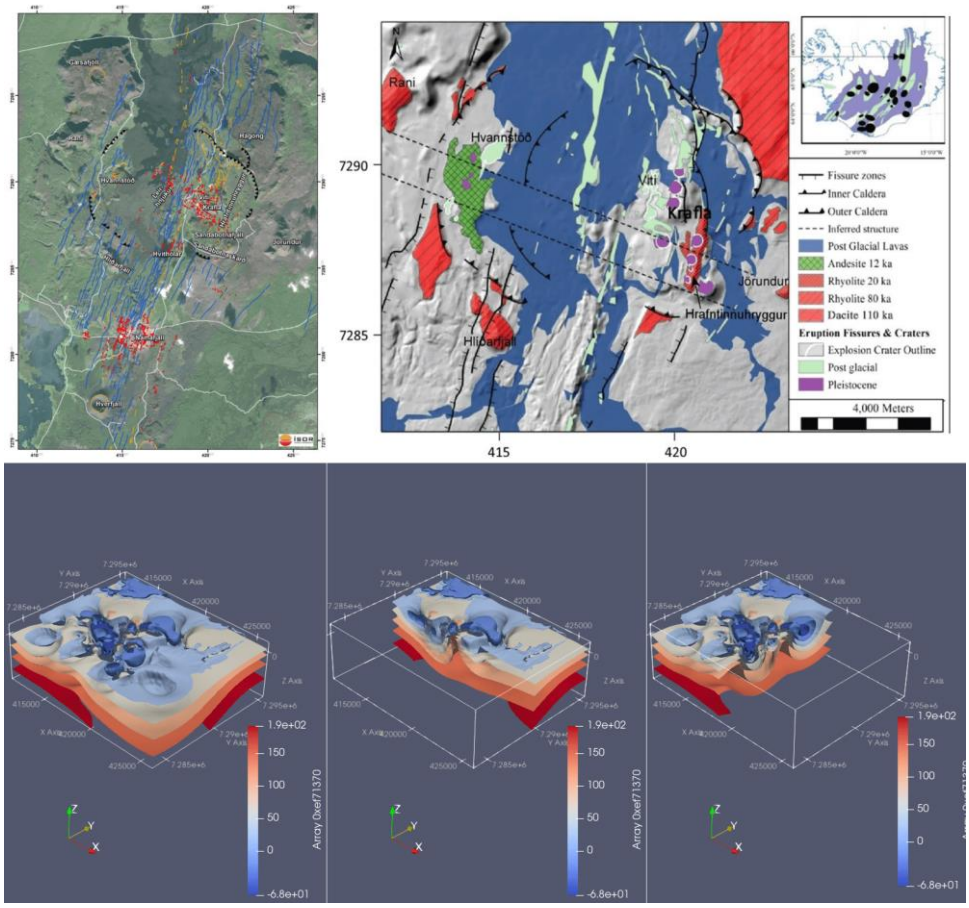

The upper panel of the figure above shows the geological map of Krafla (Northern Volcanic Zone of Iceland) on the right and an aerial view of the same area, ovelayed with the surface tectonics markers and the main caldera frontiers on the left (figures from Arnason, 2020). The bottom panel shows sections in the inverted density model recovered from gravity data (inversion carried out with the new numerical tool, relying on the Integral Equation Method (IEM))

Mustapha BENZIANE

Receiver extension strategies for time domain FWI

Year 2

Supervisors: **Romain Brossier, Ludovic Métivier**

Ondes & structures / Waves & structures

Receiver-based extension strategy introduces additional degrees of freedom to full waveform inversion, in order to improve the fit between the observed and calculated data at earlier iterations. This helps circumvent the cycle-skipping phenomenon. The additional degree of freedom is the receiver position, in our work we make it time-dependent, meaning that the receiver position varies during the acquisition time. The resulting problem is a two nested-loops minimization problem, where the outer loop is the conventional FWI loop to update the subsurface mechanical parameters, and the inner loop finds the optimal time-dependent virtual receivers' positions.

This inner loop problem is heavily nonlinear and non-convex finding the global minimum is a challenging task. We resort to a computational intelligence technique, particle swarm optimization (PSO). PSO is a heuristic optimization method, where at each iteration there are many realizations of model parameters called particles. This makes it possible to thoroughly explore the search space with few iterations. We take a closer look on the inner loop problem, we introduce an improvement to our PSO implementation, by judiciously choosing the starting inner loop parameters.

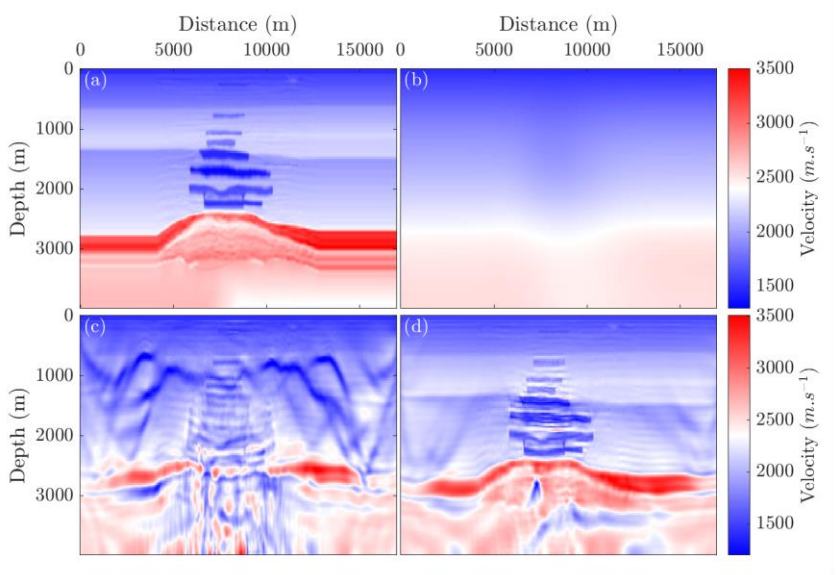

North Sea 2D synthetic model, (a): true model, (b): starting model, (c): final model obtained with conventional FWI and (d): final model obtained with receiver extension strategy.

Dorian BIENVEIGNANT

Fault analysis to understand the structuring dynamics of the W-Alpine foreland

Year 2

Supervisors: **Matthias Bernet, Stéphane Schwartz**

Tectonique, Reliefs, Bassins / Tectonics, Reliefs, Basins

The long-term study of fault system activity is essential for understanding the dynamics of orogeny structuring and their peripheral basins, the impact of tectonic inheritance, seismic risk assessment, and the coupling of deformation and erosion. At the junction of several orogenic domains, the foreland basin of the Western Alps possesses a complex structural scheme, inherited from the overlay of tectonic events since the end of the Paleozoic. Despite this knowledge, the deep geometry of different fault systems and the age of fault formation/reactivation remain poorly constrained, mainly due to the inaccessibility of these structures and the difficulty of dating minerals that are typically low in uranium found in sedimentary environments. In this doctoral thesis, it is proposed to use an approach combining structural analysis of deformations in the field, the recent method of in-situ U-Pb dating on syn-tectonic calcite, and numerical modeling (3D Geomodeling and Landscape Evolution Modeling) to bridge this gap. By targeting the Subalpine massifs (from the Vaucluse massif to the Helvetic nappes), the goal of this thesis project is to absolutely constrain the dynamics of structuring of the Alpine foreland on a large temporal and spatial scale. Furthermore, this study region presents diverse geodynamic characteristics, making it an ideal site to test the applicability of new dating methods.

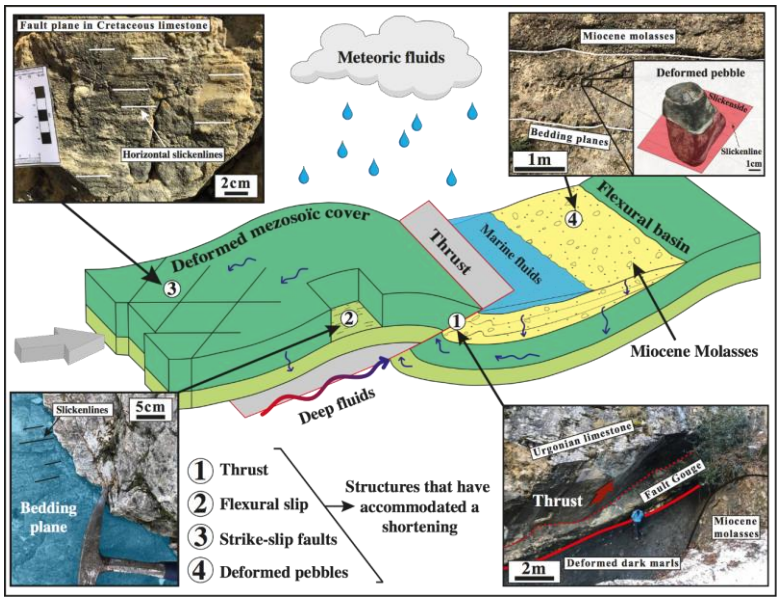

Figure 1: Non-exhaustive example of geological structures that accommodate shortening and can be dated using the U/Pb method on calcite.

Louise BOSCHETTI

Orogenic evolution of the south Alps and SE France basin: Impact of Variscan and Alpine rift structures

Year 2

Supervisors: Frédéric Mouthereau (GET, Toulouse), Stéphane Schwartz

Minéralogie et Environnements / Mineralogy and Environments

The impact of pre-Alpine tectonic and thermal events on the mountain building and deep crustal structure of the basins of SE France is currently poorly understood. In particular, the temporal and tectonic setting of the pre-Alpine phases remains to be clarified. The transition between the Mesozoic rifting and the beginning of the Cretaceous (Pyrenean?) shortening, and the paleogeography of the Vocontian basin in the complex plate framework between Europe, Iberia-Ebro and Adria must be established. The EOALP project combines different geochronological approaches over SE France. New low-temperature thermochronological dating will be carried out in the Pelvoux and Maures-Esterel massifs to constrain the pre-alpine thermal evolution of the Variscan basement. (U-Th)/He dating on hematite will be applied to the bauxites of Provence in order to link paleogeographic reconstructions of the Durancian uplift to tectonics and pre-Alpine paleo-topography. The thermal evolution of the Vocontian Basin will be constrained by U-Pb dating of fault-related calcites and the temperature of fluids associated with extension. These results, together with new crustal geophysical imagery from the AlpArray project, will provide new constraints on the still debated tectonic models and their impact on the structure and thermal evolution of the region.

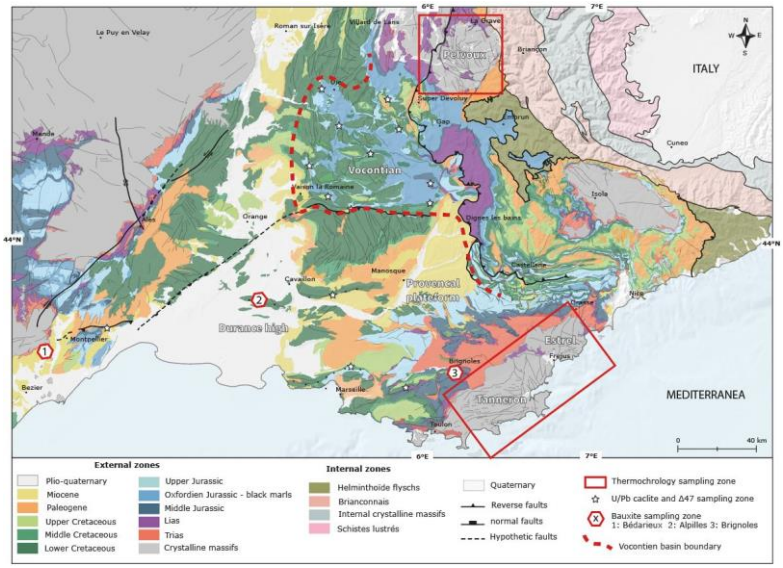

Geological map of the studied zone with sample locations.

Pierre BOUYGUES

Characterization of volcanic activity at Semeru volcanoe using high resolution radar and optical imagery.

Year 1

Supervisors: **Virginie Pinel**

Géophysique des volcans & Géothermie / Geophysics of volcanoes & geothermal energy

Explosive volcanic activity located in Indonesia associated with the Sunda subduction arc is causing 20% of worldwide reported volcanic fatalities. Among the 116 Indonesian volcanoes, Semeru is one of the most active and showed an increase of activity in December 2021 associated with the formation of lava and pyroclastic flows that threatened the population living nearby. To better understand and the dynamic of the volcano, it is important to detect precursors signs such as ground deformation related to magma movements inside a reservoir and/or a shallow conduit beneath the edifice. Interferometric Synthetic Aperture Radar (InSAR) uses satellite radar signals to detect and measure ground deformation caused by volcanic activity. However, such deformation signals caught by InSAR can be masked by the contributions of atmospheric delays that could be particularly strong in tropical volcanic regions and topographic residuals due to Digital Elevation Model that is not representative of the current topography. First, I will develop methods for improving the quality of the InSAR processing and reduce noise in InSAR time series. To reduce atmospheric delays, I will derive reliable atmospheric delay maps on Semeru based on external weather models and ground GNSS stations. To minimize topographic residuals, I am currently building an up-to-date and high-resolution DEM (spatial resolution of 5 meters) over Semeru. I analyze bi-static radar acquisition obtained during the period of 2015-2016 from the TanDEM-X mission and a stereo optical image acquired from the Pleiades database in July 2021 covering the crater and the southeastern flank of the volcano. In 5 years, the 2016 crater has been covered by the extrusion of a 200 meters lava dome leading to the December 2021 paroxysmal eruption. Furthermore, the southeast channel (yellow in figure 1), with a depth of 150 meters (P1 in figure 1) and served as the primary deposition and erosion area for volcanic products in 2016, has migrated toward the west due to infilling, leading to the formation of a new preferential channel with a depth of 40 meters (P2 in figure 1) in 2021 (orange in figure 1). The dynamic nature of Semeru volcano's topography requires the use of precise digital elevation models (DEMs) that accurately describe the current terrain, thus mitigating topographic residuals in InSAR deformation analyses.

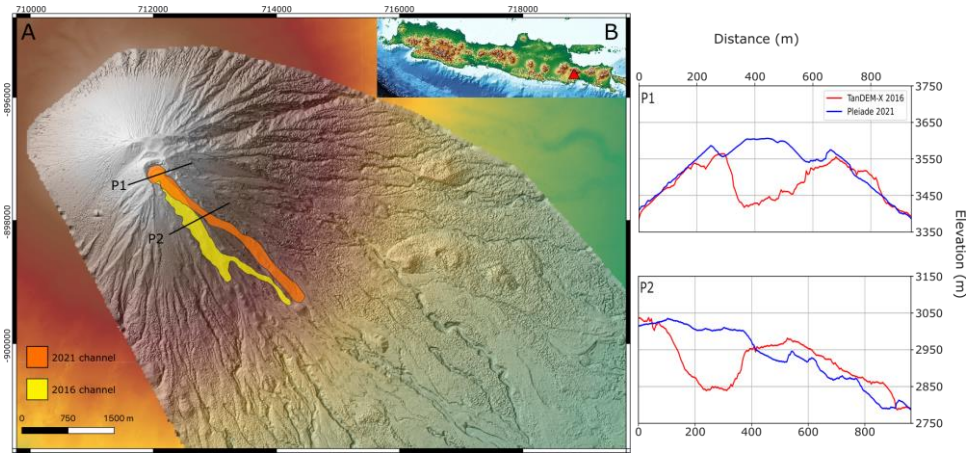

Map showing the dynamics of topographic changes at Semeru volcano during the 2016-2021 period: A) Hillshades of the DEM derived from the December 2021 Pleiades stereoscopic image. B) Localization of Semeru volcano (red triangle) on Java island, Indonesia. The old 2016 main deposition channel is highlighted in yellow, based on the 2015-2016 TanDEM-X analysis, while the 2021 main deposit channel is marked in orange. Profile 1, situated atop the crater, illustrates a 200-meter topographic difference between the 2016 crater and the 2021 lava dome. Profile 2, positioned on the southeast flank, emphasizes a 150-meter depth channel filled between 2016 and 2021, along with the emerging new main deposit channel.

Mirko BRACALE

Wavefield gradient methods to monitor the Earth's crust

Year 3

Supervisors: **Michel Campillo, Helle Pedersen**

Ondes & structures / Waves & structures

This research project aims to study the effects of seismic wave scattering to detect and monitor heterogeneity in the shallow crust. The study is divided into three parts, each of which considers different regimes and contexts:

1. This study investigates the sensitivity of seismic wavefields and their gradients to detect velocity variations at shallow depths using numerical simulations. Two case studies consider shallow localized velocity changes of -10% and -70%, analyzing phase shifts and amplitude change. We show that wavefield gradients have higher sensitivity in detecting strong heterogeneities than traditional seismological observables. Our results were validated through an ad hoc experiment comparing linear strain using DAS and horizontal acceleration in a field where a concrete foundation is buried.

2. We explore the behavior of seismic waves in a highly scattering medium through numerical simulations based on the Spectral Element Method. Three cases with increasing heterogeneity fluctuation (10% to 25% standard deviation) were analyzed, confirming theoretical predictions regarding mean free path, long-term energy decay, and energy partitioning. Our findings suggest that existing simulation codes can effectively replicate wave propagation, offering new possibilities for inversion studies and improving the characterization of environmental heterogeneity.

3. Conventional interpretations attribute stability in volcanic tremor spectra to source consistency. Our study, employing numerical simulations, reveals that stable features arise from the interference of multiply scattered waves on structural heterogeneity within volcano plumbing systems. By using a model obtained through magma injections in an elastic medium, we show how highly heterogeneous structures induce strong multiple scattering, influencing the observed complexity and stability of seismo-volcanic signals.

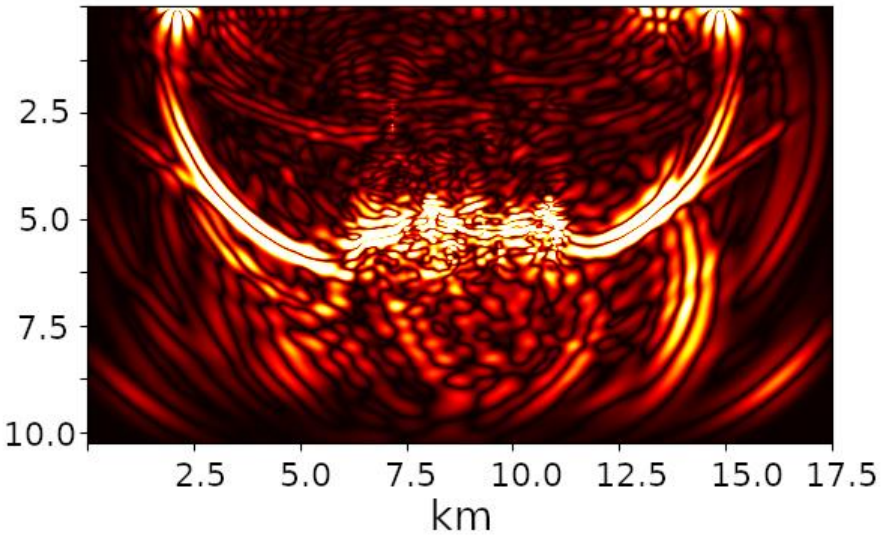

Screenshot of a seismic simulation related to the third project. Waves propagate in a magmatic plumbing system, the ballistic wave front is completely altered by the heterogeneous structure. A large amount of scattering is produced in the central area of the structure.

Margaux BUSCETTI

Development of multi-approach strategies for integrating site response into site-specific seismic hazard estimates.

Year 3

Supervisors: Fabrice Hollender, Vincent Perron (CEA Cadarache)

Géophysique des Risques sismiques et gravitaires / Geophysics of seismic and gravity risks

Site-specific Seismic Hazard Assessment (SHA) is becoming standard practice for critical facilities such as nuclear sites. This involves taking into account the specific characteristics and seismic response behaviour of the site under study as accurately as possible. To assess the seismic site response, Standard Spectral Ratio (SSR) or 1D (2D/3D) numerical modelling are usually used. Nevertheless, the SSR method requires choosing a reference site near the target one, and for ground motion numerical simulations, costly geotechnical and geophysical measurements are needed. For several years, empirical approaches based on national/regional ground motion databases, such as empirical ground-motion models (GMMs) and Generalized Inversion Techniques (GITs), have proven their reliability to estimates ground-motion properties, including site response, for various database types. One of the advantages of such methods is that the reference condition can be regional or a selection of one or plural sites that not need necessarily be located near the target site. Thus, in the objective to integrate site response estimates into SHA, the Epos-France database (Buscetti et al. submitted) was implemented in order to apply two types of GITs (Oth et al. 2011 and Grendas et al. 2022), as well as an Ad hoc GMM for metropolitan France. The site terms obtained with these three approaches are compared to SSR and 1D Transfer Function that are available at the site of study (CEA site), to attest of their reliability. The epistemic uncertainty associated to GITs results was investigated in the same time, and decimation of the local dataset has allowed deducing the minimum number of recordings required to infer a reliable site response with these approaches, and therefore the instrumentation period required. The final objective is to explore signal duration specificities, which is site-dependent, and plays an important role in the computation of response spectrum used in building design and SHA.

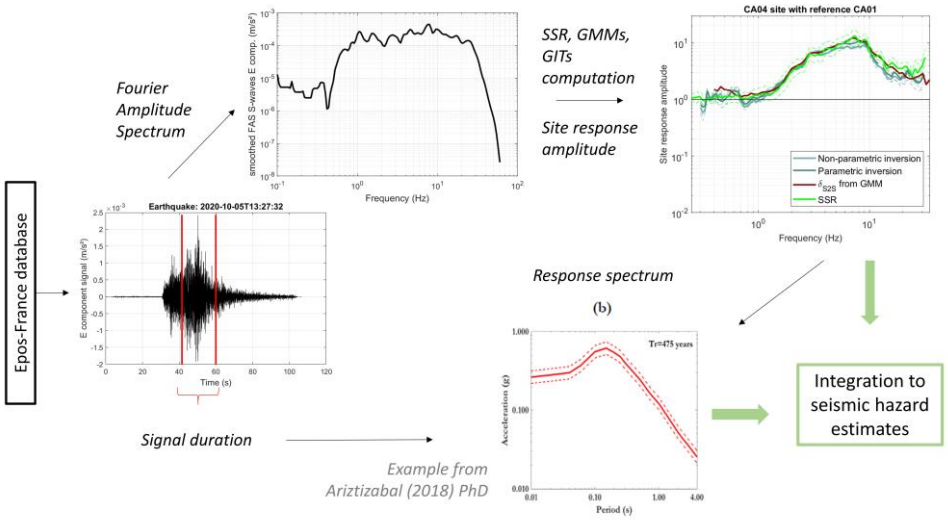

Scheme representing the different work done since the beginning of my PhD and the objective. From left to right: Database implementation, GMMs and GITs computation (assessment of epistemic uncertainty related to results and estimates of the minimum recordings required). Perspectives (lower part): signal duration analyses to compute response spectrum from amplitude Fourier spectrum.

Lucie CANET

Volatiles behavior during terrestrial evolution

Year 1

<u>Supervisors:</u> Guillaume Morard, Angelika Rosa (European Synchrotron Radiation Facility, Grenoble)

C-H-O-N-S are known as volatiles elements which constitute the outgassed atmosphere and have been delivered by comets and chondritic materials. Surface habitability of terrestrial planets and exoplanets is governed by the possibility to store and preserve volatile compounds, such as H_2O, CO_2 or N_2, over geological time.

Planets in their early stage experienced a fully molten state, the so-called Magma Ocean, which has strong implications for the subsequent evolution of the planet, from internal processes such as mantle convection and plate tectonics, up to the distribution of chemical elements, and notably the distribution of volatiles between the atmosphere and the interior of the planet.

The aim of this PhD is to study the densities and structure of Fe-rich/volatile-rich silicates melts, using X-Ray diffraction and pulsed laser heating at high pressure and high temperature, in order to better understand the existence of a volatiles reservoir at the Core-Mantle Boundary (BMO).

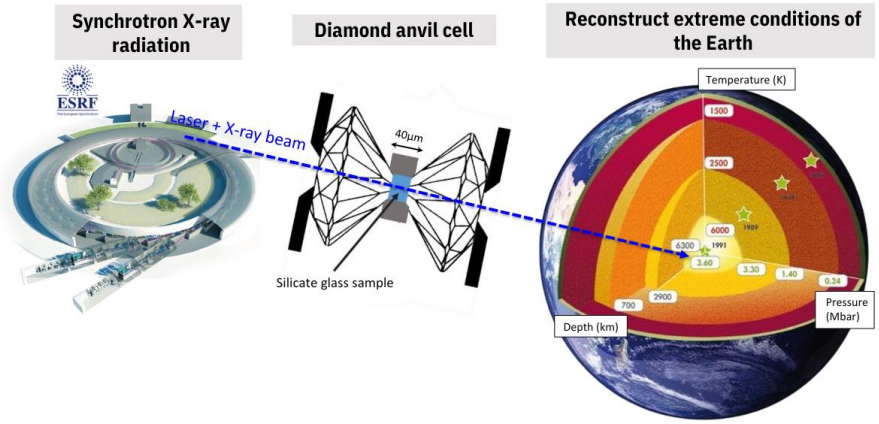

The combination of the extremely brilliant X-ray source, using X-ray diffraction, and time-resolved laser heating at the European Synchrotron allows to reconstruct high-P and high-T conditions that prevail in deep Earth interior. The silicate glass samples, composed of (Mg, Fe)SiO_3, are compressed between two diamonds, i.e., the strongest materials in the Earth, up to 150-200GPa and heated (>3000K) with a pulsed laser, in order to track high P-T processes at the microsecond to second timescale.

Menghan CAO

Well water-level response to seismic waves revealed by a decade's worth of high-rate hydraulic data recorded near Parkfield

Year 1

Supervisors: **Mai-Linh Doan**

Mécanique des failles/ Fault mechanics

Understanding the interaction between earthquakes and groundwater is crucial for elucidating variations in subsurface properties as well as fault structure and activity. For this purpose, we develop an automatic detection program to identify coseismic water level oscillations, which integrates time- and frequency-domain detection methods. Application to a decade's worth of high-rate pore-pressure data recorded near Parkfield shows that the coseismic water-level oscillations are primarily influenced by the seismic energy density, and the well-bore construction, aquifer hydraulic properties and dilation of seismic waves can also influence water-level responses. However, the specific impact of each factor cannot be distinguished, which requires further investigation in the future.

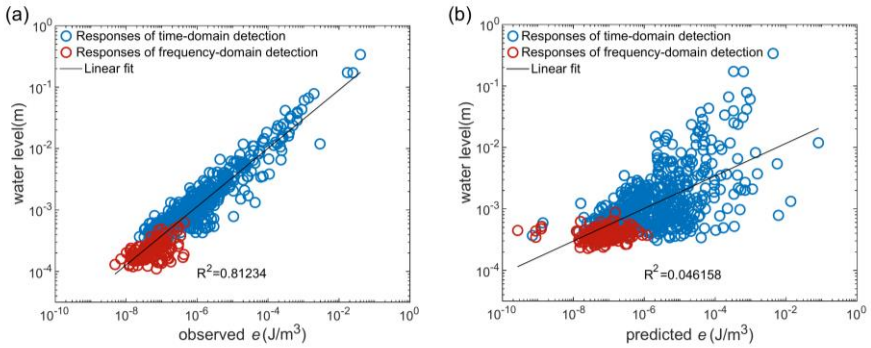

(a) Relationship between water-level oscillation and seismic energy density estimated from the observed peak ground velocity. (b) Relationship between water-level oscillation and seismic energy density predicted by the empirical relation of Wang (2007). The red and blue circles represent the water-level responses detected by spectral analysis in the frequency domain and by STA/LTA in the time domain, respectively. The black lines are the linear fits to all data, and R2 is the coefficient of determination (the closer the value to 1, the better the fitting).

Estela Juana CENTENO MONCADA

Detailed study of crustal faults and associated seismicity in the Colca Valley, Peru

Year 1

Supervisors: Hugo Sánchez-Reyes, Anne Socquet, Hernando Tavera (Instituto Geofísico del Perú)

Cycle sismiques et déformations transitoires / Seismic cycles and transient deformations

The Colca Valley region in southern Peru (Figure 1) is noted for its prominent seismic activity, which can cause considerable damage to vulnerable infrastructure typical of the region. This activity is influenced by both volcanic phenomena and the presence of tectonic fault systems. Among the notable volcanoes in the area we found Sabancaya volcano. This important volcano began its seismic activity in 2013 with earthquakes up to a local magnitude greater than 4.5 [Machacca, R. et al. (2023)]. To the north of Sabancaya there is another important volcanoe, Hualca Hualca, in addition to that, several active tectonic faults are present as well in the area. Therefore, the high seismic activity in this region may have different causes (e.g., seismic swarms, magmatic movements and landslides).

With respect to the fault systems present in the Colca Valley, we can highlight the Ichupampa Fault and the Trigal Fault System. Activity on these two major faults contributes significantly to the high seismicity in the region. Understanding the interaction between volcanic activity and these faults is crucial to assess and mitigate seismic hazards in the area. Therefore, my work focuses on the detailed study of the crustal faults in this area and the seismicity probably associated with tectonic or volcanic events. For this study, we used continuous seismic records from 13 seismic stations of the Local Seismic Network of the Colca Valley of the Geophysical Institute of Peru (IGP). These records were collected from 2015 to 2018. Preliminary results of automatic detection (using Artificial Intelligence tools) using SeisBench software [Woollam, J. et al. (2022)], has managed to detect 61,639 seismic events between January 2015 and December 2018. The seismic events present local magnitudes from -0.05 to 6.14. These results evidence the intense seismic activity in the Colca Valley region. The next steps in my work will be to analyze this activity to unveil the different sources that originate these events. In addition, my work will seek to answer to what extent the volcanic activity in this area is related to the activation of tectonic faults and landslides.

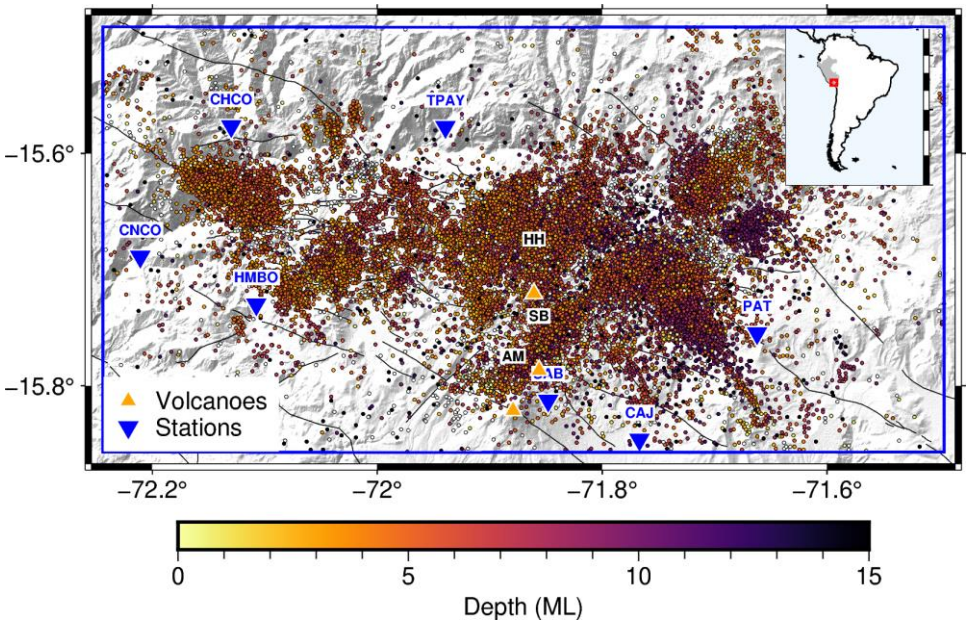

Figure 1. Map of seismic activity detected by Seisbench sofware from January 2015 to December 2018. The colored circles represent the epicenters of the detected earthquakes. The colors represent the depth of the hypocenter. The blue triangles represent the stations of the Local Seismic Network of the Colca Valley of the Instituto Geofísico del Perú (IGP). The orange triangles represent the three important volcanoes in the study area, Sabancaya (SB), Hualca Hualca (HH) and Ampato (AM).

Jacques CHARROY

Resource and risk assessment for medium enthalpy geothermal energy by passive geophysical methods

Year 2

Supervisors: Jean-Luc Got, Yajin Yan (LISTIC, Université Savoie Mont Blanc)

Géophysique des volcans & Géothermie / Geophysics of volcanoes & geothermal energy

Geothermal energy is an attractive source of renewable energy; however, its exploitation requires a sound knowledge of the nature, quality and boundaries of the reservoir to evaluate the resource potential with a good level of confidence and reduce the risk of induced seismicity. We have acquired broadband magnetotelluric (MT) data and ambient seismic noise measurements to investigate a medium-enthalpy geothermal prospect zone in the region of Annecy, France. In this pre-alpine area, karstic limestones constitute a deep aquifer (up to ~2 km) intersected by the Vuache fault, an active strike-slip fault where a M5.3 earthquake occurred in 1996.

An MT data set consisting of 34 MT stations was acquired with satisfactory data quality up to periods of ~1s. Major data quality issues arise at longer periods, related to the presence of pervasive electromagnetic noise in this urbanized region, mitigated by the reliance on long acquisition times and careful use of advanced processing methods (FFMT). 1D and a 3D MT models were produced by inverting first for tippers and phase tensors, then full impedance tensors, using the ModEM inversion code (Kerlbert, Meqbel et al, 2014). The sensitivity of our model was then evaluated on the basis of normalized euclidian sensitivities calculated from the Jacobian matrix (1,2,3) of the resulting 3D MT model.

We produced a 3D geological model on the basis of geological field surveys, 2D seismic reflection sections, and borehole information and aim at using this model as a basis for re-inversion of the MT data by turning off smoothing across interfaces detected by seismic reflection, with the intention of allowing refined imaging on either side of these interfaces and testing the detectability of the presence of permeability within karstic aquifers at depth based on inverted bulk resistivities.

References:

(1) Egbert, G. D. and Kelbert, A. (2012). Computational recipes for electromagnetic inverse problems, Geophys. J. Int., 189, 251-267, 2012, doi: 10.1111/j.1365-246X.2011.05347.x
(2) Kelbert, A., Meqbel, N., Egbert, G.D., Kush, T. (2014). ModEM: A modular system for inversion of electromagnetic geophysical data, Computers and Geosciences 66, 440-53.
(3) Muñoz, G. and Rath, V. (2006). Beyond smooth inversion: the use of nullspace projection for the exploration of non-uniqueness in MT, Geophysical Journal International, 164, 301–311, 2006, doi: http://dx.doi.org/10.1111/j.1365-246X.2005.02825.x

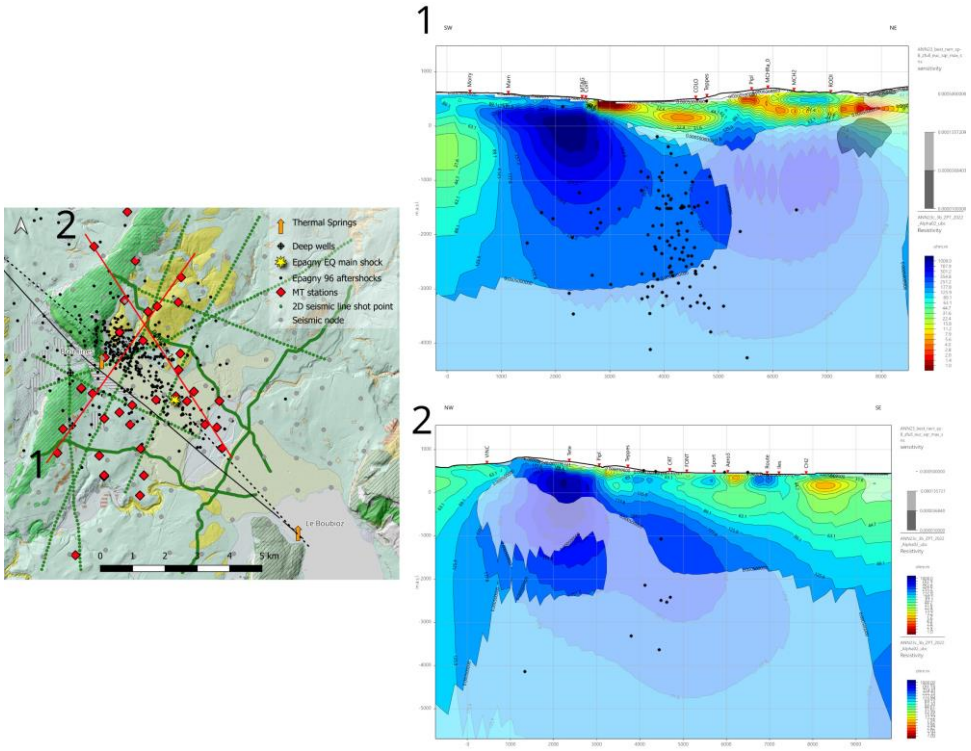

Map of MT stations (red diamonds), seismic nodes (grey dots) and 2D seismic lines (green dots) acquired over the area of the Epagny 96 mainshock (yellow) and aftershocks (black dots); Sections of 3D MT models produced along profiles 1 and 2 showing resistivity contours with normalized euclidian sensitivity contours overlay (gray).

Audrey CHOULI

Seismicity and deformation in subduction zones: from intermediate-depth intraslab earthquakes to shallow megathrust events

Year 3

Supervisors: Anne Socquet, David Marsan, Sophie Giffard-Roisin

Cycle sismiques et déformations transitoires / Seismic cycles and transient deformations

The 2011 M_w 9 Tohoku-oki and 2014 M_w 8.3 Iquique subduction earthquakes were both preceded by shallow foreshocks, occurring sometimes synchronously with intermediate-depth seismicity (deeper than 60 km).

To assess the possibility of a causal link between deformation at depth and ruptures of the shallow interface, we systematically pinpoint the interactions between shallow and intermediate-depth activity, and assess their statistical significance. We use correlation to detect synchronous deep-shallow bursts lasting some days in the seismicity rates, and clustering techniques to extract from the earthquake catalogs spatio-temporal patterns connecting the deep and shallow parts of the subducting slab.

Significant correlations emerge in the months before both megathrust earthquakes, with an increased occurrence of along-dip seismicity lineaments in the Tohoku area.

A candidate model involves pressure bursts traveling along the slip interface, caused by the release of over-pressurized fluids trapped at intermediate depth, that trigger activity over months along the interface and participate in the slow unclamping of the megathrust.

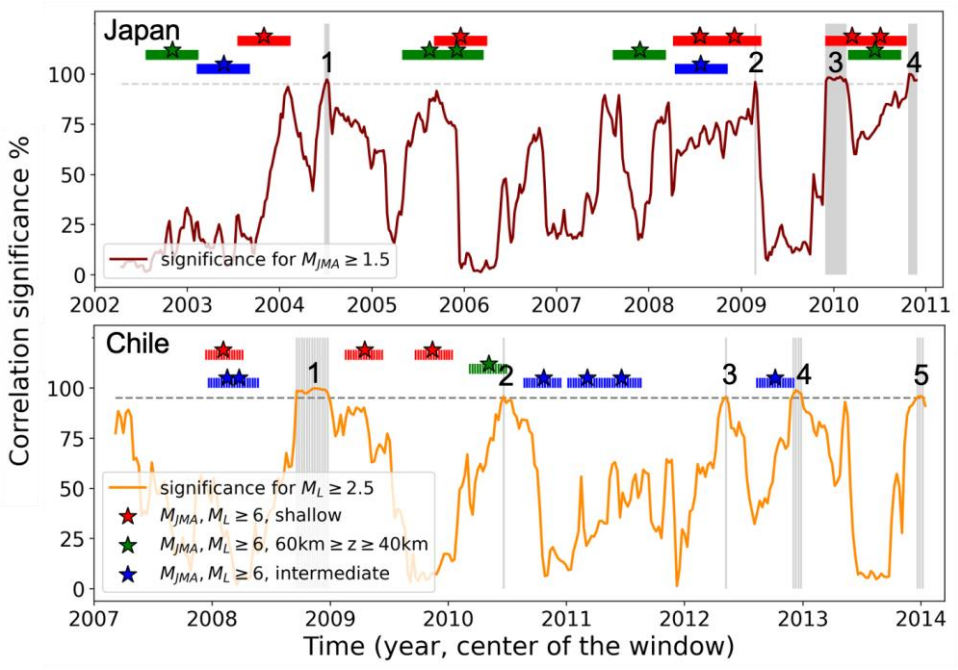

Evolution of the significance of the correlation coefficient between intermediate-depth and shallow seismicity rate with time in Japan and Chile. Windows with significant correlation are highlighted by vertical grey lines. In Japan, the correlation coefficient has been calculated with the seismicity rate smoothed over 7 days, and each window has a duration of 210 days.
In northern Chile, the seismicity is smoothed over 4 days, and the correlation coefficient is calculated on 120 day-long windows.

Rajkumar CHOWDHURY

Physical and chemical characterization of Nannoconus, the main planktonic bio-producers of early Cretaceous oceans

Year 3

Supervisors: **Fabienne Giraud, Alejandro Fernandez-Martinez**

Tectonique, Reliefs, Bassins / Tectonics, Reliefs, Basins

My doctoral thesis is on the subject of the "Physical and Chemical characterization of Nannoconus, the major planktonic bio-carbonate producers in Early Cretaceous Seas." Early Cretaceous (~ 150-100 Ma) is characterized by huge marine carbonate deposits. Calcareous nannofossils are bio-calcitic remains (~1-30 µm), formed by planktonic algae living in the photic zone of the ocean. Nannoconus is a group of calcareous nannofossils (~5-20 µm) with massive exoskeleton (40-1000 Picogram). However, very little is known about the successful calcification of this particular group of calcareous nannofossils to form this huge mass of bio-calcite. Thus, we applied several physical and chemical characterization techniques to understand this success story with respect to the paleobiology and paleoceanography.

Physical Characterization:

The physical structure of Nannoconus is formed by the interlocking arrangement of calcitic plates, around a central canal (Fig 1). The interlocking arrangement is developed by two different inclinations of plates (Fig 2). The organisation of the plates to form the entire exoskeleton of Nannoconus is not well-known. To understand this micro-structural development, we applied a high-resolution (~40 nm) Ptychography computed X-ray tomography with synchrotron radiation in several species of Nannoconus. The results were a series of tomographic image slices for the entire exoskeleton of Nannoconus. The results were combined together in ORS-Dragonfly software to virtually segment one plate. Then this plate has been used to reconstruct the entire exoskeleton. Two different models have been defined for the reconstruction of the exoskeleton.

1. Model-1: Two separate layers of plates are formed. Each layer has a particular inclination of the plates. The entire exoskeleton is built by alternatively placing these two layers one after another. (Fig 3).
2. Model 2: The exoskeleton is built by several segments of plates. Each segment is formed by alternately stacking plates of the two different inclinations. (Fig 4).
   The reconstruction of the exoskeleton from one plate is fairly new approach to understand the micro-structural development. However, this information can be used to infer about the non-existent knowledge of the process of the exoskeletal calcification of the living cell(paleobiology) of Nannoconus.

Chemical Characterization:

The major composition of Nannoconus is calcite. To understand the chemical characterization of Nannoconus at sub-micron level, we applied Raman micro-spectroscopy and X-ray micro-fluorescence with synchrotron radiation.

Raman Micro-spectroscopy: The spectrum of Nannoconus obtained contain several peaks of calcite. These peaks can be compared to the peaks of the spectrum of pure calcite (Fig 5A). The υ1, L peaks of Nannoconus (Fig 5B) show shift of positions with respect to the respective peaks of pure calcite. This shift is due to the chemical heterogeneity in calcite. This heterogeneity is a result of the replacement of Ca+2 of calcite by trace elements like Strontium and Magnesium.

The results of the µ-XRF give elemental maps of Calcium (Fig 6A), Strontium (Fig 6B) and Magnesium (Fig 6C) of Nannoconus. The value of the Sr/Ca and Mg/Ca ratios from these elemental maps can be calculated. These ratios can quantitively indicate the chemical heterogeneity of the bio-calcite of Nannoconus. One of the reasons, of the chemical heterogeneity in bio-calcite of calcareous nannofossils is the adaptation of the algae to the paleoceanographic changes. High nutrient availability of the ocean (photic zone) generally increases the Sr/Ca value in bio-calcite. Similarly, the increase in temperature of the photic zone results high Mg+2 intake during bio-calcification (thus increased Mg/Ca value). Considering this, the quantitive results of the chemical characterization of Nannoconus can indicate the paleoceanographic conditions responsible for the successful calcification of Nannoconus.

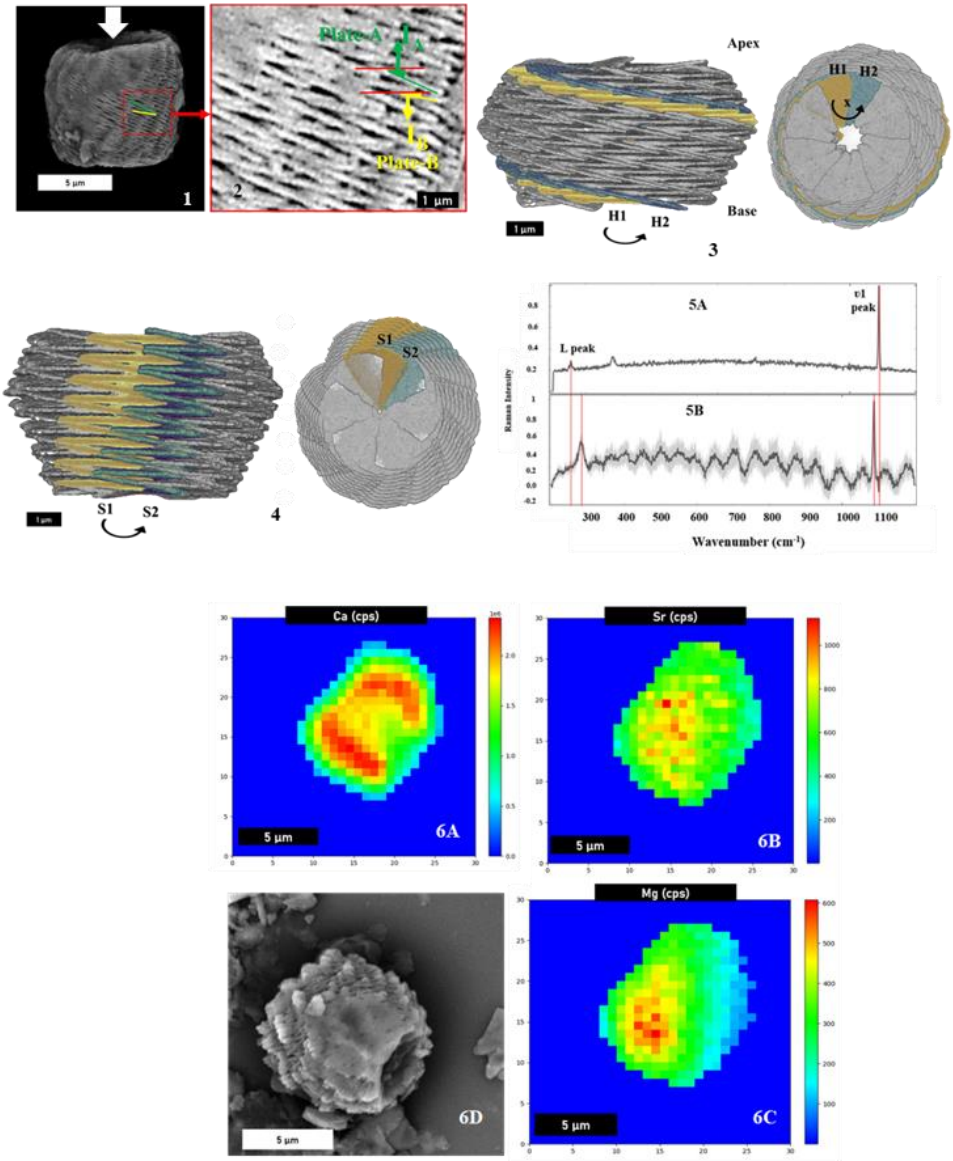

Scanning Electron Microscopic image of Nannoconus circularis (Fig 1). The central canal is shown by the white arrow. The red box shows the interlocking arrangement of the calcitic plates. In the enlarged view of the red box (Fig 2) the two distinct angles of inclination of the plates are given. These two angles of inclination cause the interlocking arrangement of the calcitic plates. The higher value of inclination (IA) given by green line (Plate-A) and the lower value of inclination (IB) given by yellow line (plate-B). Fig 3 shows the reconstruction of the exoskeleton using Model 1, where the two layers (H1 and H2) of low and high angle of inclinations are shown by the yellow and green colours. Similarly in Fig 4, the reconstruction is generated from Model-2 where two consecutive segments are given by the yellow and green colours (S1 and S2). The shift (in wavenumber) of L and υ1 peaks between the Raman spectrum of pure calcite (Fig 5A) and calcite of Nannoconus (Fig 5B). The positions of the peaks are marked by the red lines. The elemental maps of Calcium (Fig 6A), Strontium (Fig 6B) and Magnesium (Fig 6C) resulted from the µ-XRF with synchrotron radiation of Nannoconus globulus. "CPS" indicates "Counts per Second". SEM image of different specimen of Nannoconus globulus, is given in Fig 6D.

Aleksandr CHUGUNOV

Evolution of Archean Earth mantle composition: The evidence from magmatism of Kaapvaal Craton

Year 4

Supervisors: Alexandre Sobolev

Minéralogie et Environnements / Mineralogy and Environments

Komatiites are unique volcanic rocks that form from extremely hot and magnesium-rich magmas deep within the Earth's mantle. Olivine phenocrysts found in Archean komatiites have proven to be effective containers for preserving melt inclusions. The goal of my PhD is to present new findings regarding composition, assimilation, temperature, oxygen fugacity, Rb-Sr model ages of mantle sources for Archean komatiites in the Barberton greenstone belt, which are identified through in-situ examination of melt inclusions and host olivine phenocrysts. Over 400 melt inclusions from high-Mg olivine phenocrysts (Fo 95.3-92.5) were heated up to 1400°C to melt the inclusions, then quenched to form homogeneous glass.

We study inclusions with the help of our IMAP platform for major, minor, trace elements and Sr isotopes (EPMA and LA-IPC-MS); RAMAN for water contents. The host olivines are also studied for major, minor and trace elements (EPMA and LA-ICP-MS) and oxygen isotopes (SIMS lab in Wisconsin, USA). The reverse post-entrapment crystallization modelling was used to reconstruct the composition of the trapped komatiite melts.

The primary melt composition of these komatiites indicates over 32 wt.% of MgO, which is extremely high. The estimated eruption temperature (Mg-Fe and Sc-Y olivine-melt geothermometers) of the primary melt is around 1500°C, which gives this melt a high potential for country rock assimilation. This is indicated by intercorrelated enrichment of melt by Cl, K, Rb, Ba, Sr, Pb, H_2O, and depletion of 18O (Chugunov et al., 20024, in prep). A subset of 10 inclusions yielded an average initial $^{87}Sr/^{86}Sr$ ratio of 0.69932±0.00028, corresponding to a minimum BSE model age of 4309±230 Ma (Vezinet et al., Nature, 2024, in review). Values for Ce/Pb and Nb/U are higher than BSE and suggest that the BSE mantle was involved in the production of oceanic crust, extraction of continental crust from the latter, and the recycling of residual components deep within the mantle to form plume-produced komatiites by 3.27 Ga.

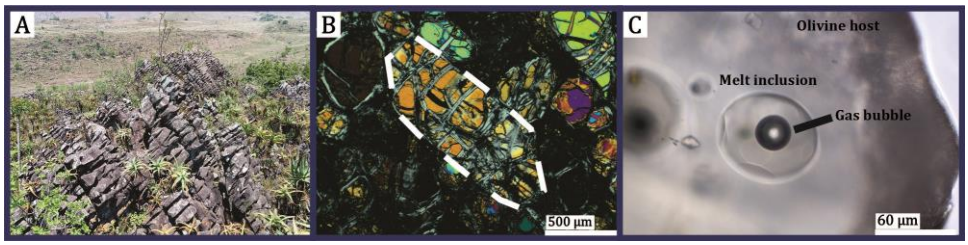

A - Field view of the 3.27 Ga Weltevreden formation (Pioneer Complex), Barberton Greenstone Belt, South Africa. B - Photomicrograph of partially serpentenized cumulate komatiite from Weltevreden formation. Fresh melt inclusions occur in the remaining cores of olivine grains (dotted line). C - Olivine-hosted melt inclusion after high temperature experiment.

Lucile COSTES

Evolution of intraslab seismic activity during intense aftershock sequence

Year 1

Supervisors: **David Marsan**

Cycle sismiques et déformations transitoires / Seismic cycles and transient deformations

In subduction zones, earthquakes at depths between 60 and 100 km occur within the subducting slab rather than at the slab interface. The presence of fluids resulting from dehydration reactions in the medium would favour these earthquakes by fluid embrittlement, but the relation between the two processes is not yet fully constrained.
We study the aftershock sequence following the M7.1 2003/05/26 intraslab earthquake which was located off the Miyagi prefecture coast, in Japan. This sequence displays characteristics that are promising for studying relations between seismicity and fluid pressure (high aftershock rate, expanded instrumentation…).

The analysis of the catalogues of seismicity and focal mechanisms provides information on the principal characteristics of the aftershock sequence (Omori-Utsu law, Gutenberg-Richter law). In particular, the aftershock sequence follows nearly perfectly an Omori's law. This good agreement between the data and the model appears to be due to the absence of large aftershocks. An application of the ETAS model to the sequence suggests that most of the sequence would be triggered by the M7.1 itself, i.e the aftershocks play no role in triggering more aftershocks. Moreover, the temporal distribution and inversion of stress field in the small aftershock zone show that, unlike the slab interface, the area inside the slab does not seem to be disturbed by the nearby occurrence of M9 Tohoku-oki earthquake (2011/03/11).

We conclude from our analyses that this intraslab sequence is characteristic of a very critically stressed crustal and upper mantle volume implying strong faults that are not sensitive to large stress perturbations. Moreover, if fluids are involved, then they are likely to be drained off from the top of the activated volume as proved by the depth dependence of the Omori-Utsu's *p*-value, possibly playing a role in the subsequent occurrence of the 2011 megathrust Tohoku-Oki earthquake which hypocenter is updip this sequence.

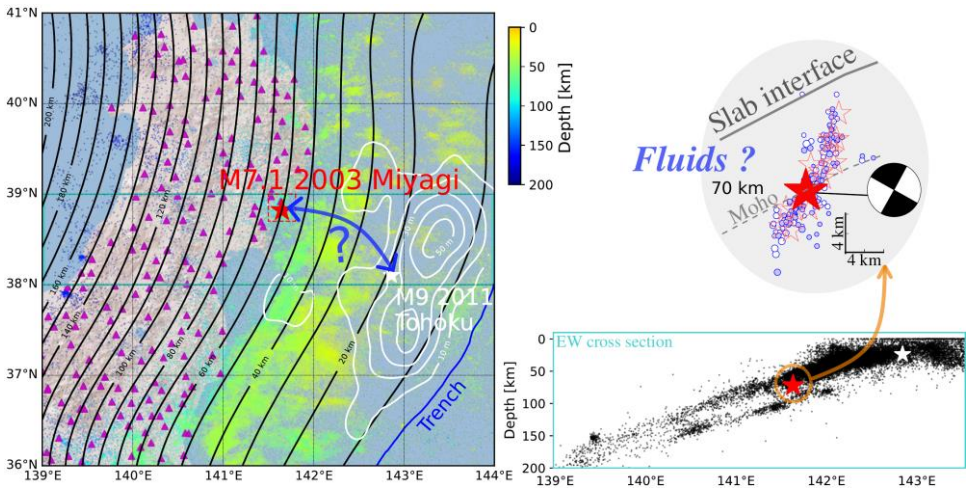

The M7.1 26 May 2003 Miyagi earthquake
(left) Seismicity map of NE Japan subduction zone. Are represented the seismicity (depth-coloured), NIED stations (triangles), slab depth contours (black lines), epicenters and M9 2011 Tohoku earthquake slip contour.
(bottom right) Cross-section of the seismicity (38°N-39°N).
(top right) Graph modified after Okada & al (2004) : early aftershocks of the sequence, aligned along an intraslab sub-vertical plane, and focal mechanism of the mainshock (side view).

Charline COUDUN

The Cretaceous continental margins of the Demerara plateau

Year 2

Supervisors: Christophe Basile

Tectonique, Reliefs, Bassins / Tectonics, Reliefs, Basins

The Demerara plateau is a submarine bathymetric high, 230 km long and 170 km wide, located north of French Guiana and Suriname. It is bordered by oceanic domains of different ages: the Jurassic Central Atlantic domain and the Cretaceous Equatorial Atlantic domain. This two-stage evolution has segmented the Demerara Plateau into three margins: westward a Jurassic divergent margin, an eastern Cretaceous divergent margin and a northern Cretaceous transform margin. As a planar submarine relief extending the continental shelf, and bounded by a transform margin, the Demerara plateau is a typical Transform Marginal Plateau.

Since 2003, four oceanic cruises collected several types of data on the Demerara Plateau: mainly seismic profiles (vertical and wide angle), and dredges. Seismic profiles reveal the existence of a regional Albian age unconformity. The dredges recovered pre-Albian magmatic rocks and showed that the Jurassic margin was a magmatic divergent margin. It was supposed that its formation was related to hot spot activity, but the lack of samples did not allow to confirm this hypothesis. In early 2023, a new oceanic cruise called DIADEM took place. The aim of this cruise was to sample and observe the pre-albian units in order to verify the hot spot hypothesis and to bring new informations that would allow to reconstitute the unexplained vertical movements of the Demerara plateau.

In order to do this, we used two complementary methods, dredges and manned deep underwater dives (Nautile) in four sites: the 60° Ridge, the Bastille Plateau and the Juillet Block, the Buteur Ridge and the Waste Canyon. At these sites the topography allows the Jurassic-Cretaceous rocks to the outcrop. Nearly 400 magmatic rocks and 100 sedimentary rocks were sampled. During my thesis, I will focus on the Cretaceous margins of the Demerara plateau by describing and analyzing the sedimentary samples at a macroscopic and microscopic scale, with X-Ray and with a Scanning Electron Microscope. I will then date sedimentary and magmatic samples (apatite and zircon fission tracks, biostratigraphy, U/Pb zircon and apatite, U/Pb calcite, Ar/Ar, U/Th/He Goethite). In addition, the 38 hours video recording of each deep dive will be viewed in order to carry out the structural study and the log of the investigated outcrop with a new approach of photogrammetry.

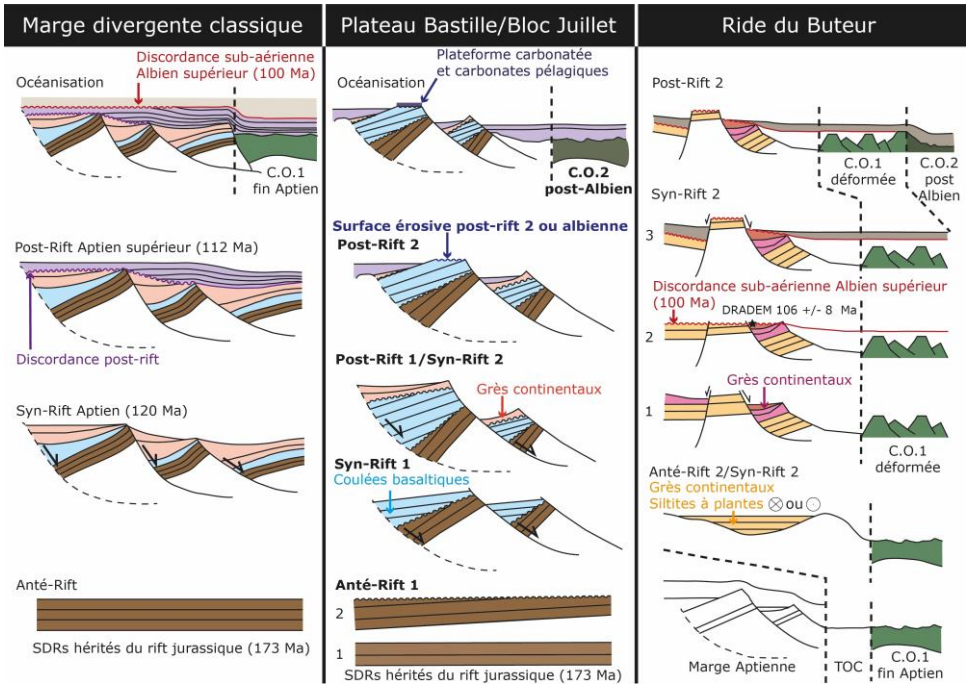

A first hypothesis about the vertical movements chronology of the Bastille Plateau/Juillet Block and the Buteur Ridge during the Cretaceous rift.

Léa COURTIAL-MANENT

Ecroulements rocheux dans les parois de haute et moyenne montagne : quelles évolutions ? Quelle temporalité ? Quels risques ?

Year 3

Supervisors: Jean-Louis Mugnier

Tectonique, Reliefs, Bassins / Tectonics, Reliefs, Basins

Rockwall erosion due to rockfalls is one of the most efficient erosion processes at high elevations. It is, therefore, important to quantify this erosion to understand the long-term evolution of mountain topography. This is especially crucial since rockfall frequency is increasing in high-Alpine areas, such as in the Mont-Blanc massif (MBM), due to regional scale permafrost degradation (which occurs through thickening of the active layer, the subsurface layer freezing and thawing throughout the year), a consequence of climate warming and the multiplication of heat waves.

To better understand rockfalls as a permafrost-related process, we quantify the erosion rates at different time scales by i) a short-term (~ ten-year scale) quantification of the dynamics of the rock walls based on the diachronic comparison of topographic measurements carried out by terrestrial laser scanning (LiDAR) and ii) a long-term quantification (10^2-10^4 year scale) based on the ^{10}Be concentration of sediment sampled downglacier on medial moraines. Our analysis considered that once the rockfalls have occurred, clasts are transported within the ice stream and amalgamated by ice melt in the ablation zone, forming medial moraines. The ^{10}Be concentration is linked to the rockwall erosion rate and the time needed to transport from the glacier equilibrium line to the sampling location.

Scanned rockwalls and rockwall sources vary in elevation, aspect, slope, and area, allowing us to assess whether these factors influence the measured ^{10}Be concentration and erosion rates. We studied rockwalls located on the French side between 2800 m and 4200 m a.s.l. and between 2500 m and 4600 m a.s.l. on the Italian side. We collected 8 (Géant basin and Vallée Blanche, France) and 10 supraglacial samples (Brouillard and Frêney glaciers, Italy), respectively.

Our results reveal substantial variations in 10Be concentrations. On the French side of the MBM, ^{10}Be concentrations vary from 1.2 ± 0.2 to 6.7 ± 0.4 x 104 atoms g^{-1}, while they range from 3.0 ± 0.2 to 92.0 ± 3.2 x 104 atoms g^{-1} on the Italian side. These results suggest that the long-term erosion rates vary between 0.8-1.7 and 0.1-0.3 mm.yr^{-1}, respectively. The short-term erosion rates for the French side are 4.3 mm.yr^{-1} for 2005-2014 and 39.3 for the period of 2015-2022. On the Italian side, they are 0.8 mm.yr^{-1} for 2005-2011 and 6.1 for 2011-2017.

Our results show spatial differences in erosion rates on both sides of the MBM. Short-term erosion rate is lower on the Italian side, and ^{10}Be concentrations are higher, meaning that the rock walls are more stable in this area. However, on both sides of the MBM, erosion rates have increased significantly recently, with a further acceleration during the last decade. This suggests that high-altitude rockwalls, previously unaffected by global warming, are progressively entering a state of permafrost degradation.

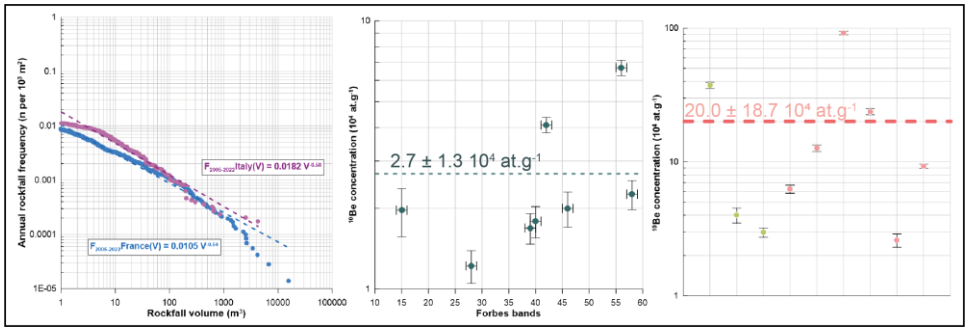

Magnitude-frequency distribution for all rockfalls on the French and Italian side of the Mont-Blanc massif. In total, 671 rockfalls have been documented. ^{10}Be concentration of the supraglacial sediments. Dark-green dashed line for the average concentration of medium-altitude rock walls. Pink dashed line for the average concentration of high-altitude rock walls.

Juliette CRESSEAUX

Large-scale interactions during sequence of large subduction earthquakes in South-America

Year 4

Supervisors: **Anne Socquet, Mathilde Radiguet, Marie-Pierre Doin**

Cycle sismiques et déformations transitoires / Seismic cycles and transient deformations

Major earthquakes, thousands of kilometers away, can happen close in time. For example, it is the case of the Maule 2010, Iquique 2014 and Illapel 2015 earthquakes in South America. After an earthquake, post-seismic deformation signals are observed in GNSS data: a rotation pattern from adjacent segments towards the broken one (Klein 2016, Yuzariyadi 2021); velocity changes at the location of the neighboring asperity. Corbi et al. explain the increase or the decrease of velocity after an earthquake by the state of maturity of the fault based on laboratory experiments. These observations request a larger scale process. The viscous rheology, that is usually neglected in earthquakes studies, has the potentiality to affect this order of magnitude. Can and how viscoelastic relaxation, medium parameters, fault maturity affect the post-seismic deformation? Does it correspond to what is observed in the data?

A 3D Finite Element Model answers these questions. By imposing an ad-hoc slip on the subduction interface, we can visualize the surface deformation pattern. The variation of the viscosity of a low-viscosity mantle wedge showed that lower viscosity leads to more extensive deformations. Viscoelasticity can drive surface displacements at thousands of kilometers from the fault. In the context of the South-American subduction zone, it could link the 2010 M_w 8.8 Maule and the 2015, M_w 8.3 Illapel earthquakes. However, the mechanisms responsible for the interactions between distant lateral asperities need to be further investigated. Following Corbi et al., we explore the effect of a megathrust seismic rupture on a distant lateral asperity in an elastic framework. We add viscoelasticity in our model in order to explore the effect of post-seismic relaxation processes leading to possible distant interaction in a more realistic framework.

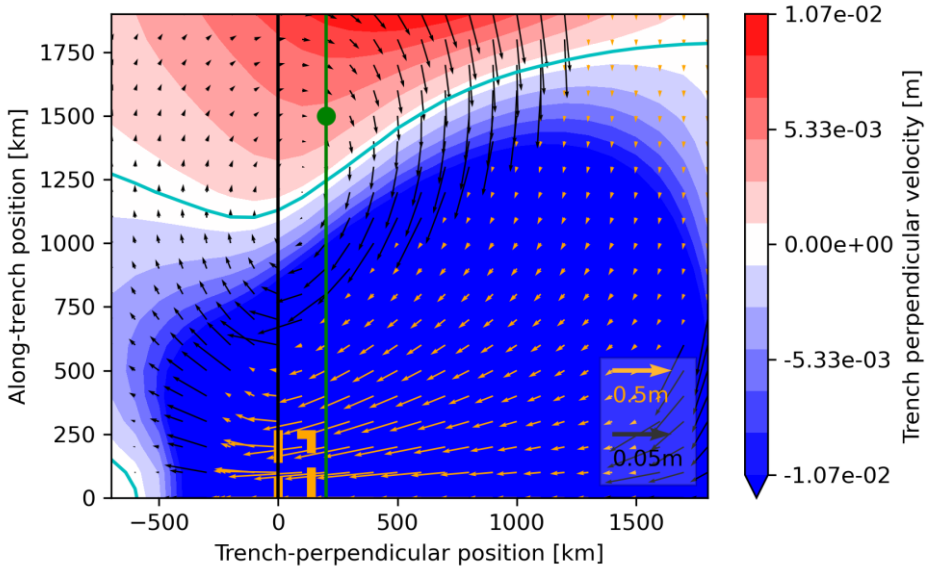

Surface velocity change after a major earthquake for a model with a visco-elastic mantle. We can observe that if the surface displacement is towards the ocean near the rupture patch (orange rectangle), the adjacent location (further than 1000km) shows a landward motion. It may be due to the visco-elastic relaxation in the mantle.

Djamilatou DABRE

Impact of gold mining on the contamination of aquatic ecosystems and populations in Burkina Faso and Guinea

Year 2

Supervisors: Stéphane Guédron, Jacques Gardon (Hydrosciences Montpellier-Epidemiology)

Géochimie / Geochemistry

Artisanal small scale gold mining (ASGM uses various processes to extract gold, including mercury (Hg) amalgamation and cyanidation (CN), which easily contribute to the degradation of the aquatic and terrestrial environment. In West Africa, this lucrative activity, increasingly practiced by underprivileged populations, has negative externalities that are currently poorly assessed. Our study concerns Burkina Faso and Guinea, where the impact of these activities on the contamination of these ecosystems, the trophic chain, and humans is poorly assessed. The aim of this study is to understand the impact of ASGM activities on the contamination of surface waters and soils, food chains and populations in gold mining camps in Burkina Faso and Guinea, where gold is the main export product. The first year of my PhD was focussed on the assessment of levels of contaminants in and around of mining sites, with a particular focus on mercury (Hg) and its speciation, together with lead (Pb) and arsenic (As). In the second year of my PhD, I focused a part of my research on the Niger River and its tributaries (Guinea), and sampled sediments and the trophic chain (fish).

Results from the first year showed that mercury concentration ([THg]) in soils from ASGM sites ranged from 200 $ng \cdot g^{-1}$ to 5$\mu g.g^{-1}$ in Guinea, compared with 500 ng.g-1 to 2 $\mu g.g^{-1}$ in Burkina Faso. Hg speciation in ASGM soil showed that at least 19% of THg was found as Hg(0). [THg] measurements in water show that most of the Hg is absorbed onto suspended particles, with dissolved Hg accounting for <6% in Burkina Faso and Guinea. Arsenic concentrations in water are generally low in both countries (< WHO standard of 10 $\mu g \cdot L^{-1}$), with the exception of one site in Burkina Faso where [As] in a water well was >10 times the WHO threshold of 10 $\mu g \cdot L^{-1}$ recommended for drinking water. [Pb] is also below the Who recommendation value of 10 $\mu g \cdot L^{-1}$ in water.

These first results show that soils and unfiltered well water used by the local population in ASGM areas are highly contaminated with Hg. This shows that Hg-enriched particles are potential sources of contamination for downstream aquatic ecosystems. Human exposure is also expected through inhalation of dust and elemental Hg and, to a lesser extent, through consumption of well water.

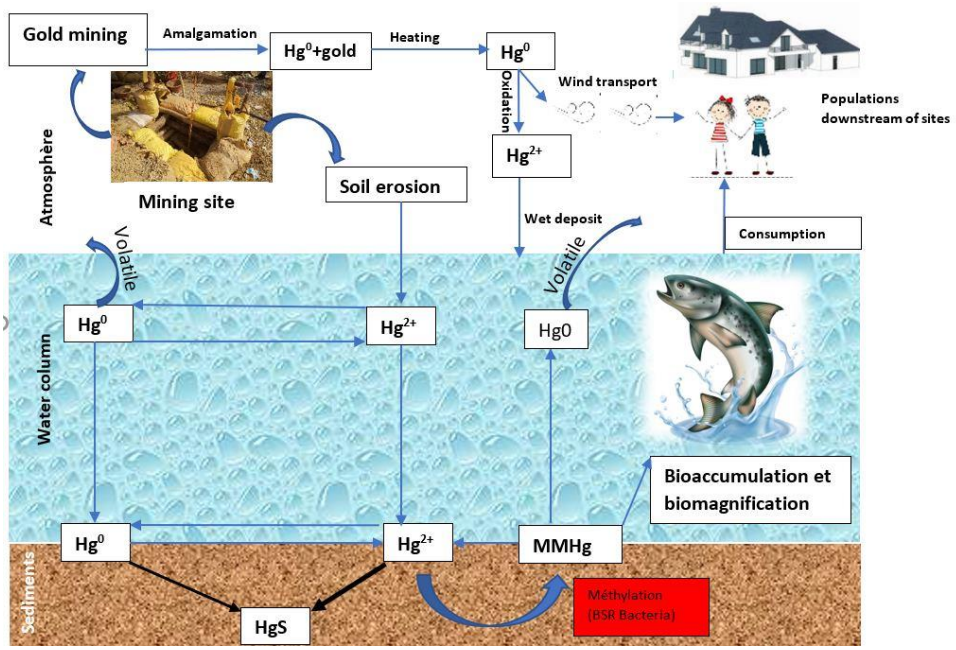

Gold mining impact (Especially mercury) on aquatic ecosystems and populations

Mathilde DEHUE

Reducing the carbon footprint of cement through the CO_2 mineralization of recycled concrete

Year 2

Supervisors: Alejandro Fernandez-Martinez

Géochimie / Geochemistry

The use of concrete has been growing continuously in the 20th and 21st century, leading to an increase of its environmental footprint. The current global warming crisis and the significant consumption of natural reserves have pushed the building industry to search for new and sustainable solutions. New breakthrough technologies for lowering the CO_2 footprint include a circular utilization of demolished concrete. Recent developments have shown that most of the CO_2 originally released by limestone calcination during clinker production can be sequestered by carbonation of the recycled cement paste. This technology, currently under development by the cement industry, consists in the carbonation of a part of recycled concrete in a humid/aqueous medium, leading to the formation of carbonate minerals and therefore to the permanent storage of the CO_2 in solid form.

A successful deployment of this technology at large scale needs a good understanding and, eventually, a control of the $CaCO_3$ polymorphism. The project of this thesis is to characterize the carbonation reactions using both laboratory and synchrotron X-ray scattering experiments. The effect that different ions from cement hydrates –e.g., silicate, aluminate, magnesium- and different organics used as modifiers of the hydration kinetics –e.g., gluconate, have on the calcium carbonate crystallization kinetics will be investigated in the framework of classic and non-classical theories of mineral formation.

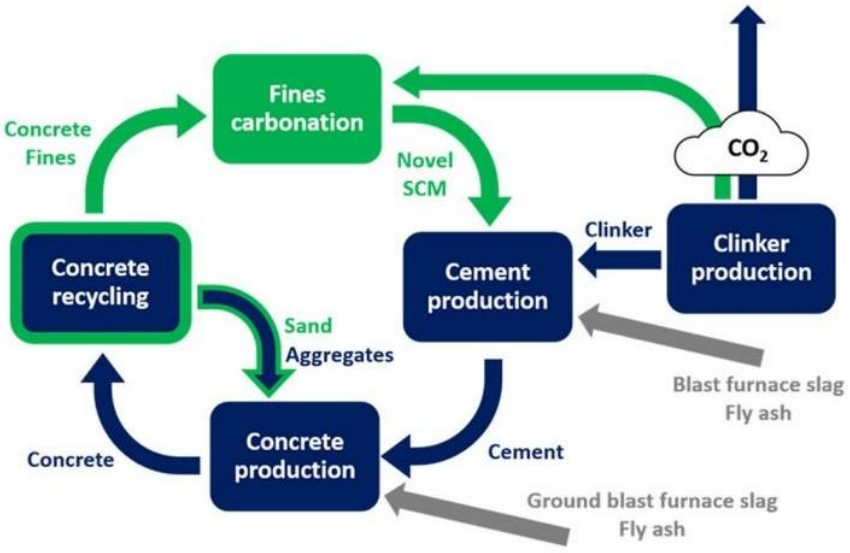

Scheme of the production of the cement characterized by substantially lower CO_2 emissions. The green color highlights improvements of the process compared to the current situation shown in blue. The gray color highlights the traditional supplementary cementitious materials input with uncertain future availability.

Laetitia DRUMARE

Modélisation de la banquise par approche de champ de phase

Year 1

Supervisors: **Véronique Dansereau, Luiza Angheluta Bauer (Université d'Oslo)**

Mécanique des failles/ Fault mechanics

La banquise, comme plusieurs autres objets géophysiques (par exemple, les roches de la croûte terrestre, les sols, la neige), est un matériau très complexe qui présente divers comportements mécaniques, en fonction de son état local et des échelles de temps et d'espace auxquelles elle est observée. En effet, lorsqu'elle est dense (en hiver et dans le centre de l'Arctique), elle se comporte comme un solide continu et endommageable. Lorsqu'elle est localement très fragmentée (comme dans la Zone Marginale de Glace), elle se comporte plutôt comme un milieu granulaire frictionnel. Entre ces deux régimes, solide et granulaire, l'intensité des échanges d'énergie, de gaz et de quantité de mouvement entre la glace, l'atmosphère et l'océan est très différente, d'où l'importance de capturer leur essence dans des modèles continus tels que ceux utilisés pour les prévisions climatiques. Il est tout aussi important de pouvoir simuler la transition entre ces régimes, ou granularisation, car elle contrôle fortement l'évolution locale/saisonnière et globale/long terme de la banquise polaire. Ce projet de doctorat vise à développer un modèle continu capable de capturer cette transition de granularisation, en représentant la propagation d'une phase fragmentée (c'est -à-dire endommagée) dans un solide continu par approche champ de phase. Du point de vue de l'approche champ de phase, le projet s'attaquera à plusieurs défis fondamentaux qui découlent du contexte de la banquise et d'objets géophysiques au comportement similaire, par exemple : le couplage du champ de phase à une équation constitutive viscoélastique de type Maxwell, qui permet des déformations irréversibles dans la phase endommagée, ainsi que la formulation et le traitement numérique d'un critère d'énergie critique pour la rupture par cisaillement compressif. Le projet, axé sur le développement d'un modèle, ouvre la voie à plusieurs applications géophysiques. Par exemple, le modèle développé pourrait être comparé aux modèles existants de banquise qui sont basés sur une approche classique de la mécanique de l'endommagement, afin de contraster leur comportement mécanique simulé et de leur efficacité numérique. Il pourrait également être utilisé pour étudier l'évolution de la résistance mécanique macroscopique de la glace de mer ou d'autres objets géophysiques à travers la transition de granularisation et ainsi informer les équations constitutives à grande échelle et les paramétrisations de cette transition.

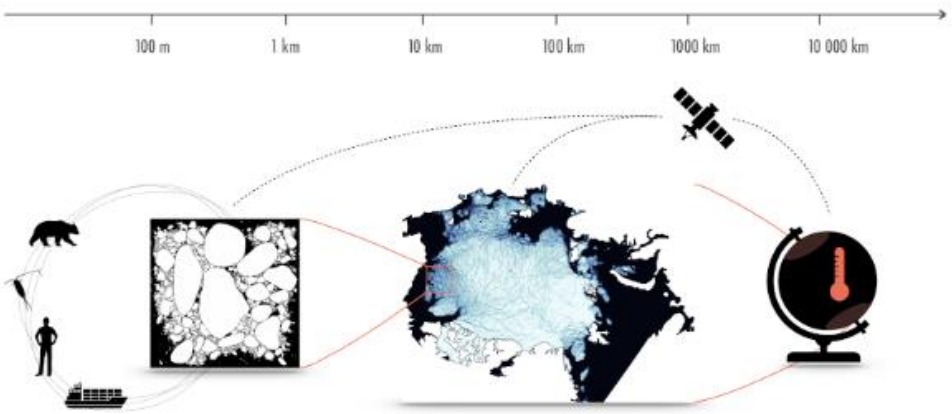

The Scale-Aware Sea Ice Project

https://sasip-climate.github.io/

Part of the SASIP project

Hugo DUTOIT

Exploration and modelling of natural hydrogen and helium sources and migration pathways

Year 3

Supervisors: Frédéric Donzé, Laurent Truche

Minéralogie et Environnements / Mineralogy and Environments

Hydrogen (H_2) and helium are two actively sought resources that have gained in interest in recent decades. The former could play a helpful role in the transition to low-carbon energies while the latter is essential to many sectors for its distinctive physicochemical properties. Most if not all of the current He reserves originate from fortuitous discoveries mainly made during oil and gas exploration in intra-cratonic sedimentary basins. However, global demand for helium has been experiencing a consistent upward trajectory, while production is struggling to keep pace. In the case of H_2, although its exploration is booming, pathfinders for efficient exploration and reservoir characterization are still lacking. Hence there is on one hand an emergent need to diversify helium sourcing by investigating alternative geological environments in order to mitigate the industry's reliance on hydrocarbon extraction and on the other hand a need of fundamental knowledge about hydrogen natural system.

Helium was investigated along a major fault rooted in the Corso-Sardinian batholith (France) in two thermal springs: Caldanelle and Guagno-Les-Bains. Both show significant outgassing activities of crustal He with concentration up to 1.45 vol% and flow rate of 110 m^3 STP ^4He/year. Besides He, the gas phase is dominated by N_2 (≈ 98 vol%) and minor CH_4. Based on a survey employing multidisciplinary methodologies, it is revealed that i) Variscan rocks represent efficient ^4He source rocks, ii) the main source of He comes from the underlying Eo-Variscan basement, iii) A deeply rooted fault and dense fractures networks drain the He, iv) the helium loss is limited, v) faults and fractures may act as partial traps, and finally vi) the presence of an efficient trap could promote a He-rich reservoir with high flux but low reserves. In that sense, young post-orogenic granites represent promising helium plays. The geological context in which Caldanelle and Guagno-Les-Bains are embedded is ubiquitous in European Variscan batholiths. This case study is therefore intended to serve as a guide for helium exploration and to provide insights into helium behavior within Variscan geological context.

The ICDP project “Drilling the Ivrea Verbano zonE (DIVE)” explores the Ivrea Verbano Zone in the Southern Alps of Italy, the probably most complete pre-Permian lower crust–upper mantle transition worldwide, by deep scientific drilling. Two boreholes have recently been completed, reaching a final depth of 578.5 m and 909.8 m, with excellent drill core recovery (100 %). The drilling was accompanied by various scientific experiments, including the continuous extraction, measurement and sampling of gases from the circulating drilling fluid (OLGA). The gas phase was continuously measured with two quadrupole gas mass spectrometers (miniRUEDI and Pfeiffer Omnistar) for Ar, H_2, He, N_2, O_2, CH_4 and CO_2, a gas chromatograph for hydrocarbons (CH_4, C_2H_6, C_3H_8 and i/n C_4H_{10}), and a radon detector for ^{222}Rn. Initial results show, that H_2 (up to 1.2 vol%), He and CH_4 were the most gases extracted from the drilling mud and a correlation between formation gases in drilling mud and the drilled fault and fracture zones. Continuous real time detection of hydrogen helium and radon while drilling has proven to be a good indicators of deep fracture fluid migrations and appear to be a strategic tool for H_2 and He exploration.

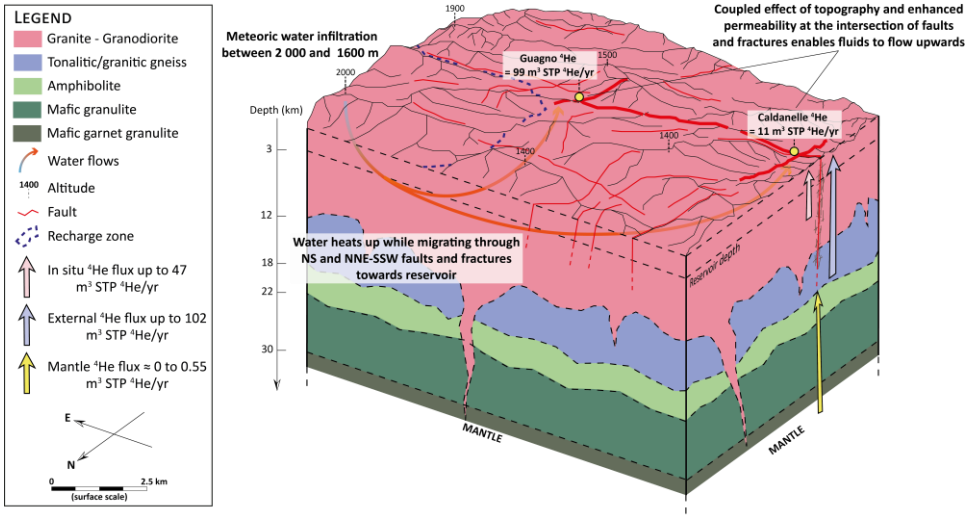

Schematic 3D block summarizing the thermal system of Caldanelle and Guagno-Les-Bains thermal springs and showing the source, migration and escape of helium. Layer geometry is not representative.

Paula DÖRFLER

Natural Layered Double Hydroxides in Serpentinites

Year 1

Supervisors: Benjamin Malvoisin, Bruno Lanson, Fabrice Brunet, Alejandro Fernandez-Martinez

Minéralogie et Environnements / Mineralogy and Environments

Serpentinization describes the hydration and oxidation of mantle minerals such as olivine and pyroxene to form serpentine minerals, magnetite, brucite and hydrogen. Brucite often contains a considerable amount of Fe^{2+}. The formation of hydrogen is buffered by the equilibrium between Fe-component in this ferroan brucite and magnetite. While at T > 200°C, magnetite formation explains at first order the measured concentrations of hydrogen, the generation of hydrogen at lower temperatures is not well understood. The low temperature phase assemblage consists mostly of Fe-brucite and layered double hydroxides such as pyroaurite [1] or iowaite [2, 3].

To gain a better understanding of the reaction pathways at lower temperatures, experiments exposing brucite suspensions to water at 105 and 130 °C were performed by [4]. Their study showed that brucite oxidation may be charge compensated by incorporation of CO_3^{2-}, leading to pyroaurite formation. At the same time, ferrian (Fe^{3+}) brucite, described for the first time during these pioneering experiments, was another reaction product forming after 3-7 days. In ferrian brucite, deprotonation accounts for charge balance in the structure.

We propose an experimental approach to investigate further how the parameters (CO_2-availability, oxygen fugacity and T) change the reaction pathway of brucite. First results from ambient temperature experiments with brucite suspensions exposed to synthetic air showed that pyroaurite formation correlates with the amount of CO_2 dissolved in the water and that brucite oxidation to form ferric brucite under these conditions is limited. This finding implies that LDH formation is favored and that it is likely not proceeded by deprotonation and thus hydrogen production to form ferric brucite under ambient conditions.

Our experiments will provide better thermodynamic and kinetic constraints as well as insights on the involved reaction mechanisms to understand and model low temperature serpentinization.

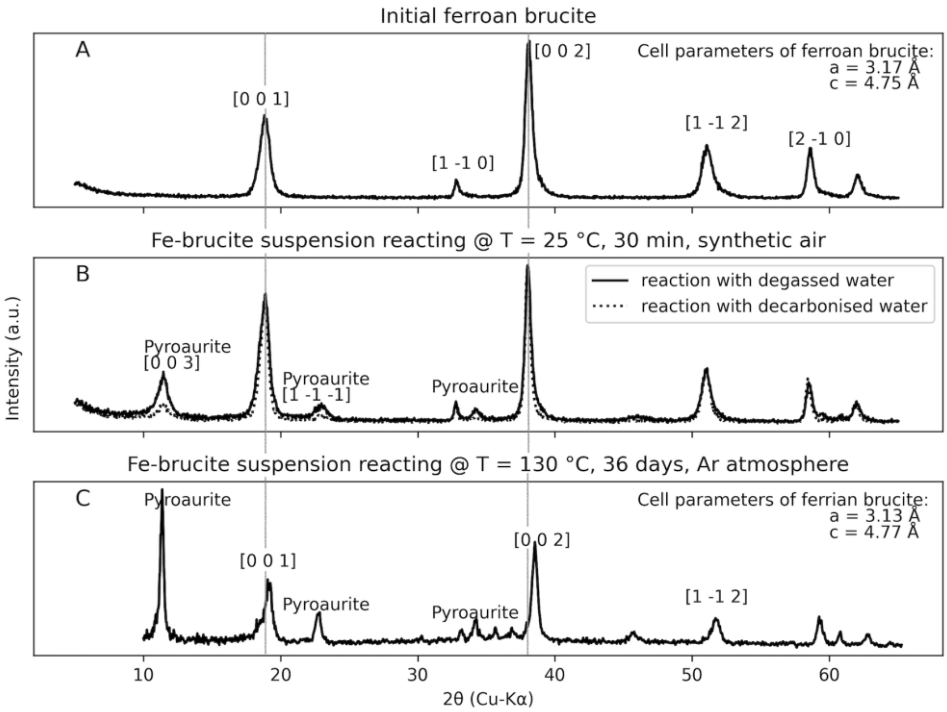

Figure 1. XRD results of A: $(Fe_{0.2}, Mg0_{.8})(OH)_2$, B : after reaction with degassed water, app. 20 wt. % of pyroaurite formed vs. 10 wt. % of pyroaurite after reaction with decarbonised water, C: ferrian brucite (note shift in [001] and [002]) and pyroaurite formed, data from [3].

Zaccaria EL YOUSFI

Insights on along-dip fault transition zone rheology through LFE clustering

Year 2

Supervisors: **Mathilde Radiguet**

Mécanique des failles/ Fault mechanics

In all active fault zones, the distribution and variety of seismic and aseismic events is driven by physical parameters. Brittle to Ductile behaviors can observed, with a transition done in a section of the fault called 'transient zone', which houses brittle-ductile conditions for geologic materials, and a wide variety of seismic and aseismic slip events (Tremors, Low Frequency Earthquakes (LFEs) and Slow Slip Events (SSEs)).

Transient zones are bounded on the updip side by a seismogenic zone, housing earthquakes and large SSEs, and on the downdip side by a stable creep zone. In the transient zone small SSEs, micro-seismicity and creep are observed (Luo et al., 2021).

I focus on the micro-seismic activity in transient zones, in particular on the evolution of LFE activity in the along-dip direction of several fault zones. I gathered LFE catalogs for 3 subduction zones: Nankai (Japan), Cascadia, Guerrero (Mexico), and for the Parkfield strike slip fault. And I analyzed the LFE activity through the computation of auto-correlation spectra (Frank et al., 2016, Prieto, 2022), allowing to compute the recurrence time of LFE episodes in the along-dip direction of all these fault zones.

The results (Fig. 1) show that the recurrence times are similar for all the studied transient zones, and decrease systematically with depth, even though the depth range varies from one fault zone to the other (see Fig. 1). Other rheological parameters vary, such as the pressure-temperature conditions, which gives us perspective on other rheological parameters such as the pore pressure shear strength and the healing time of fault asperities.

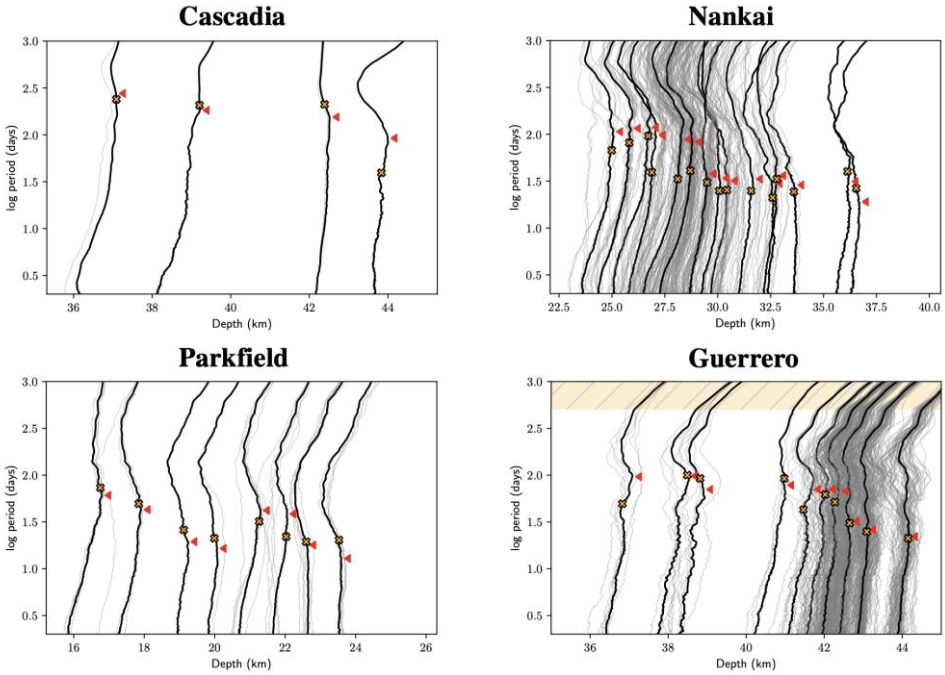

Spectra of auto-correlation of LFE counts in 4 fault zones. The black lines are the smoothed spectra for bins of LFE families along-dip. The grey lines are the spectra for single families of LFE, and the red triangles point recurrence time (highest PSD).

Mateo ESTEBAN

Origin of Archean komatiites and their mantle sources: focus on the Neoarchean era

Year 1

Supervisors: **Alexandre Sobolev**

Minéralogie et Environnements / Mineralogy and Environments

Komatiites are high-MgO (>18 wt% MgO) ultramafic lavas which erupted predominantly during the Archean [1], providing some of the few clues to understanding the early earth's mantle. However, the scarcity of preserved materials and their degree of alteration limits the study of these ancient rocks. In that respect, melt inclusions hosted and protected in magnesian olivine are highly valuable to characterize komatiites' parental melts and probe the Archean mantle composition. Furthermore, the study of melt inclusion has proven fruitful in revealing chemical and isotopic heterogeneities so far undescribed [e.g., 2].

This study will focus on Neoarchean komatiite formations (ca. 2.7 Ga) from the Zimbabwean craton and Canadian and Australian shields (fig. 1). More than 200 olivine-hosted melt inclusions from komatiite flows of the reliance formation in the Belingwe Greenstone Belt (Zimbabwe) were hand-picked and exposed to be analysed. State-of-the-art in-situ analyses for major, minor & trace elements, and H_2O concentration will be conducted in the near future. Additionally, the first Rb-Sr isotope data from melt inclusions of this formation will be retrieved. The results will then be compared with other Archean and Proterozoic komatiites and Picrite. The same protocols will eventually be performed for Canadian and Australian samples.

We expect a depleted mantle source component for the Belingwe komatiite, with Hadean Rb-Sr model age which will provide some insight into the processes of this poorly documented era, as suggested for the 3.2 Barberton formation in [3].

1. Arndt, N., et al., Komatiite, Cambridge university press, 2008.
2. Sobolev, A. V., et al., A young source for the Hawaiian plume, Nature, 2011. 476(7361).
3. Sobolev, A. V., et al., The processes in the Hadean mantle detected by the in-situ study of melt inclusions in komatiite olivine phenocryst, AGU Fall meeting, Chicago, 12 Dec. 2022, DI15A-04.
4. Hasterok, D., et al., New map of geological provinces and tectonic plates, Earth Sci., 2022.

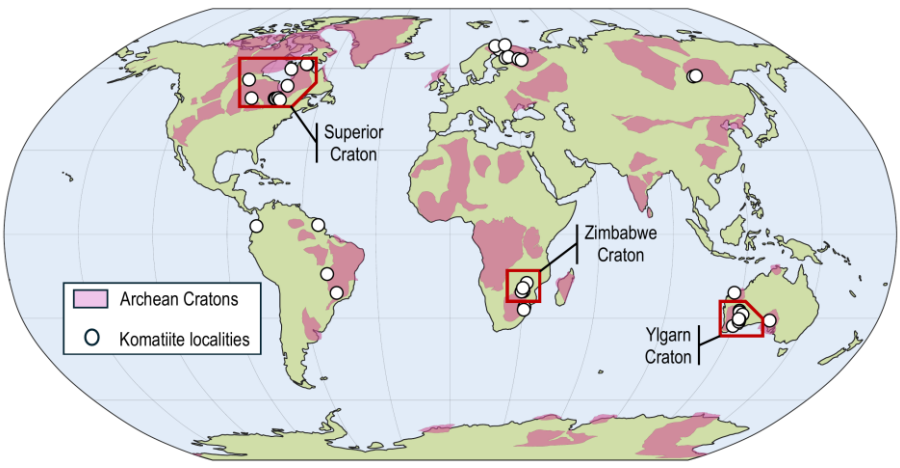

World map of global komatiite localities and Archean cratons, compiled respectively in [1] and [4]. Regions of interest are highlighted by the red polygons.

Fandy Adji FACHTONY

4D FWI with reflection oriented workflow for CO_2 monitoring

Year 3

Supervisors: **Romain Brossier, Ludovic Métivier**

Ondes & structures / Waves & structures

Carbon capture and storage (CCS) is becoming increasingly significant in global climate change mitigation according to IPCC reports, with the Sleipner CCS facility serving as a pioneer in offshore carbon storage operations since 1996, injecting 1 million tons of CO_2 annually into the Utsira formation. Monitoring the CO_2 at the Sleipner facility has garnered great interest among the geophysical community over the years, with many utilizing full waveform inversion (FWI) as a mean to estimate high-resolution CO_2 properties. However, a common challenge arises from offset limitations within available streamer data, constraining FWI to behave in migration mode at the deeper part, due to the lack of penetration of diving waves. Moreover, these studies have predominantly focused on velocity parameter estimation, neglecting other parameters like impedance, which could complement the characterization of the CO_2 plume.

In our study, we adopt a reflection-oriented workflow employing Joint Full Waveform Inversion (JFWI) to address the offset limitation issue. By utilizing both diving and reflected waves, JFWI compensates for offset limitations and enhances the reconstruction of low wavenumber components along reflection wavepaths. Additionally, JFWI works with parameterization separating P-impedance and P-wave velocity, treating the monitoring problem in a multi-parameter sense, obtaining both structural and quantitative properties based on the impedance and velocity models within a single workflow. We apply this reflection-oriented workflow to the Sleipner field data, illustrating that the reconstructed impedance and velocity model delineate the CO_2 anomaly effectively and are structurally consistent with the migration image. To further showcase the potential of the reflection-oriented workflow for CO_2 monitoring, we compare different time-lapse strategies, including parallel and simultaneous time lapse, in the application of Sleipner field data.

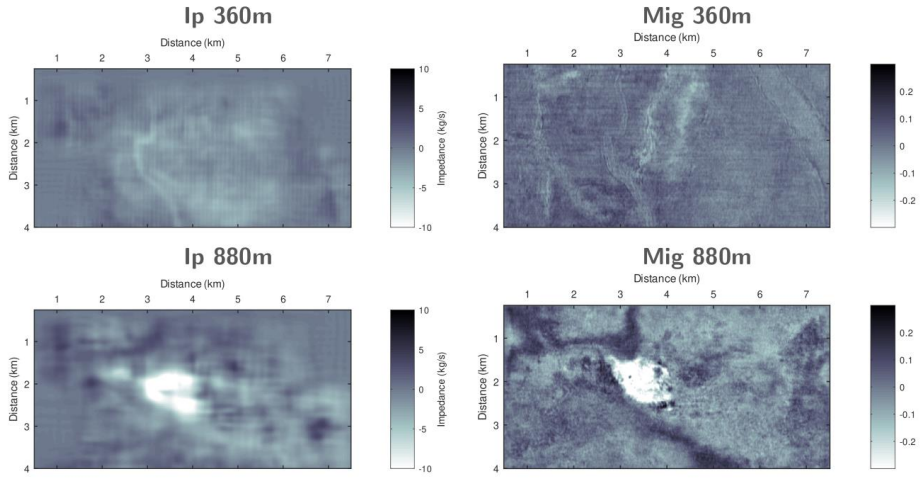

Comparison of Impedance model with the migration image. The results of impedance model able to predict the channel and CO_2 anomaly structure in high resolution, consistent with the results from migration image.

Adrien FAUSTE-GAY

Study of agrarian metabolism using a thermodynamic approach

Year 1

Supervisors: **Olivier Vidal**

Minéralogie et Environnements / Mineralogy and Environments

Every organism or complex structure functions as a non-equilibrium thermodynamic system, characterized by minimal entropy production relative to its environment. Metabolism encompasses the essential processes required to maintain such a system, including the transformation of matter into usable forms and the extraction of energy from the environment. This conceptual framework is increasingly used to retrospectively analyze the transformations of human societies through the flows of energy, matter, and information they manipulate. This study aims to further develop these tools and adapt them for use in future-oriented analyses and serious gaming applications.

Agriculture underwent significant transformations throughout the 20th century. Prior to World War II, agriculture was predominantly organic, relying mainly on human and animal labor for energy, and was characterized by integrated processes among various components of the system, particularly through mixed crop-livestock farming. At this time, agriculture was a net energy provider to society. Post-World War II, the introduction of machinery and chemical inputs revolutionized agricultural metabolism. The sector now heavily depends on massive imports of oil as well as biomass from other countries. These changes have increased productivity at the expense of the "reproductive" constituents of the system: the agro-ecosystem and the agrarian population. These developments raise questions about the viability of the agricultural system, especially in light of climate change and the scarcity of resources and fossil fuels. This study aims to explore the possibilities of constructing an agricultural system suited for the 21st century.

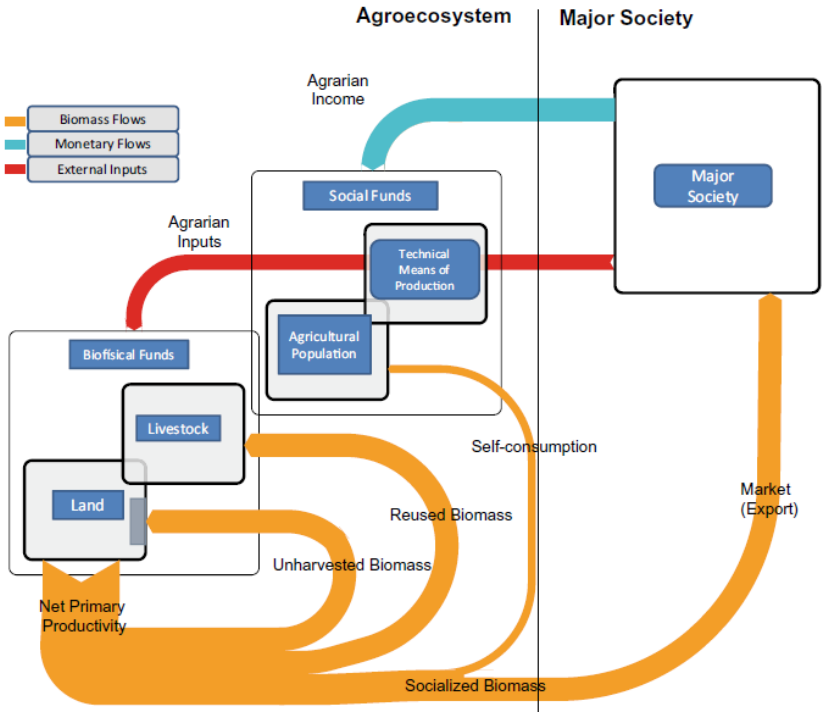

Flowchart of Agrarian Metabolism taken from The Metabolism of Spanish Agriculture (M González de Molina et al. 2020)

Maaike FONTEIJN

Combining InSAR and seismo-thermo-mechanical models to understand earthquake sequences in complex fault systems: application to the central Apennines (Italy)

Year 1

Supervisors: Erwan Pathier, Anne Socquet

Cycle sismiques et déformations transitoires / Seismic cycles and transient deformations

A recent study of Daout et al. (2023) published a multi-temporal InSAR analysis of the central Apennines. This study revealed along-strike variation in strain partitioning throughout the central Apennines. However, no large wavelength uplift of the Apennines could be detected, as is suggested by previous GNSS studies. This raises new questions about the mechanism driving deformation and seismicity in the central Apennines. Multiple mechanisms have been suggested to drive the extension in the central Apennines: 1) differences in gravitational potential energy; 2) dynamic mantle support linked to slab break-off; and 3) rotation of the Adriatic plate.

So far, no large-scale numerical model exists in the central Apennines. I use a 2D tectonic scale seismo-thermo-mechanical (STM) model with a realistic present-day setup of the central Apennines, to test the importance of the different driving mechanisms in reproducing observed seismicity and surface deformation. The model uses a visco-elasto-plastic rheology and a slip-rate dependent friction, which allows for the spontaneous development of faults and the simulation of earthquakes. The use of a realistic rheology allows to compare the model surface velocities with the InSAR velocities. Furthermore, the model will be validated against earthquake distribution and focal mechanisms, stress orientations in the crust and the Bouguer anomaly.

The initial setup integrates a geological cross-section, Moho data and tomography. As the lithospheric structure is poorly constrained, multiple setups will be tested, with different configurations of plate overlap, asthenospheric upwelling and height of slab break-off. Additionally, a model with slab window and a model with subducting slab will be run to test whether a slab window can explain the deformation in the central Apennines.

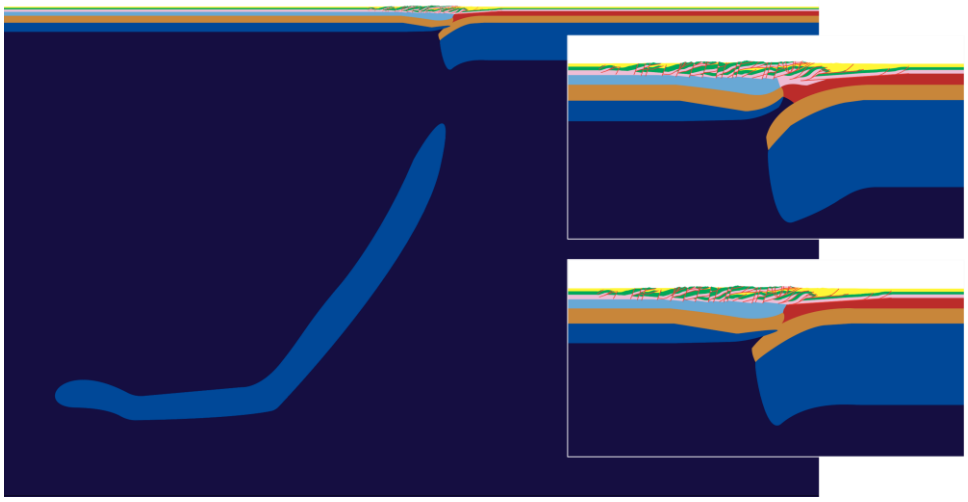

First sketches of the compositional setup for the 2D STM model, with two different interpretations for the lithospheric structure. Geology is based on Cosentino et al., 2010, the moho follows Lanari et al., 2023 and the slab is based on tomography from Rappisi et al., 2022.

Thomas FRASSON

How does mantle convection affect magnetic reversals?

Year 3

Supervisors: **Henri-Claude Nataf**

Géodynamo / Geodynamo

Paleomagnetic evidence shows that the behaviour of the geodynamo has changed during geological times. These behaviour changes are visible through variations in the strength and stability of the magnetic dipole. Variations in the heat flux at the core-mantle boundary (CMB) due to mantle convection have been suggested as one possible mechanism capable of driving such a change of behaviour.

Coupling mantle convection models and geodynamo models is crucial to understanding how the geodynamo can react to variations in mantle convection. This coupling can be studied by applying heterogeneous heat flux conditions at the top of the core in geodynamo models. Previous studies have notably shown that large-scale heat flux heterogeneities at the CMB can have a large impact on the stability of the magnetic dipole and thus the reversal frequency in viscous and moderately viscous dynamo models.

In order to better constrain the core-mantle coupling, we exploit numerical models of mantle convection and numerical geodynamo models. We use mantle convection models corrected for true polar wander (TPW) to obtain realistic CMB heat flux conditions at the top of the core in the reference frame useful for core dynamics. We then apply heterogeneous heat flux conditions at the top of the core in low viscosity geodynamo models. We show that an equatorial cooling of the core is the most efficient at destabilizing the magnetic dipole, while a polar cooling of the core tends to stabilize the dipole. The destabilizing effect of an equatorial cooling of the core is stronger for dynamo models that have larger magnetic Reynolds number and lower magnetic to kinetic energy ratios. Complex heat flux patterns tend to destabilize the magnetic dipole, except when it is dominated by polar cooling.

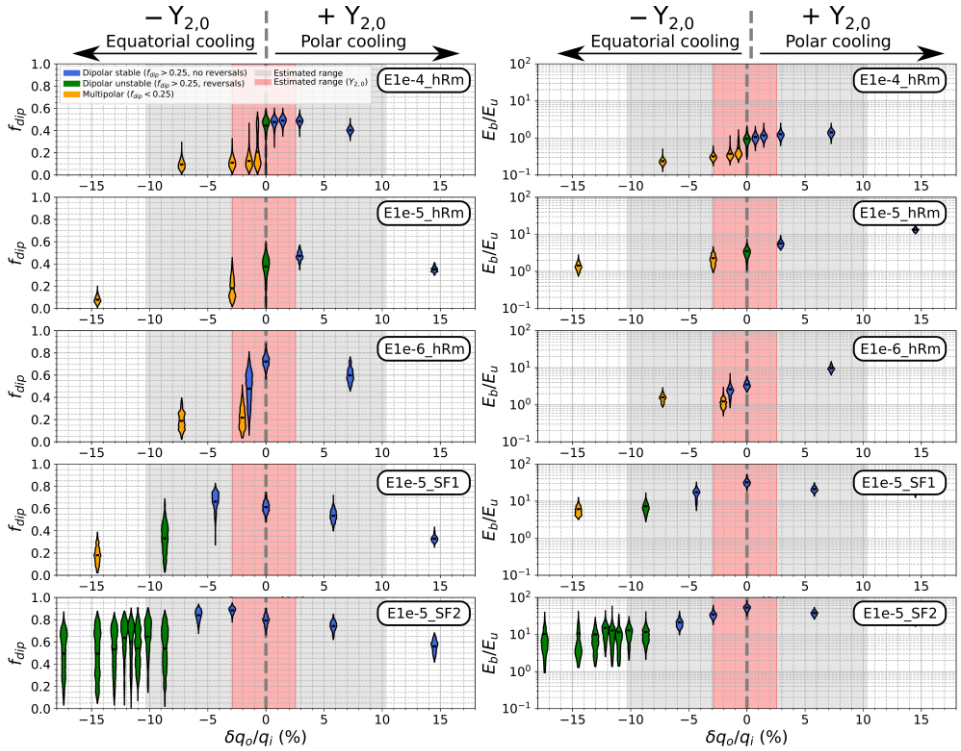

Probability distributions as violin plots of the dipolar fraction of the magnetic field at the CMB (f_{dip}) and of the ratio of magnetic to kinetic energy (E_b/E_u) in the five dynamo cases considered. The results are shown as a function of the amplitude of the degree 2 order 0 heat flux pattern imposed at the top of the core. The colour of the violin plots shows the behaviour of the dynamo. The red and grey ranges show the values of dq_o/q_i estimated for the Earth from a mantle convection model.

Bastien FÉAUD

Post-glacial geomorphic response and erosive dynamics in the Western Alps and Eastern Pyrenees

Year 1

Supervisors: Pierre Valla

Tectonique, Reliefs, Bassins / Tectonics, Reliefs, Basins

Quantifying landform dynamics remains problematic in the context of current climate change, partly because geomorphological processes operate on nested and partly independent time scales. The Alpine relief were progressively sculpted during the Quaternary by glacial-interglacial oscillations, yet the impact of glaciations on moutain environnements remains variable on a global scale. Furthermore, the current erosion of mountain ranges incorporates both the impact of recent climate change (10-100 years) via the retreat of present-day glaciers and the degradation of permafrost, and long-term (1-10ka) to deglaciation and (post-)glacial topographic conditionning. Anticipating the geomorphological response of high and mid-mountain environnements to future climate scenarios therfore remains an excerice with uncertainty. It requires a better understanding of the sensivity of moutain environnements to climate forcing on several time scales using a multi-processes approach. During this doctoral project, we will study the geomorphological record in two natural laboratories from a comparative angle: The Western Alps (AO) and the Eastern Pyrenees (PO).

The aim is to quantify postglacial erosion and sediment transfer since the Last Glacial Maximum (LGM, ca. 20ka), in response to the folowing question: What are the interactions and response times between climate change, deglaciation and erosive dynamics in Alpine environments?

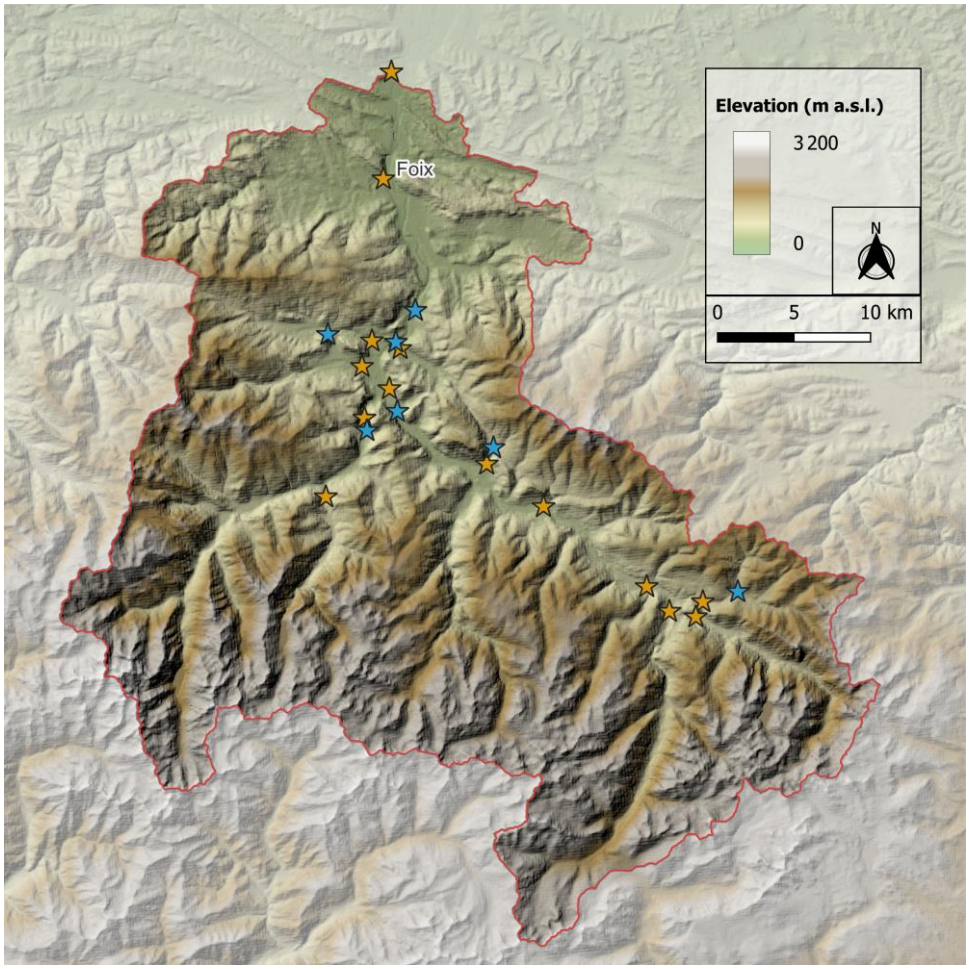

Location map of ^{10}Be samples in the Ariege catchment (red line). Samples in actual rivers are represented in orange and samples in terrace are represented in blue.

Pauline GEORGES

Regionalisation of seismic ground-motion prediction models

Year 2

Supervisors: **Emmanuel Chaljub, Sreeram Reddy Kotha**

Géophysique des Risques sismiques et gravitaires / Geophysics of seismic and gravity risks

The complex physics of earthquake rupture, wave propagation and site effects are simplified and modelled into generic Ground-Motion Models (GMMs) for use in seismic hazard and risk assessment. However, the complexity of geology and seismicity in Europe leads to a high variability in the ground motion prediction compared to observed data. Recent GMMs partially resolved this variability by regionalising their model and adapting to the specificity of each region. We focus this study on the apparent anelastic attenuation variability, to understand the underlying physics of wave propagation in the crust and better model the variability in GMMs. The GMM regionalisation model used in the recent European Seismic Hazard Maps 2020 (ESHM20) divides Europe in several polygons, each with a specific apparent anelastic coefficient adjustment. This model has certain limitations due to ambiguity in the criteria to define these polygons, which have led to non-reproducible maps and geologically diverse regions being grouped into a single large polygon, especially in France. Two hypotheses have been made to improve the current regionalisation. Firstly, France was divided following the contrast of Rayleigh wave velocity in the ambient noise tomography of France. Secondly, a null hypothesis was defined where no prior geological information is used, and Europe is simply regionalised into a regular grid. Linear mixed-effects regressions were performed on the pan-European ground-motion dataset, complemented with a French dataset, to quantify the apparent anelastic attenuation variability. The regionalisation based on Rayleigh wave velocity captures attenuation variability better than the current model for France. However, the grid-based regionalisation is more accurate in the representation of the attenuation variability which leads to keep this choice as the best regionalisation. Analyses of variance statistics confirmed this result. The size of the grid was also discussed based on these statistical tests and the number of records. The apparent anelastic attenuation variability captured on a regular grid can now be examined for a physical meaning producing this variability and improve the parametrisation of GMM.

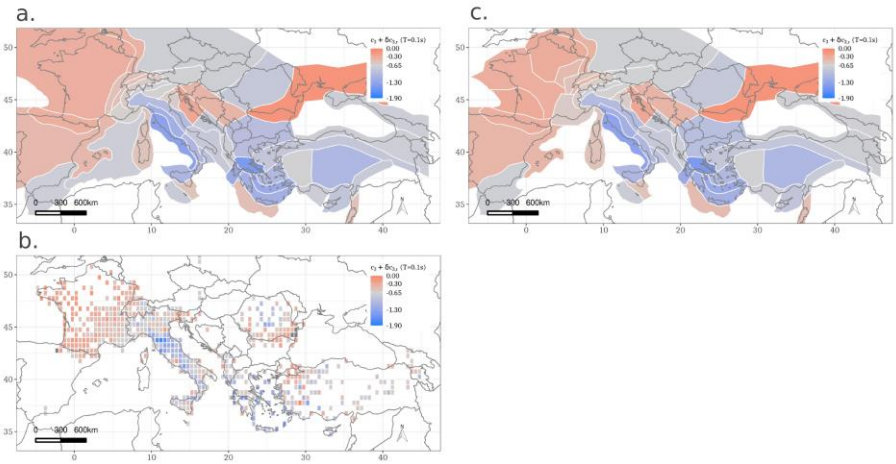

Comparison of apparent anelastic attenuation in three different regionalisations of Europe at a period of 0.1s. a) The figure shows the tectonic-based regionalisation used in ESHM20. b) The figure shows the crustal property based regionalisation for France. c) The figure shows regionalisation based on a null hypothesis with a regular 0.5*0.5° grid.

Elisabeth GLÜCK

Multiscale and multiphysics imaging of Krafla volcano, NE Iceland

Year 3

Supervisors: **Stéphane Garambois, Jean Vandemeulebrouck**

Ondes & structures / Waves & structures

Krafla, one of the five central volcanoes of the Northern Volcanic Zone in NE-Iceland, last erupted during the Krafla Fires in the 70s and 80s. During the same period, a geothermal power plant was built within Krafla caldera, first operated in 1978. Both scientific and industrial interest led to an increase of knowledge of the complex system through systematic exploration with a wide variety of geophysical methods including seismic and electromagnetics coupled with borehole information.

Among them, a local seismic network operated by Landsvirkjun and Iceland GeoSurvey, comprising 12 permanent broadband stations, has been continuously recording seismic data since 2013. We supplemented this network in June 2022 with a dense network of 98 nodes, resulting in two arrays, one large-scale, the other small-scale, operating in parallel.

Here we present multi-scale 3-D velocity models for P-, S- and surface waves, independently derived for both networks through local earthquake and ambient noise tomographies. These models offer a glimpse into the subsurface structures of the volcanic system by utilizing various types of waves that are responsive to distinct rock/fluid properties and depths. The relocated and clustered seismic activity, documented by both permanent and temporary networks, underscores active structures pinpointed through tomography. With this we hope to strengthen the understanding of the connected volcanic and geothermal systems. Indeed, both the seismicity and strong velocity anomalies are located at similar depths as the magma batch that was drilled into with the IDDP1.

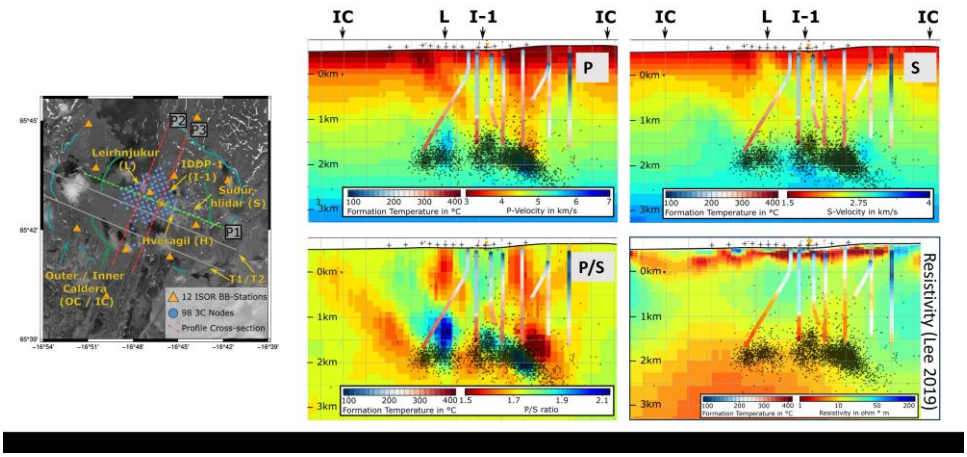

Left: Overview of the multiscale seismic experiment and the main geological and tectonic features of the Krafla caldera and its geothermal system
Right: Crossection P1 perpendicular to the rifting system - Velocity models (Vp, Vs, Vp/Vs) from local earthquake tomography, resistivity, seismicity from 2017-2022 and formation temperature at production and injection wells

Arthur GRANGE

High resolution 3D characterization of the Argentière glacier structure by waveform inversion.

Year 2

Supervisors: **Ludovic Métivier, Romain Brossier, Philippe Roux**

Ondes & structures / Waves & structures

Glaciers represent almost 70% of the Earth's drinking water. In the context of current climate change, they are undergoing major modifications, their melting is accelerating and some of them are already beginning to disappear. A better understanding of their behavior and mechanisms is therefore crucial for the years to come. A dense seismic array of 98 3-component seismic stations has been deployed on the Argentière glacier, in order to record displacements on the surface continuously over 35 days in early spring 2018. In this project, we are interested in the high-resolution 3D characterization of the Argentière structure. We are going to apply a full waveform inversion algorithm to the data recorded on the glacier surface. Before proceeding with this step, we need to characterize the sources at the origin of the recorded signals. This includes spatial localization, characterization of their mechanism and temporal signature. We start by using the Matched Field Processing method to detect events in the data and spatially localize the icequakes within the glacier. We then build a 3D model of the glacier's surface topography using digital elevation models. Finally, we invert the focal mechanism and time signature associated with each icequake using an iterative alternating optimization algorithm. The inversion is performed in the elastic approximation and the 3 data components are used. The method is based on a decomposition of the solution of the elastodynamic equations into the derivatives of the Green functions associated with the moment tensor coefficients (characterizing the source mechanism). The results are encouraging: surface waves are generally well reconstructed in the calculated seismograms. Moreover, the estimation of mechanisms yields an interesting result: most icequakes (84%) seem to behave like isotropic sources.

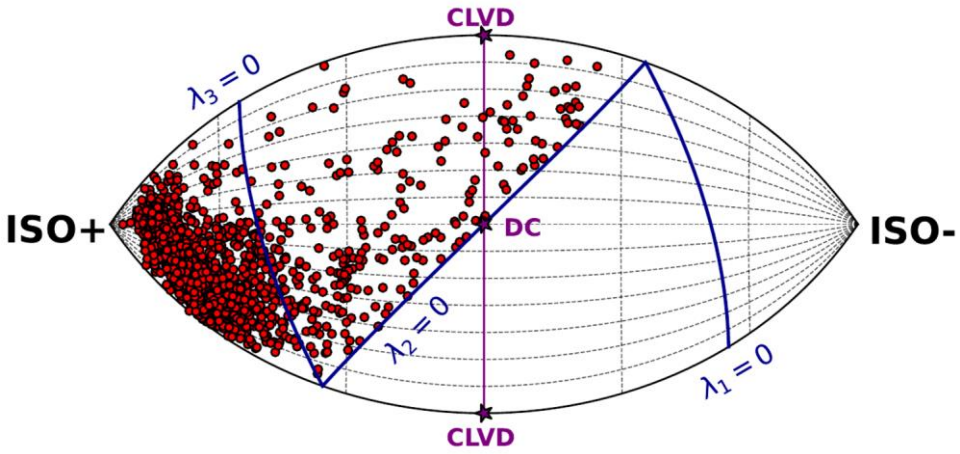

Repartition of the inverted moment tensors (red points) for the icequakes on the fundamental lune of the unit sphere in the eigenvalue space. Only the left side has been considered here, in order to study the distribution of mechanisms between isotropic and deviatoric: 84% of inverted moments are isotropic.

Julius GRIMM

Coherence-based methods for new instruments and heterogeneous datasets

Year 3

Supervisors: **Piero Poli**

Ondes & structures / Waves & structures

As large and heterogeneous datasets (such as Distributed Acoustic Sensing [DAS] and dense arrays of nodes) become more widespread, uncovering new, 'hidden' signals besides earthquakes becomes increasingly feasible. We develop and apply coherence-based methods for new instruments and heterogeneous datasets, leveraging the different sensitivities of various sensors. This approach enables us to detect tiny and exotic signals (such as tremor-like and emergent events), which are often overlooked in routine analysis. The obtained coherence features offer a global overview of the seismic wavefield, facilitating the rapid identification of anomalous signals and the classification of large seismic datasets through clustering algorithms. Throughout the project, we explore diverse datasets, including DAS deployments in urban environments, volcanic regions, and landslide areas.

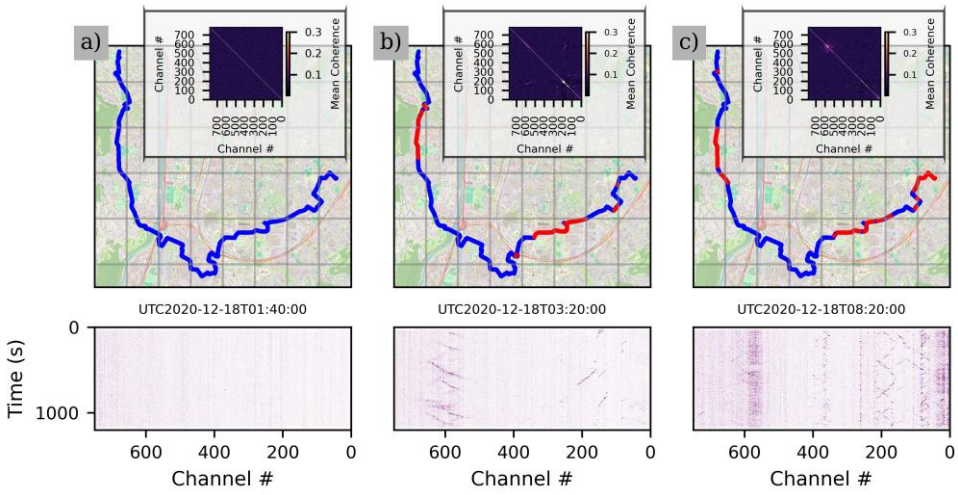

Examples of three coherence matrices from December 22, 2020. Moving from left to right are three distinct settings: a) middle of the night, b) early morning hours, and c) rush hour. The coherence matrices encode information about coherent signals in the strain-rate data, which can then be mapped to sections of the cable.

Shan GRÉMION

Improving the monitoring of Merapi volcano, Indonesia, using radar and optical imaging

Year 3

Supervisors: Virginie Pinel, François Beauducel

Géophysique des volcans & Géothermie / Geophysics of volcanoes & geothermal energy

Merapi volcano is located on the South coast of Java Island (Indonesia). It exhibits a typical subduction andesitic volcano morphology and activity: steep vegetated slopes with a volcanic activity of effusive viscous lava dome emplacement and growth alternating with explosive, sometimes very destructive events. Assessing the location, shape, thickness, and volume of viscous domes is crucial to evaluate the risks associated with sudden pyroclastic density currents (PDCs) for the numerous surrounding crops, villages, and cities.

In this PhD, we take advantage of the capabilities of remote sensing images to track for surface changes at Merapi to better understand volcanic hazard. We use both high resolution and medium resolution satellite images to follow the evolution of Merapi summit activity since 2017 up to now.

The joint use of high resolution on-demand bistatic radar acquisitions of TanDEM-X satellite, and optical acquisitions from Pléiades satellite enabled to produce 53 TandDEM-X and 11 Pléiades derived Digital Elevation Models (DEMs) over the summit area of Merapi volcano, between July 2018 and September 2023. We calculated the difference in elevation between each DEM and a reference DEM derived from Pléiades images acquired in 2013, to track the evolution of the summit. Uncertainties are quantified for each dataset by a statistical analysis of areas with no change in elevation. The DEMs derived from the TanDEM-X data show very good agreement with the DEMs calculated from Pleiades optical images and local drone measurements made by the BPPTKG in charge of monitoring the volcano. The dataset allows to quantitatively track lava volumes and effusion rates during the last two episodes of dome construction, in 2018-2019 and 2021-now respectively.

We show that the 2018-2019 dome was hosted in the crater and reached a maximum volume of ~0.64 Mm3 in 5 months, before undergoing a phase of balanced lava supply and gravitational destabilization leading to no apparent change in volumes.

We also show that the last eruption of 2021 was different from the prior in many aspects: an additional dome appeared on the South-West flank, and both the crater and flank domes show ~3 Mm3 volumes, which is ~ 3 times higher than before. Moreover, thanks to additional Sentinel-1 and Pléiades horizontal image correlation timeseries, we show that prior to the 2021 lava domes apparition, several important changes occurred in the summit area. A brutal block sliding of more than 10 m towards North-West starting June 2020, and continuing until August 2022, along with an inflation of 7 cm until the eruption on the Eastern flank. In August 2020, another block slided at the same location of the 2021 flank dome. We interpret all these flank modifications as potential precursors of the 2021 lava dome eruptions.

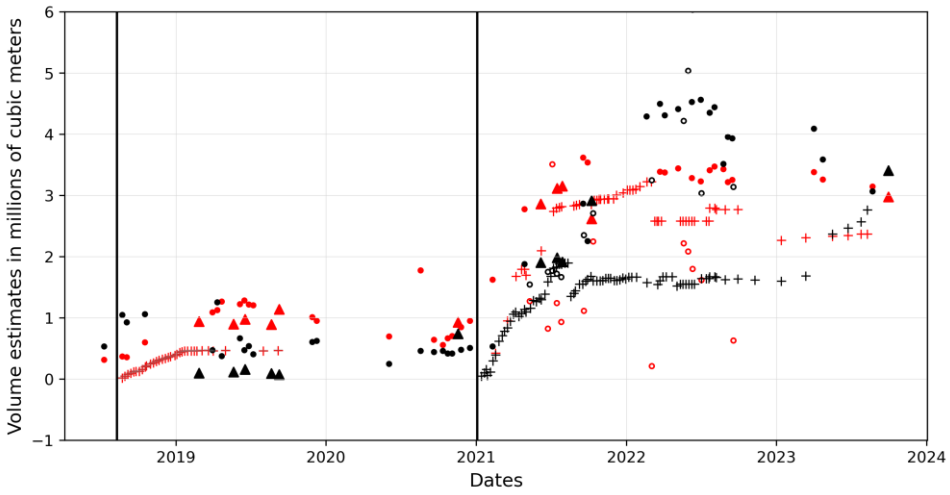

Lava dome volumes estimates between 2018 and 2023 from TanDEM-X (circles), Pléiades (triangles) and BBPTKG drone (crosses) DEMs. Red color refers to the crater dome, and black color to the flank dome.

Maureen GUNIA

L'ophiolite de Chamrousse est-elle seulement le vestige d'un océan cambrien ?

Year 2

Supervisors: Carole Cordier, Émilie Janots

Minéralogie et Environnements / Mineralogy and Environments

Chamrousse, située à quelques kilomètres de Grenoble dans le Massif Cristallin Externe de Belledonne (Alpes), est connue pour sa station de ski de moyenne altitude. La géologie de Chamrousse est singulière puisqu'elle présente une succession lithologique typique d'une ophiolite (portion de lithosphère océanique), bien que celle-ci apparaisse « la tête en bas », du fait d'un renversement lors de son charriage sur le continent. L'ophiolite de Chamrousse est donc considérée comme une structure majeure en France, car elle est la section de lithosphère océanique la plus ancienne, 496 Ma, et la mieux préservée de France.

Cependant, les nouvelles données géochimiques et géochronologiques obtenues in situ sur les zircons et apatites remettent totalement en question l'existence d'un océan cambro-ordovicien à Chamrousse.

L'ophiolite « vraie », composée de gabbros et serpentinites (Fig. 1) affleure au sommet de Chamrousse. Les gabbros ont été datés par Uranium-Plomb sur zircons et apatites au LA-ICP-MS à ISTerre au Carbonifère inférieur (~350 Ma), et les éléments en traces contenus dans ces minéraux présentent une signature magmatique et océanique.

En revanche, la base du complexe, jusqu'à présent interprétée comme une unité volcano-sédimentaire avec un complexe filonien, est formée d'unités amphibolitiques basiques et des intrusions plagiogranitiques acides associés à un complexe filonien basaltique (Fig. 1). Les unités basiques et acides ont toutes deux étés datés par Uranium-Plomb sur zircons à ISTerre au LA-ICP-MS ce qui donne un âge cambro-ordovicien (~500 Ma), mais surtout révèle une signature continentale de par leurs éléments en traces.
Le massif de Belledonne permet ainsi d'étudier, sur un territoire réduit, l'évolution à grande échelle des terrains nord-gondwaniens : le rifting cambro-ordovicien, l'ouverture océanique dévono-carbonifère et la collision varisque.

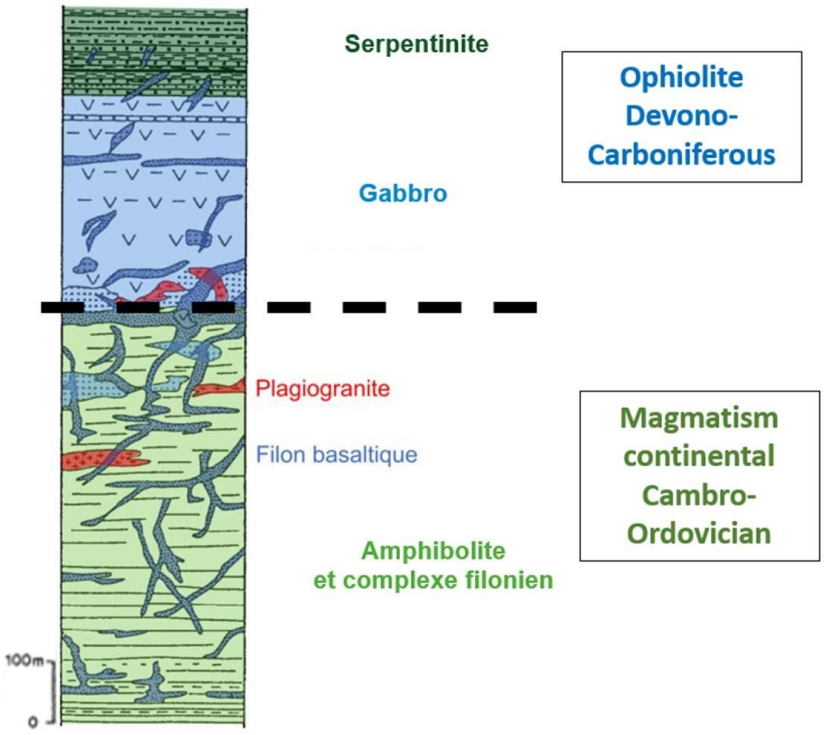

Figure 1. Pile stratigraphique schématique de l'unité de Chamrousse.

Olivier HAUTERVILLE

Régionalisation du modèle de flux physiques MATER

Year 1

Supervisors: **Olivier Vidal**

Minéralogie et Environnements / Mineralogy and Environments

Our society is changing at a rapid pace and its now facing big environnemental challenges (climate change, resources consumption, land use, pollution management). To overcome these challenges, one could use a model of the resource stocks and flux of our society with a prospective angle (i.e., different scenarii and trajectories about possible futures, like the work of the IPCC). More precisely, the work of the thesis will be to integrate a new way of looking at the world into the existing model via Geographgical Information System data (GIS).

Capture of the land use and of the anthropogenic infrastructures and modifications of the environnement

Carlos HEREDIA

Multi-isotopic tracing of historical mining pollution in European environmental archives and their impact on populations

Year 4

Supervisors: Alexandra Gourlan, Stéphane Guédron

Géochimie / Geochemistry

Knowledge of the sources, chronology and intensity of historical metallurgical activity in Europe are based on archaeological discoveries and paleo environmental studies that are unevenly spatially distributed. Although emissions of pollutants such as lead (Pb) from these activities have been recorded as far back as the polar archives, it is still difficult to pinpoint local sources and trace a regional map of metal flows from past activities.

Here, the combination of metal accumulation rates, enrichment factors, and isotopic fingerprinting in five new records from the Balkans and Carpathians clearly assess the contribution of these sources at the local and regional scales. Records from the Carpathians testify to almost continuous and intense mining activity over the past 2,000 years, with trends independent of the main mining periods known in Western Europe.

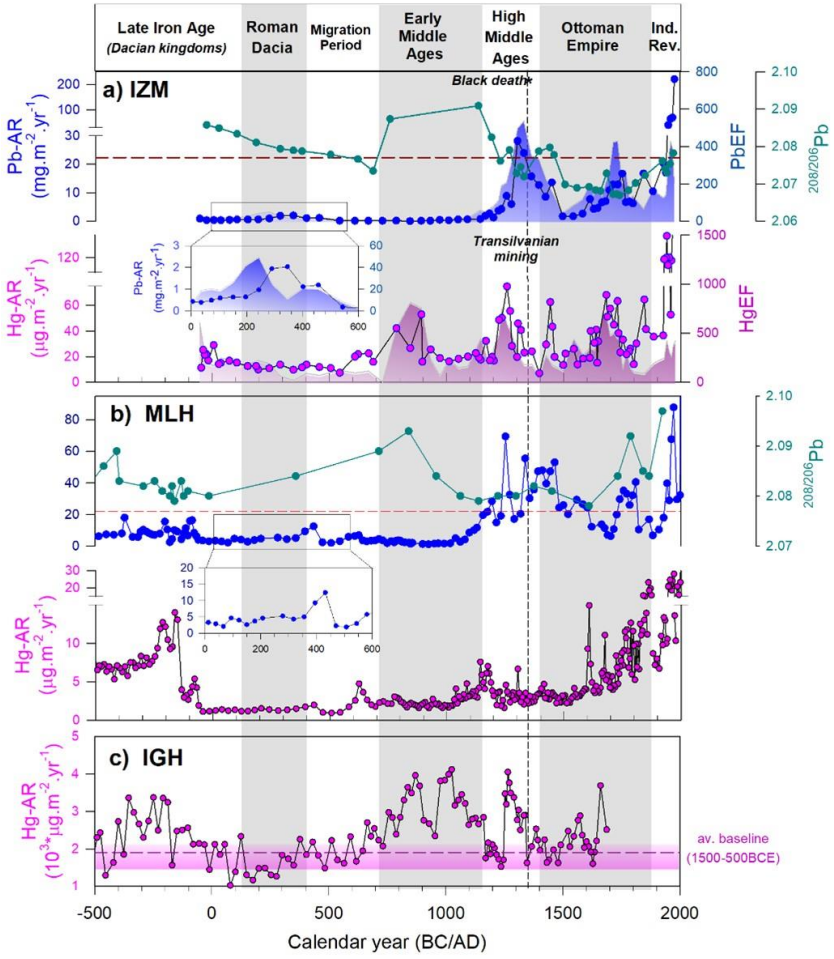

Figure 1. Lead (Pb) and mercury (Hg) accumulation rates (AR, left Y axes), enrichment factors (EF, right Y axes) relative to background concentration normalized to Ti, and Pb isotopes (208/207Pb) in the two Carpathian mires; A) Izul mare mire (IZM), and Mlhua (MLH), and C) lake Ighiel (IGH) sediment records. Red dotted line shows the averaged 208/207Pb value (2.07787 ± 0.00148 (1σ)) reported for Au-Ag ores mined by the Roman in the Apuseni Mountais.

Quentin HIGUERET

Seismic study of the San Jacinto Fault dynamics using dense arrays

Year 3

Supervisors: **Florent Brenguier**

Ondes & structures / Waves & structures

Seismic interferometry is widely used to monitor seismic velocity changes in the crust. However, the complex signal emerging from noise correlations makes it difficult to assess the wave content (body vs. surface waves, cross-terms) and thus to properly localize these velocity changes laterally and at depth. In this work, we use 3D numerical simulations and adjoint method to model noise correlations and assess the sensitivity of travel-time perturbations of reconstructed wave packets to localized velocity variations. We focus on the San Jacinto Fault (South. Cal.) and use real noise correlations obtained from stations across the fault including a 300 nodes array deployed at the Piñon Flat Observatory. We identify two distinct wave packets and use the moveout information from the array to show that they are bodywaves. One body-wave packet appears at low frequency (0.5-1 Hz) and the source is attributed to wind-driven microseismic noise along the coastline of California near San Diego, and the other at high frequency (4-6 Hz) with a source attributed to freight train activity in the Coachella valley. We use estimated noise source localization for both microseismic activity and trains to model these body-waves in noise correlations and compare the result to the observed correlations. Our result show that while we are able to reproduce the clear body-wave emerging from train tremor correlations, the modelled and observed correlations don't match for low-frequency microseismic noise highlighting the fact that we still have poor constraints on the source localization and that we probably observe complex cross-terms between body- and surface-waves. For the train noise correlations, we investigate the sensitivity of the reconstructed body-wave (P wave) travel perturbations to velocity perturbations induced by either environmental changes or velocity changes within the San Jacinto fault zone. We also examine the impact of train source spatial variability on travel time variations and discuss the use of ballistic body-waves for fault zone monitoring purposes.

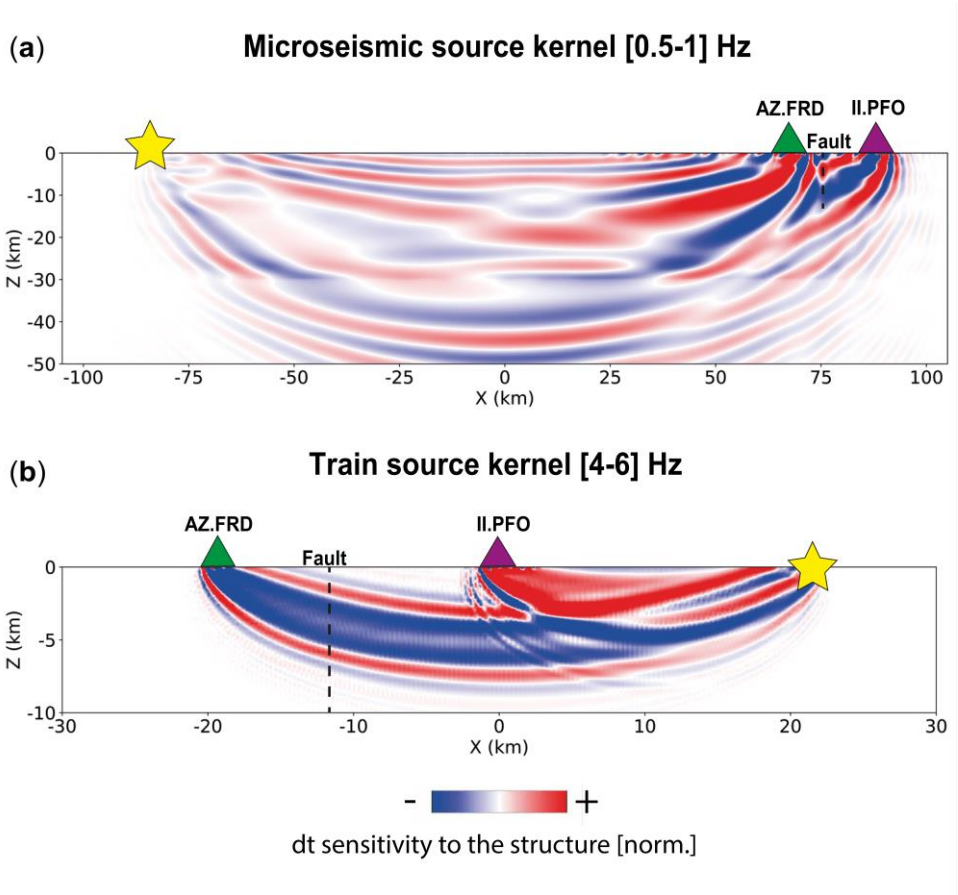

Figure 5. a) 2D Sensitivity kernels for traveltime shifts for two station pairs: II.PFO (purple triangle)-AZ.FRD (green triangle) for the microseismic source case (yellow star). b) 2D Sensitivity kernels for traveltime shifts for two station pairs: II.PFO (purple triangle)-AZ.FRD (green triangle) for the train source case (yellow star). For both a) and b) the SJFZ is represented using a black dash line.

Robin HINTZEN

Abiotic reactivity of minerals at elevated H2 concentrations

Year 3

Supervisors: **Laurent Truche, Roland Hellmann**

Minéralogie et Environnements / Mineralogy and Environments

Using H_2 gas as an intermittent energy carrier for the large-scale storage of excess renewable energy in different geologic subsurface environments such as salt caverns, depleted natural gas fields and porous aquifers has recently become a political and economic interest. Pyrite commonly occurs as an accessory mineral phase in reservoir lithologies such as sandstones. In the presence of H_2, pyrite dissolves and produces toxic and corrosive H_2S gas. In our project, the aqueous reductive dissolution kinetics of pyrite (FeS2) in the presence of H_2 has been investigated over a wide range of parameters (60-150 °C, 0-150 bar PH_2, in-situ pH 3.5-9.5). The experimental work ultimately aims at enabling the long-term modelling of S-II(aq.) release from pyrite dissolution at reservoir conditions via a kinetic rate law.

Beyond macroscopic bulk solution chemistry, the dissolution and growth mechanisms between primary pyrite (FeS_2) and secondary authigenic phases (pyrrhotite, FeS; magnetite, Fe_3O_4) in reducing H_2-rich environments are investigated on the µm- to the (sub)nm-scale by FEG-SEM imaging and FIB-TEM techniques. Congruent dissolution of pyrite is indicated by structurally and chemically sharp mineral-mineral interfaces. The embedded growth of authigenic phases points to a fluid-assisted mineral-mineral replacement mechanism. In addition, the PH_2 seems to affect the growth and morphology of pyrrhotite that changes from idiomorphic monocrystalline crystals at low PH_2 to polycrystalline amalgams at high PH_2.

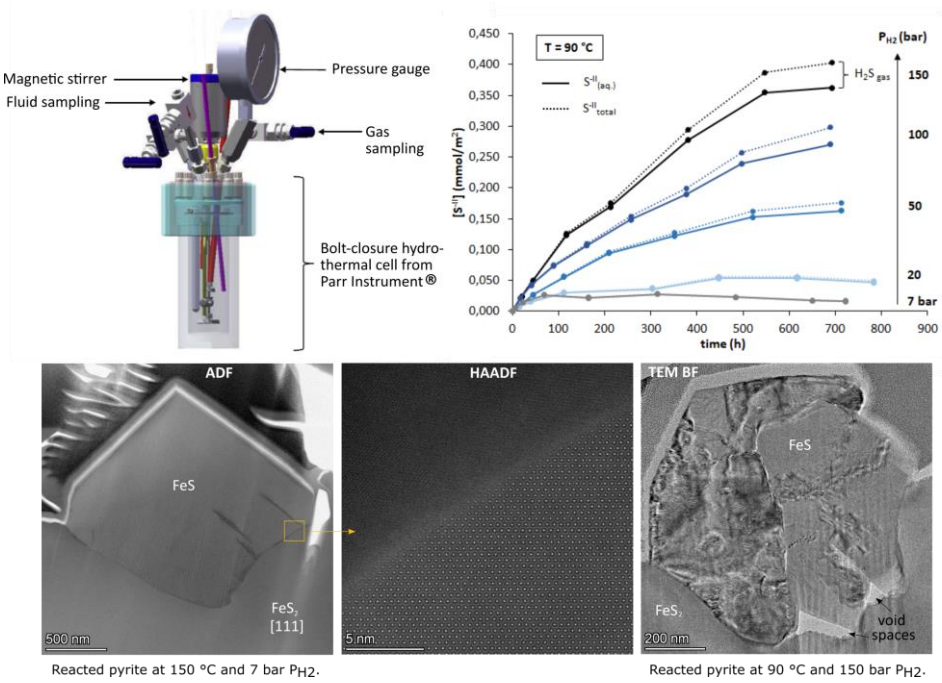

Upper left: Continuously stirred batch reactor design applicable for in-situ fluid and gas sampling. Upper right: Measured dissolved S-II(aq.) and modelled in-situ H_2S(gas) (mmol/m2) as a function of time (h) in pyrite alteration experiments at varying PH_2 from 7-150 bar at 90 °C. Bottom: FIB-TEM images illustrating pyrite dissolution and pyrrhotite growth features.

Jafar KARASHI

Spatial and temporal diversity of rupture characteristics and impact on ground-motion prediction for earthquake

Year 2

Supervisors: **Mathieu Causse, Sreeram Reddy Kotha**

Géophysique des Risques sismiques et gravitaires / Geophysics of seismic and gravity risks

The 2016 Amatrice-Visso-Norcia (AVN) seismic sequence occurred on Laga (LFS) and Vettore-Bove (VBFS) normal fault systems in the Central Apennines. The AVN triggered approximately 3600 aftershocks with $M_w \geq 2.5$, which were recorded at 278 permanent and temporal strong-motion and seismic stations. We compiled a catalog comprising approximately 135,000 data to investigate spatial and temporal variability of ground motion. A non-parametric Random-Forest GMM was employed to model the combined impact of magnitude and distance on the recorded PGA. Theoretical and observational studies indicate that the between-event variability of ground motion (δBe) is mainly controlled by stress drop. However, the level of the correlation between the stress drop (adopted from Kemna et al., 2021) and the δBe varies along the strike of the fault system. For the events located on the LFS, the correlation was the lowest (0.39) obtained, where events with small stress-drop values had high δBe. This suggests that the ground-motion variability in this region is likely influenced by another physical process, possibly due to a weaker attenuation than the VBFS region. Conversely, in VBFS, a higher correlation (0.65) was observed, indicating that the ground motion variability is primarily controlled by stress drop. A strong correlation (0.67) between hypocentral depth and δBe was also observed, implying that depth exerts first-order control on ground motion, and the ground motion variability decreases by increasing depth.

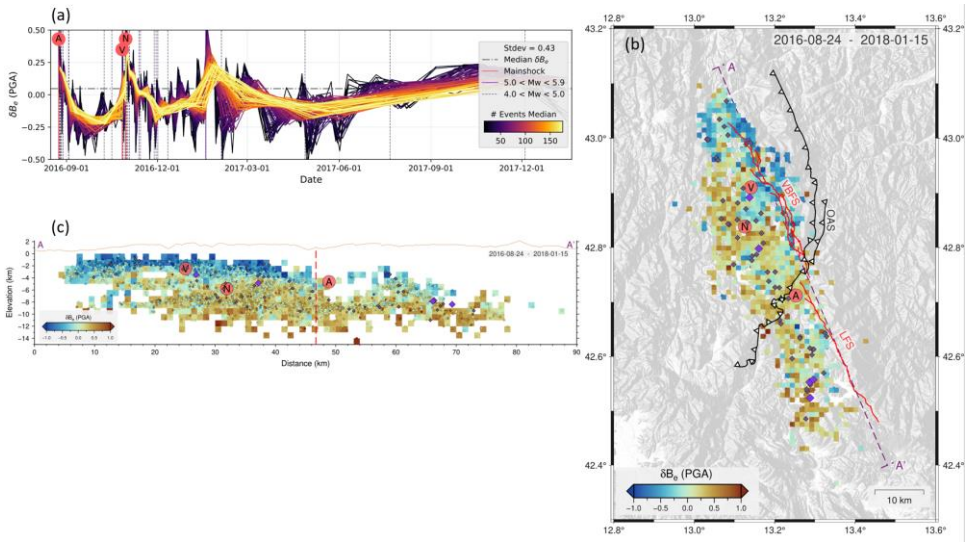

(a) Temporal variability of the between-event residual for recorded PGA during the central Italy seismic sequences. (b) Spatial distribution of the between-event residual over the entire central Italy. (c) Spatial distribution of the between-event along the VBFS and LFS corresponding to the cross-section AA'.

Tatiana KARTSEVA

Source parameters of volcano-tectonic earthquakes (M<3) and laboratory acoustic micro-fractures (M<-6) from coda-waves

Year 3

Supervisors: **Nikolai Shapiro**

Ondes & structures / Waves & structures

Source spectra parameters such as corner frequencies (f_c), seismic moments (M_0), stress-drops and source radii of volcano-tectonic (M < 3, tens of meters size) and laboratory (M < -6, milimetric size) earthquakes are estimated based on empirical Green's function (eGf) approach with the use of amplitude spectra of signal's coda.

The use of eGf approach allows to remove usually poorly known propagation effects in both cases and unknown sensor response particularly in laboratory case. Spectra of coda amplitudes instead of direct waves allow to avoid several conditions that can not be fulfilled but are necessary for using eGf method. Coda waves due to its formation mode (scattering, attenuation and reflections in laboratory case) average radiation pattern and have stable envelope shape on all stations. As eGf functions we use a set of smaller scale events that allow to stabilize estimations. Source parameters f_c and M_0 are extracted after approximation of data spectral ratio with source models.

The method was applied to volcano-tectonic earthquakes occurred in the summit of the Piton de la Fournaise (PdF) volcano on La Réunion island (West Indian ocean). They precede eruptions appearing as a swarm, located around ring-fault system likely hosting repetitive collapses of the summit caldera. This seismicity is triggered by the over-pressure of the magma body and according to our results demonstrate inverse cubic relation $M_0 \sim f_c^{-3}$ and stress-drops 1-10 MPa that is usually observed for tectonic earthquakes

Such a scenario of seismicity generation consisting of repetitive triggering of pre-existing fault system by external pressure rises can be modeled in the laboratory on a centimetric scales. Experiments were conducted on INOVA-1000 press (GO "Borok", Russia) on 6 cm high granite and sandstone samples. First stages of this experiments consisted of confining pressure steps applied to intact rock. Due to a coda-based procedure for source parameters estimation acoustic events on this loading regime also were found to follow cubic relation with a constant stress-drop (relative, since sensors are not calibrated). Applying axial loading to samples revealed high variability of stress-drops because of generation of new faults.

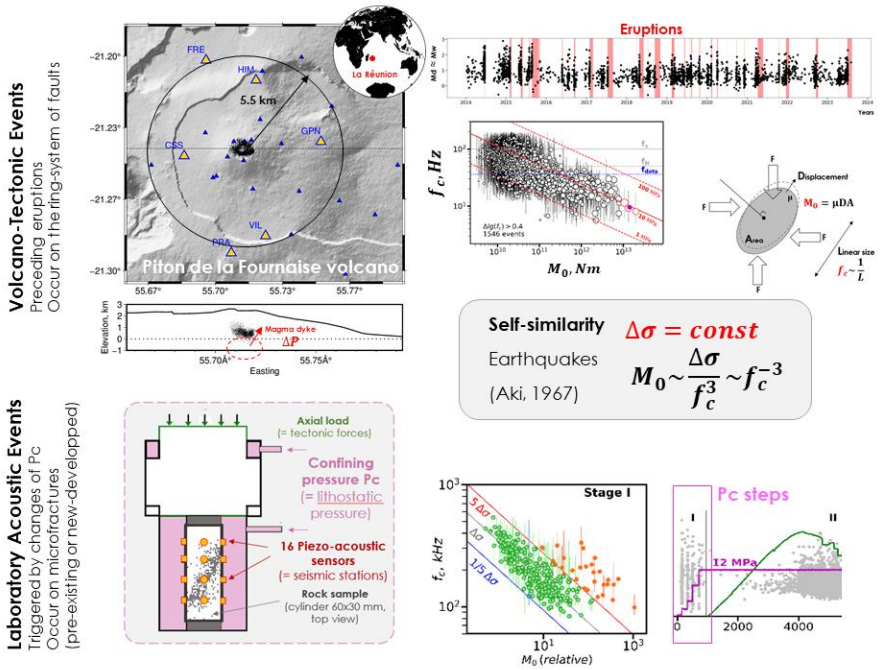

Figure shows seismicity in both scales and physical conditions to generate signals with repetitive over-pressures. M_0 vs f_c diagrams demonstrate inverse cubic relation in both cases that corresponds to the self-similarity principle for source spectra and therefore source geometry

Théo LALLEMAND

Characterization of recent seismotectonic activity on the Vuache fault (Haut-Jura) using a multidisciplinary approach

Year 1

Supervisors: **Laurence Audin, Stéphane Baize (IRSN)**

Cycle sismiques et déformations transitoires / Seismic cycles and transient deformations

A multidisciplinary study combining archeoseismology, geomorphology and structural geology on a Gallo Roman site in the Jura mountains (Jura, France), with a potentially evidence for recent tectonic deformation along the northern Montagne du Vuache Fault (MVF) a slow intracontinental fault. This site has the potential to record local seismic activity through the deformation of ancient buildings. During excavations in 2021 and more recently in the summer of 2023, numerous deformations were observed in the archaeological remains, with a clear link between the faulted substrate and this remains. In order to be able to study these deformations, a tectonic context has been established for the area through a multidisciplinary study combining structural geology, geomorphology and archaeoseismology. The preliminary results suggest the occurrence of tectonic events during Antiquity along the northern segments of the MVF. Surface-rupture faulting could have damaged and offset Gallo-roman remains, and strong local shaking during those events could have coevally damaged the constructions. The 20–30 cm wall offset observed could fit with the deformation characteristic of a shallow to very shallow moderate-magni- tude earthquake, capable of causing strong shaking in the vicinity of the fault.

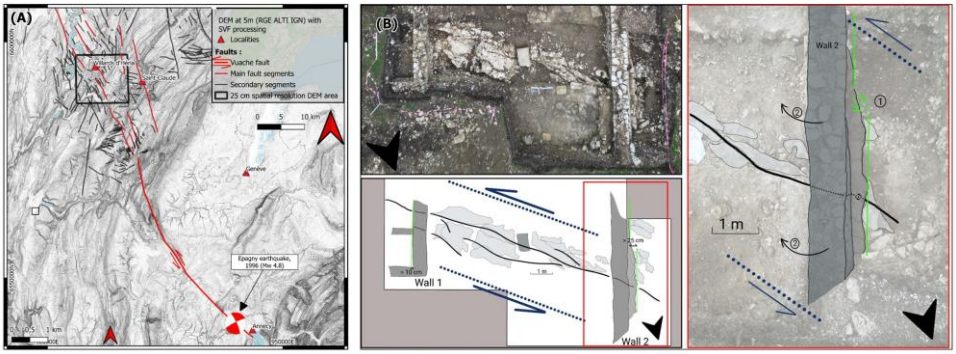

Fig 1: (A) Geomorphological imprint of the fault based on a 5-m-spatial resolution DEM, and on a 25-cm-spatial resolution DEM in the boxed area. Projected coordinate system: EPSG 2154, RGF93 / LAMBERT 93. (B): Area of archeoseismological investigations with a Zenithal view, and a structural diagram of the faulted zone. Focus (red box) on Wall 2 shows two phases of damage, 1: sinistral offset at the base and 2: tiltingof the structure in the upper part.

Emma LEGROS

Microstructural study of the dehydration/deformation coupling of serpentinites: implications for fluid mobility and geochemical

Year 1

Supervisors: Anne-Line Auzende, Fabrice Brunet

Minéralogie et Environnements / Mineralogy and Environments

The subducted oceanic lithosphere contains hydrated minerals such as serpentines and brucite formed by chemical interactions between seawater and mantellic rocks. Along a subduction geotherm, P-T conditions are met for these minerals to dehydrate. Water and other chemical components incorporated into the subducted oceanic lithosphere can be recycled into the deep mantle. One of the main products of dehydration is olivine, called metamorphic olivine. Metamorphic olivines are preserved in Zermatt ophiolite (Swiss Alps) in veins that illustrate the dehydration process of the serpentines and offer a remarkable opportunity to characterize it.

The first results obtained where acquired on these serpentinites, originally formed during the opening of the Tethys ocean and subducted to eclogitic facies during the Alpine collision (Kempf et al., 2020). These rocks reached P-T conditions leading to anhydrous phases characterized by the dehydration reaction:

Antigorite + Brucite = Olivine + H2O (1)

This reaction is often mentioned as an important dehydration reaction but is poorly investigated. In particular, we are seeking for brucite, which is rarely identified in serpentinite samples.

Two types of olivine veins are identified:

i) Small veins underlining the C/S structures and made of small grains olivine (<50micrometers). Electron microprobe results on these metamorphic olivines show a un enrichment in magnesium Mg# 93-95, in contrast to mantle olivine whose average Mg# 90.
ii) Large crosscutting veins consisting of large olivine crystals (>500micrometers). This metamorphic olivine shows higher magnesium enrichment, with Mg# 95-98.

Two types of serpentines can be distinguished by the chemical variations: i) sheared serpentines, crosscuted by olivine veins, have an enriched composition with high Al and Fe content (>1wt%). ii) serpentines within the veins, seem to grow at the expense of the metamorphic olivines, have a composition with low Al and Fe concentration (<1wt%).

Thermodynamic modelling will enable us to constrain a dehydration P-T field in relation to rock geochemistry and constrain the mechanisms of deserpentinization in subduction zones. These results will contribute to a global understanding of deep geochemical recycling across subduction zones.

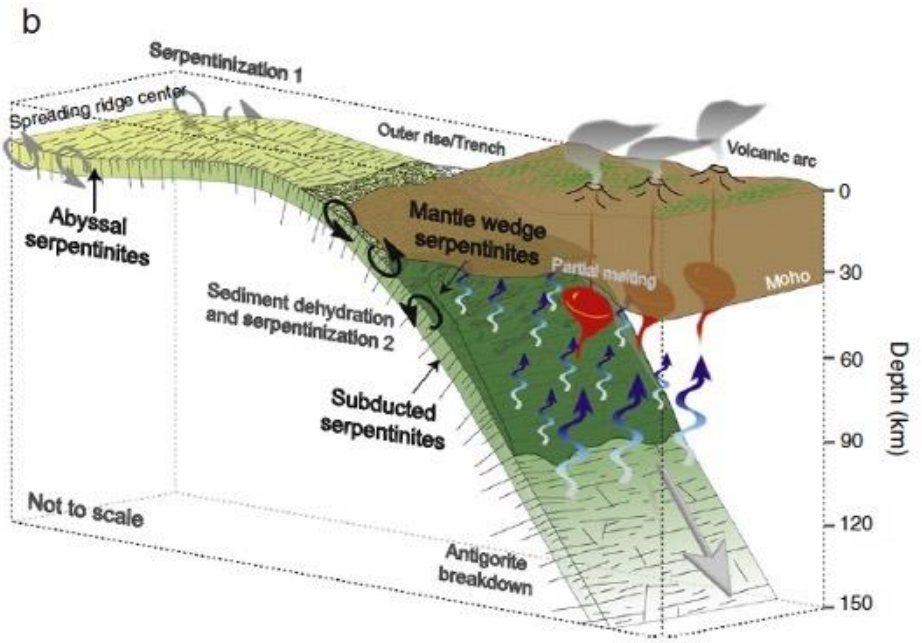

Serpentinites are formed by hydration of the ocean lithosphere at ocean ridges. They are carried to depth during subduction, then dehydrated at depths of between 70 and 150 km (ecologite metamorphic facies). The fluids released during deserpentinization will interact with the rocks of the upper mantle wedge, located at an average depth of 3 to km.

François LEMOT

Multi-lake approach to study the seismic cycle in SE Tibet

Year 3

Supervisors: **Anne Replumaz**

Tectonique, Reliefs, Bassins / Tectonics, Reliefs, Basins

The Southeast Tibet region is a tectonically active area intersected by the Xianshuihe strike-slip fault system, which is considered one of the most active faults in China. During my PhD, I sampled sediment cores from 11 small mountain lakes along these faults. Multi-proxy analyses, including XRF core scanning, loss on ignition, sedimentological descriptions, and grain-size measurements, were performed to characterize event deposits associated with earthquakes. Dating techniques, such as short-lived radionuclides (^{137}Cs, ^{241}Am, and ^{210}Pb), radiocarbon, and paleomagnetic secular variations, were employed to develop age models for each section. These techniques allowed for the dating of deposits corresponding to paleo-earthquakes.

Preliminary results from the cores indicate that the lakes registered historical earthquakes, producing local intensities above a site-specific threshold. Consequently, the lakes behave as binary paleoseismometers with intensity thresholds ranging between 5.5 and 6.5, depending on the lake. I developed a numerical simulation to test physically consistent rupture scenarios and their ability to align with both positive and negative observations of earthquake deposits. The model predicts both the magnitude range and the rupture location for a given fault network, using a combination of three lacustrine records. This provides crucial insights into the local seismic cycle. Long-term dynamics of the fault can be inferred from extended core records spanning the last 8,000 years, revealing more than 60 events with intensities above 5, which offer robust statistics on intensity-exceeding probability and earthquake recurrence times.

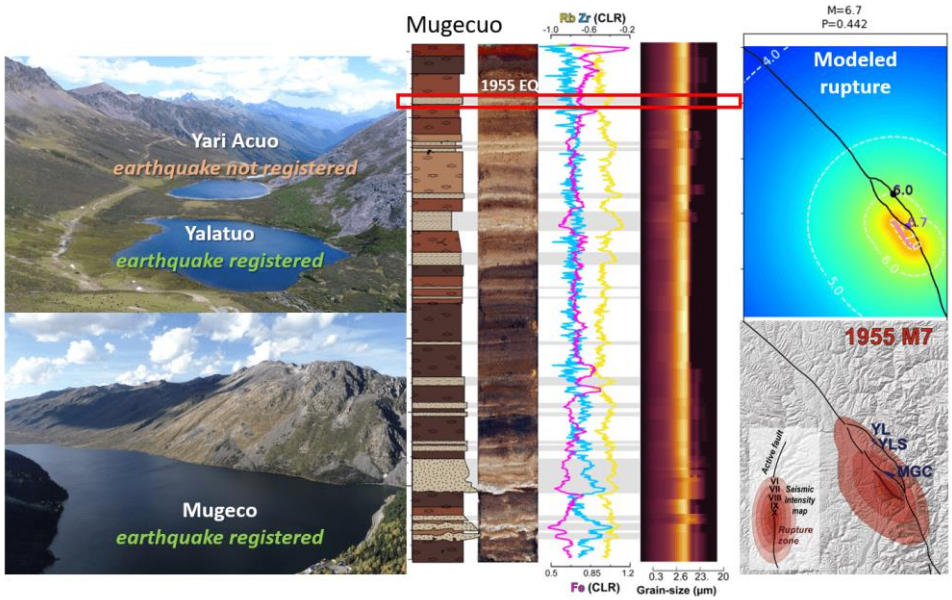

Earthquake-triggered coseismic deposits in some lakes (left) can be identified in sediment cores using various proxies (center). A model testing different rupture scenarios estimates the probability of observing deposits in the lakes for each scenario. Scenarios with high probability demonstrate remarkable agreement with historical earthquake records (right)

Thea LEPAGE

Electrical conductivity of the lowermost mantle

Year 1

Supervisors: **Dominique Jault, Nicolas Gillet**

Géodynamo / Geodynamo

The electrical conductivity σ remains a poorly understood property of the deep mantle, which however affects both core dynamics and the magnetic field observed at the surface. A thin conducting layer is suggested at the base of the predominantly insulating mantle. Utilizing geomagnetic and rotation data from both observations and simulations, the effects and implications of a conducting mantle are studied.

Assuming a thin conducting layer, relative motions between mantle and outer core coupled with temporal variations of the magnetic field give rise to an electromagnetic (EM) torque. The radially symmetric case has already been considered in several studies. In contrast, I investigate possible lateral variations of the conductance and their effects on the torque and consequently on the length-of-day (LOD). Additionally, I am comparing geodynamo simulations where the mantle is coupled to the core by the EM torque only or in combination with the gravity torque. Initial findings suggest that the EM torque cannot account alone for observed changes in LOD, thus requiring a second torque. Moreover, the EM torque involves electrical currents leaking from the interior when it acts alone whereas these currents have negligible effects when both torques are present. Furthermore, the ring current in the magnetosphere creates an external magnetic field which in turn induces a field inside both the solid mantle and the fluid core. Conductivity models of the mantle computed using geomagnetic data so far assume a shell-like mantle structure and a solid outer core. I have investigated the motions and the magnetic field arising inside the liquid core in response to changes in the external magnetic field allowing the comparison to the induced magnetic field for a solid core. Lastly, the flow at the top of the core and its radial shear are influenced by σ of the lowermost mantle. Assuming that the flow and the shear are related through the QG approximation, we can constrain σ.

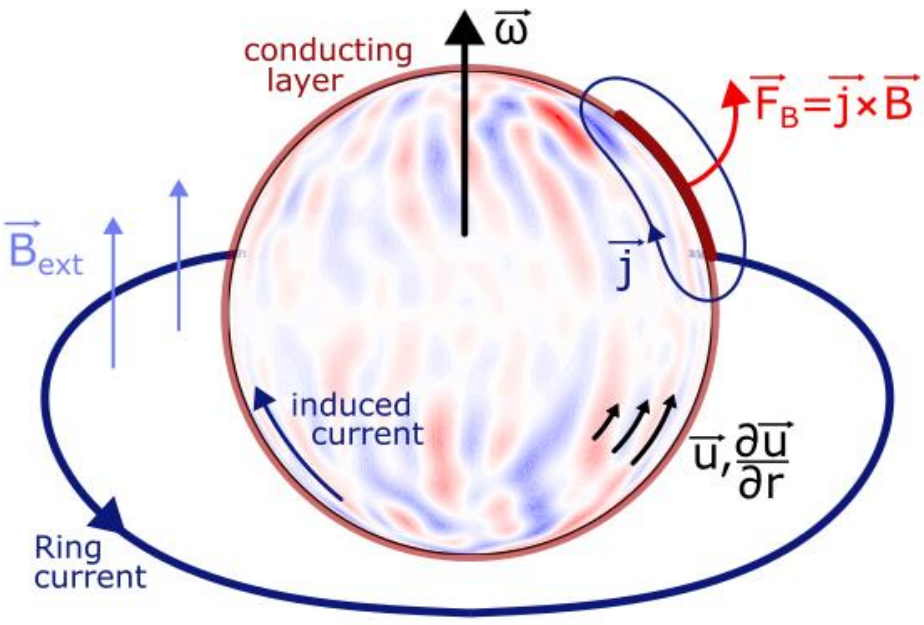

What can we learn about the deep mantle conductivity from geomagnetic and Earth's rotation data?

Manon LORCERY

Tectonic reshaping of the biosphere

Year 2

Supervisors: **Laurent Husson**

Tectonique, Reliefs, Bassins / Tectonics, Reliefs, Basins

Changes in the physical environment, whether geological or climatic, are known to be major drivers of biodiversity. At the interface between the solid Earth and the climate lies the physiography, and landscape complexity and variety may control biodiversity mechanisms at a finer scale that the large-scale patterns of plate tectonics and global climate. To test whether variation of physiography through time and space can explain the current richness pattern of biodiversity and understand the impact of landscape complexity evolution on specific mechanistic processes, we simulated the diversification of terrestrial mammals at global scale, over 125 Ma of geological and climatic changes, using a spatially explicit eco-evolutionary simulation model (gen3sis). We designed four evolutionary scenarios in which evolution was only dependent on climate and plate tectonics (M0), and scenarios where physiographic diversity was implemented in speciation (M1), dispersion (M2) and niche ecology (M3). To assess whether model predictions are consistent with the empirical distribution of terrestrial mammals, we statistically identify general emergent patterns of biodiversity within and across spatial and temporal scales.

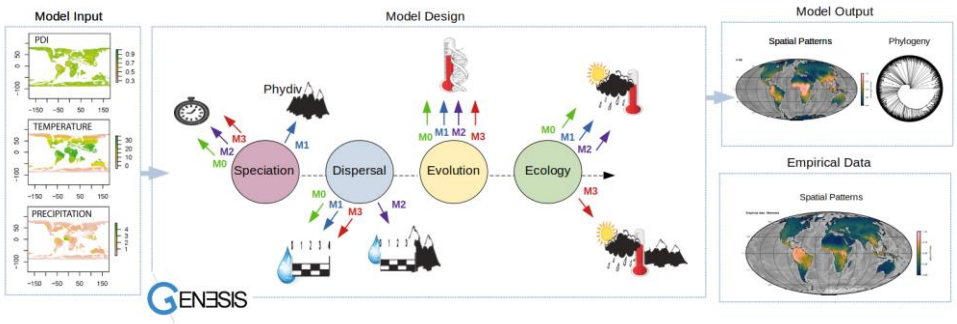

Schematic of the main components of the gen3sis model, with a model input which consists of paleo-reconstructions of environment variables (Precipitation, Temperature, Physiographic diversity). The model design defines the macroecology mechanisms implemented in the model, which will set the behaviors of the species modelled and finally a model output, with consists of richness maps, phylogenies and ecological traits.

Bertrand LOVERY

Crustal deformation associated with the seismic cycle in Central Andes from InSAR and GNSS geodetic timeseries

Year 2

Supervisors: **Anne Socquet, Mohamed Chlieh, Marie-Pierre Doin, Mathilde Radiguet**

Cycle sismiques et déformations transitoires / Seismic cycles and transient deformations

Central Andes have been the theater of numerous megathrust earthquakes, like the one of Iquique in 2014 (M_w 8.1), Pisco in 2007 (M_w 8.0), or Arequipa in 2001 (M_w 8.4). A deeper understanding of interseismic coupling distribution between tectonic plates and seismic cycle in this area is therefore a key issue in the frame of seismic hazard assessment. In this purpose, we can rely on geodetic data acquired by the dense GNSS networks that have been deployed, and on the Sentinel-1 InSAR acquisitions processed in the frame of the FLATSIM Andes project. Post-processing of these data and their joint inversion, by principal component analysis (PCAIM) and independent component analysis (ICAIM) will allow us to finely model interseismic coupling distribution along the subduction interface. From this model, we will carry out a moment budget analysis, in order to determine the maximum magnitude upcoming earthquake and its recurrence time. Finally, a significant part of the PhD will be dedicated to finite element modelling of the subduction zone, in order to determine rheological laws better suited to the various geological structures. This will enable taking into account complex visco-elasto-plastic behavior associated to megathrust events, as well as linking short-term and long-term crustal deformation.

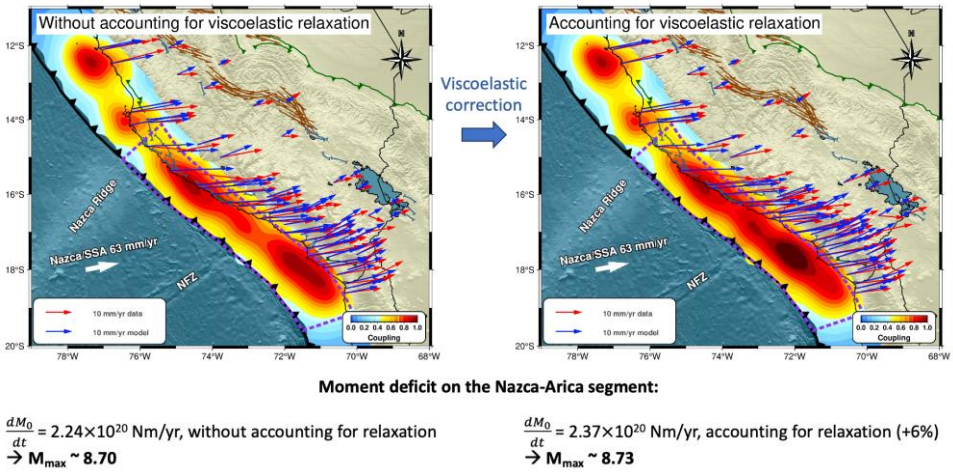

Left: Interseismic coupling distribution from our inversion of interseismic velocities in the Stable South America frame. Slab contours (dashed lines) are reported every 20-km depth, from the Slab2 model (Hayes et al., 2018). The interseismic coupling is highly heterogeneous reflecting strong variations of the frictional properties on the slab interface. Thus, there are four highly coupled areas: a very-highly coupled area close to Lima, a less coupled area near Ica, a large band of high coupling between the Nazca Ridge and the Nazca Fracture Zone (NFZ), and a highly coupled area between the NFZ and the Arica bend. Discontinuities can be observed where the Nazca Ridge and the NFZ are subducting below the South America plate. The approximate rupture area of the M_w = 8.4 2001 Arequipa has been estimated in this study, while the M_w = 8.0 2007 Pisco earthquake rupture is reported from Chlieh et al. (2011). Patches with gray hachure pattern depict areas that are not well resolved by the model.
Right: same figure but accounting for viscoelastic relaxation following the 2001 M_w = 8.4 Arequipa earthquake. Moment deficit rate is increased by 6%.

Vivien MAI YUNG SEN

Quantify

Year 3

Supervisors: Pierre Valla, Stéphane Jaillet (Edytem), Xavier Robert

Tectonique, Reliefs, Bassins / Tectonics, Reliefs, Basins

The evolution of karstic networks is intimately coupled with the topographic relief dynamics. Both are controlled by tectonic and climatic forcing on timescales ranging from thousands to millions of years. To decipher these interrelationships, we focus on the frontal limestone massifs in the Western to Central Alps, where extensive and historically renowned underground networks develop. Our goal is to reconstruct both the evolution of these karstic networks and the topographic relief since the Late Miocene.

We target three distinct paleogeographic settings:
- The Bourne River system, which drains both the underground and surface water fluxes of the Vercors Massif, and has been protected from Alpine glaciations. We aim to quantify there the long-term incision dynamics of the frontal western Alps.
- The Isère River valley has been deeply carved and overdeepened by Alpine glaciations. The neighboring karstic networks have evolved following both the Isère valley incision and successive Alpine glaciations.
- The upstream Sarine catchment affected by Alpine glaciations but preserved from glacial carving.

The extensive topographic data acquired by generations of speleologists are integrated into underground 3D models of karstic networks in order to (1) extract the fossil (epi)phreatic tubes and (2) constrain the underground phreatic flow reorganizations in response to topographic changes. Phreatic phases are identified using sedimentology and dated using burial 26Al/10Be dating and paleomagnetism. Finally, the abandonment phases of the paleo-drains are dated using U/Th and U/Pb on speleothems.

Our main results show:
- A first late-Miocene downgrading phase of karstic conduits in response to tectonic shortening and topographic uplift.
- A significant Pliocene karstification phase, during a period of stable base level (tectonic quiescence and relatively stable climate).
- Karstic evidence for Quaternary incision and first glacial incursions since ~2 Ma.
Our spatio-temporal constraints on karstification phases provide quantification of the late-Miocene/Quaternary incision and uplift dynamics in the Western French Alps, demonstrating the relevance of combining quantitative geomorphology methods (3D modelling and geochronology) in karst research.

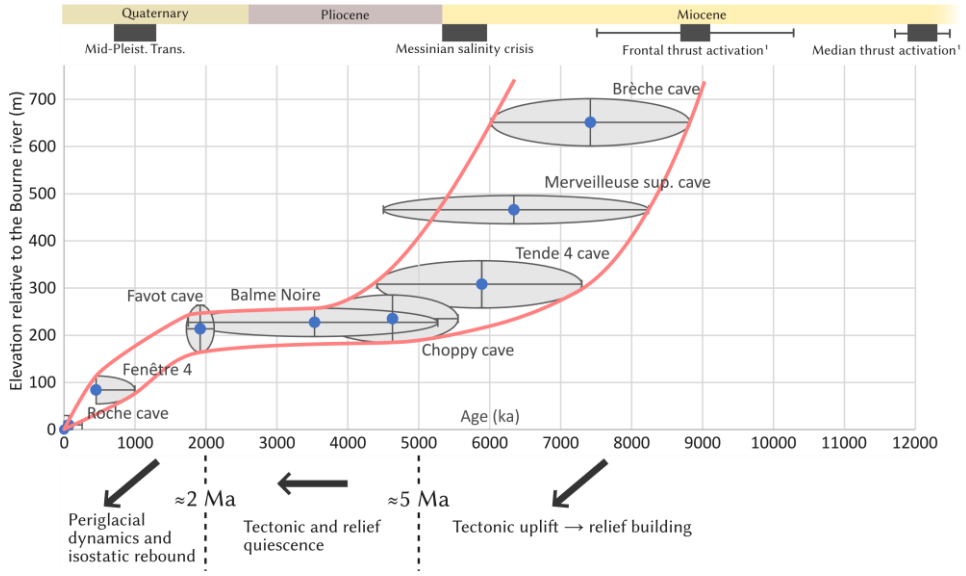

Reconstruction of the Bourne's incision since the end of the Miocene based on endokarst archives. Blue dots represent river paleo-levels reconstructed from cave sediment dating. The grey envelopes represent geochronological and altitudinal uncertainties. Three phases of incision are identified and correlated with geodynamic and climatic changes, demonstrating the coupling between the evolution of the Vercors relief, tectonics and climate dynamics.

Léo MARCONATO

Multi-sensor InSAR time-series analysis for studying active tectonics in Ecuador

Year 3

Supervisors: **Laurence Audin, Marie-Pierre Doin**

Cycle sismiques et déformations transitoires / Seismic cycles and transient deformations

Tectonics of Ecuador is dominated by the subduction of the Nazca plate underneath the South American plate, at a convergence rate of 5 to 6 cm/year. Most of this convergence occurs at the subduction interface, however, a part of the convergence is accommodated by the north-eastward motion North-Andean sliver, by about 5-10 mm/year with respect to stable South America. This crustal strain is mainly localized along the large Chingual-Cosanga-Puna-Pallatanga (CCPP) fault zone. Crustal earthquakes with important magnitudes happened in this area in the historical period, yet the associated source faults are either unknown or not much investigated. Also, recent results using block-modeling of GNSS data raise important question about the partitioning and the localization of the deformation both inside and at the limits of the North-Andean sliver.
In order to better know the active structures in this area, the goal of this PhD is to complement existing GNSS ground displacement data by high-resolution InSAR data. However, applying InSAR time-series-analysis in the region of interest is challenging, because of several factors: ionospheric perturbations in Equatorial regions, mountainous areas with strong topographic gradients, low-coherence in vegetated areas such as Equatorial forests. To overcome these issues, I use several SAR sensors (ALOS, Sentinel-1 and ALOS-2) and state-of-the-art InSAR processing techniques, with the aim of producing the most accurate ground displacement data.

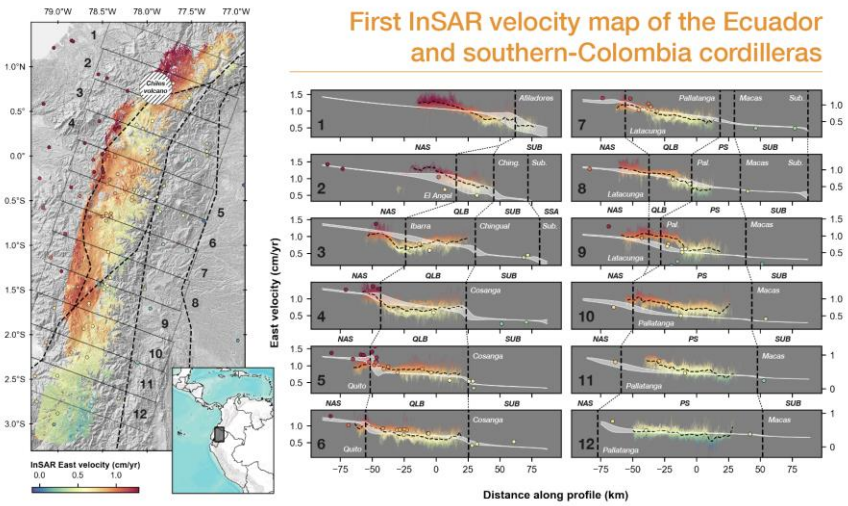

First velocity map of Ecuador and southern-Colombia cordilleras, obtained from InSAR time-series analysis of Sentinel-1 data

Cecilia MARTINELLI

Benchmarking surface rupture characteristics inferred from optical image correlation; a case study from the 2019 Ridgecrest earthquake

Year 1

Supervisors: James Hollingsworth, Céline Beauval

Cycle sismiques et déformations transitoires / Seismic cycles and transient deformations

Optical image correlation (OIC) is a geodetic technique that allows the surface deformation resulting from an earthquake to be retrieved through correlation of pre- and post-event optical satellite images. OIC is powerful at capturing near-fault and off-fault deformation around surface rupturing faults, with high spatial detail, and with precisions of m-to-cm, and can be applied to the study of modern and historical earthquakes (as long as images are available in medium/high resolution). Increasing volumes of optical data, with ever-improving spatial resolution, has facilitated the study of modern earthquake surface ruptures. There are different OIC algorithms that can be used to retrieve ground deformations, each potentially influencing the final interpretation of fault zone characteristics, such as the width, magnitude of on-fault deformation, near-field strain, and other parameters that are key to understanding how earthquakes rupture the surface. In this context of increasing data availability, it is necessary to understand the effects of the OIC on the above parameters to ensure robust interpretations, which will inform our understanding of the physics of earthquake slip. Thus, the primary objective of the study is to conduct a comprehensive statistical analysis of various algorithms (Cosi-Corr, Ames Stereo Pipeline, Mic-Mac, Ampcor, Orfeo ToolBox, and recent CNN-based approaches) and their parameters using different image sources (ADS aerial photos, and WorldView, Pleiades, and SPOT satellite images). This analysis aims to compare state-of-the-art correlation methods and examine their impact on surface rupture characteristics, using the well-studied 2019 M_w 6.4 and 7.1 Ridgecrest earthquakes in California as a case study.

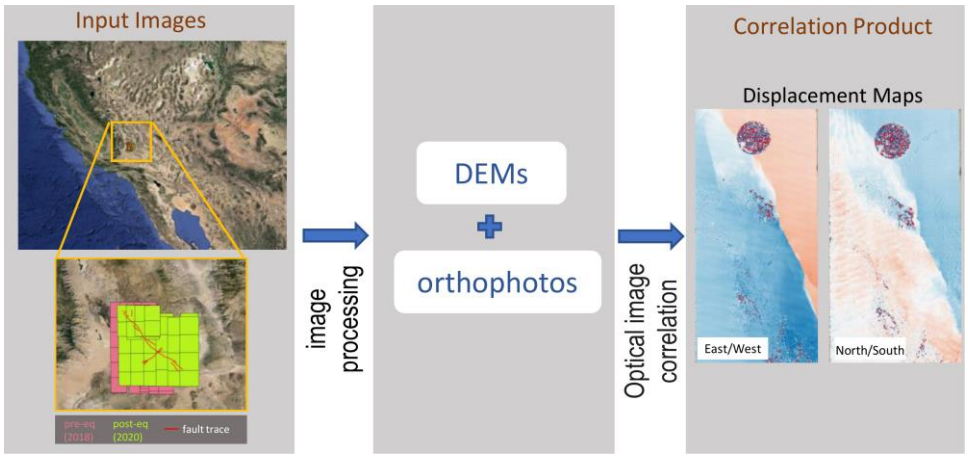

From left to right: A pair of input images of the Ridgecrest earthquake. The pre and post input images are differentiated by colors, pink and green respectively. The images are processed, and once the DEMs and the orthophotos of the area are generated, it is possible to correlate them. The correlation products are Displacement maps, generated using the optical image correlation technique.

Kristina MATRAKU

Quantification and modelling of current tectonics of Albania.

Year 4

Supervisors: **François Jouanne**

Cycle sismiques et déformations transitoires / Seismic cycles and transient deformations

Albania's current tectonics are characterized by considerable seismicity, as demonstrated by 12 earthquakes with a Ms greater than 6 in the last century and the known historical seismicity of 25 centuries, with 89 devastating events. The last strongest event in the region was the 26 November 2019, M_w 6.4 Durres earthquake, it is the first earthquake to be characterized by InSAR and GNSS in Albania. The seismic sequence started on 21 September 2019, with an M_w 5.6 earthquake, followed by an M_w 5.1 aftershock 10 minutes later considered as foreshocks, and culminated with the main shock Mw 6.38 on 26 November 2019, preceded by several immediate foreshocks (M_w 2.0-4.4), followed by numerous aftershocks (M_w > 5.0). We model the co-seismic slip distribution using InSAR, permanent and campaign GNSS measurements. Two hypotheses are tested: an earthquake on a thrust plane with direction N160°, and an earthquake on a backthrust. Varying the depth and dip angle for the first hypothesis and only the dip angle for the second, it is concluded that the optimal solution is a blind thrust at a depth of 15 km with an eastward dip of 40°, a maximum slip of 1.4 m and a M_w of 6.38. The GNSS time series obtained after 2020 shows two slow slip events (SSE): the first 200 days after the main shock up to about 26 days, and the second 300 days after the main shock up to about 28 days. We tested three hypotheses: SSE occurred along the basement thrust where the main shock was localised, SSE occurred along the flat formed by the detachment layer of the cover, and SSE occurred along these two faults. It has therefore been concluded that SSE has occurred along the detachment layer or along both the detachment layer and the basement thrust activated during the M_w 6.38 Durres earthquake.

Moreover, to characterize the current deformation of the Albanides, three Albania permanent GNSS networks and dense GNSS campaign measurements (2003, 2006, 2009, 2012, 2017 and 2022) have been processed. The horizontal and vertical GNSS velocities have been estimated. The GNSS horizontal velocities expressed in Apulia reference frame underlined the compression regime in External Albanides marked by south-westward velocities, increasing from north to south, illustrating the shortening across the western Dinarides-Albanides/Hellenides collision belt, compatible with thrust and fold faulting type and focal mechanisms covering the region, whereas an extensional regime characterizing Internal Albanides, North Macedonia, Bulgaria, Easterner Greece, marked by southward increase of horizontal velocities. The horizontal velocities field, strain rate tensors, rigid rotation rate and focal mechanisms covering Albanides lead to the analysis of deformation accommodated on the Shkodra-Peja Traversal Zone, Elbasan-Diber-Skopje fault covered by an extensional regime and the Lezha and Othoni-Llogara Pass marked by a strike-slip component.

Vertical velocities in Albania, highlight two primary trends: subsidence in the External Albanides and uplift in the Inner Albanides except the few stations installed in active grabens showing subsidence.

We propose following Handy et al., (2019) and Jolivet et al., (2021) that the rapid change between compression in external Albanides and extension in inner Albanides reflects the influence of two slab rollbacks, the eastern dipping subduction of the Hellenic Slab beneath the Albanides and North Hellenides and the subduction of the Aegean Slab beneath Crete Island.

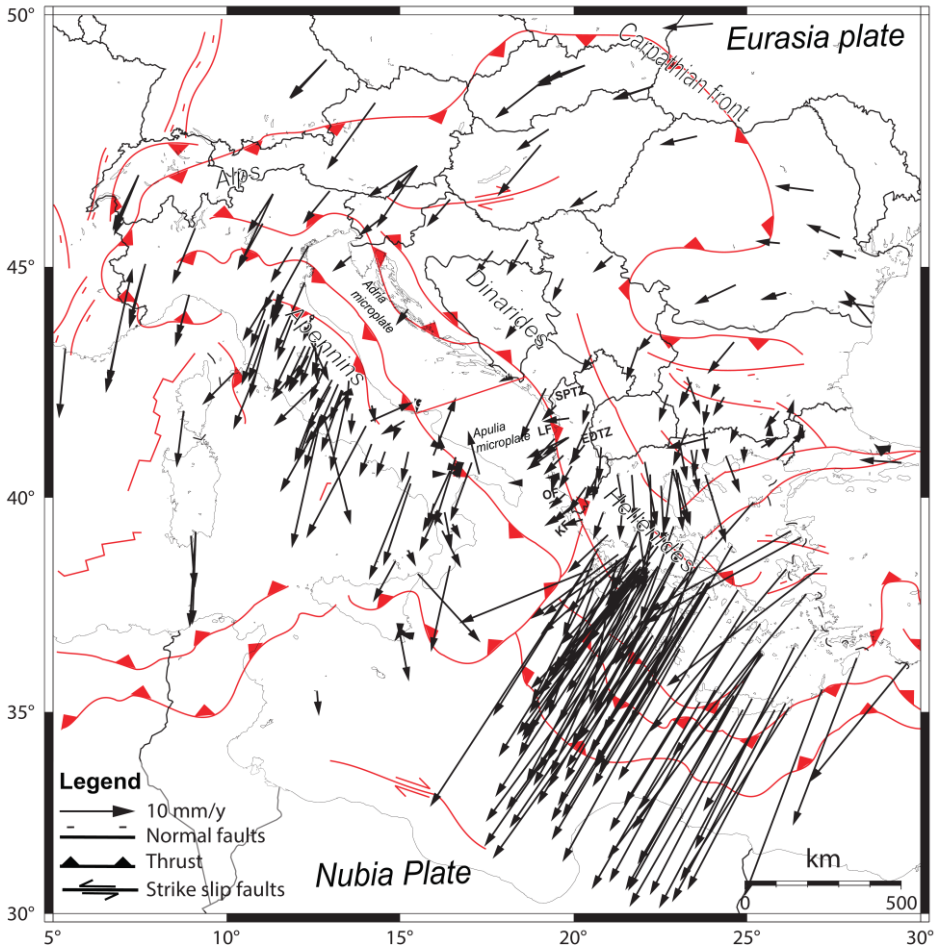

The GNSS horizontal velocity field expressed in the Apulia Fixed Reference Frame with a pole rotation at longitude −132.659± 0.3, latitude 4.041°±16.8 and rotation rate 0.340°/Ma ± 0.054 (D'Agostino et al., 2008). The location of the main structures, SPTZ = Shkodra-Peja Transversal Zone; LF=Lezha Fault; OF=Othoni-Llogara fault; EDTZ=Elbasan Dibra Transversal Zone; KF=Kefalonia Fault.

Pauline MEYER

Active tectonics of the northwestern edge of the Indian plate: observation and modelling

Year 2

Supervisors: **François Jouanne**

Cycle sismiques et déformations transitoires / Seismic cycles and transient deformations

The northwestern syntax of the Himalaya is a very rapidly deforming area at the edge of the India-Asia collision zone. Therefore, we quantify the current velocity field of the Potwar Plateau – Salt Range fold-and-thrust belt using GNSS horizontal surface velocities and Sentinel-1 interferometry line-of-sight velocities. From this velocity field which indicates a creep of the Potwar Plateau along the Main Himalayan Thrust, we infer a weak subhorizontal décollement level formed by a massive Precambrian salt layer. South of the Plateau, the Salt Range is uplifted along the Salt Range Thrust up to 5 mm/yr. The Kalabagh Fault, which forms the western boundary of the Salt Range and the Potwar Plateau, exhibits a creep rate along fault of 3.3 mm/yr. To characterize the slip distribution and coupling along the faults, we use numerical modelling with a set of dislocations in an elastic half-space. The preferred model shows the presence of a large asperity along the décollement level beneath the Potwar Plateau and several smaller asperities along the eastern basal thrust. These observations are consistent with the occurrence of the 2029 Mirpur earthquake of M_w 5.9 along the eastern part of the décollement level. Along the southern and superficial parts of the Salt Range Thrust, the model indicates a slip rate of 20 mm/yr which is greater than the 14 mm/yr slip rate along the Main Himalayan Thrust at depth. This observation suggests the existence of an internal southward flow of the massive salt layer along the upper part of the Salt Range Thrust. For the Kalabagh strike slip fault, an alternation of coupled and decoupled zones is observed, meaning that this fault can be characterised by creep and asperities where earthquakes and/or slow slip events can occur. Considering the lack of instrumental and historical large magnitude earthquakes in the area since the AD 25 Taxila earthquake, it can be concluded that the Main Himalayan Thrust and the Kalabagh Fault are likely to be affected by large magnitude earthquakes.

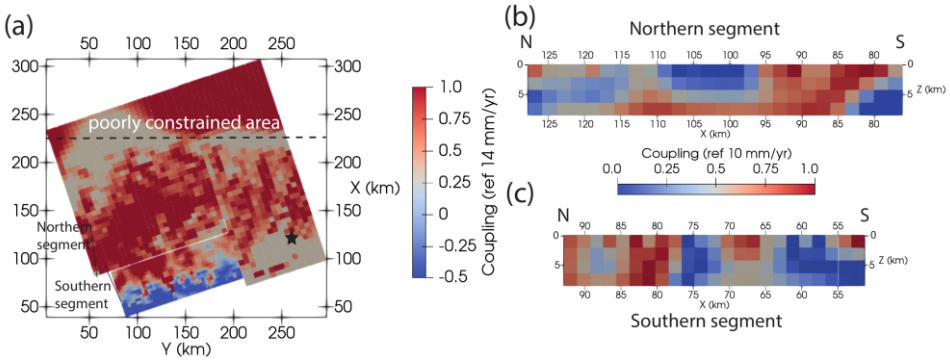

Coupling distribution: (a) along the 3 dislocations representing the décollement level with a velocity reference of 14 mm/yr which is the mean displacement rate on the MHT at depth (Kundu et al., 2014), (b) along the northern segment of the Kalabagh Fault with a reference of 10 mm/yr and (c) along the southern segment of the Kalabagh Fault with a reference of 10 mm/yr. The coupling results are represented in a local reference frame with origin fixed at 32°N 71°E. The black star indicates the epicentre of the 2019 Mirpur earthquake.

Shoaib Ayjaz MOHAMMED

Towards seismic metamaterials: From forests to wind farms to cities

Year 5

Supervisors: **Philippe Roux**

Ondes & structures / Waves & structures

It is well established that the presence of the urban agglomerate significantly modifies the free-field ground motion at the city scale. Each building can behave as a resonator, trapping a small fraction of seismic surface waves that is reradiated into the ground. But when tall buildings are densely clustered, like in a city, can we anticipate low-frequency surface waves to interact with them in unusual ways? Perhaps yes. Recent evidence suggests resonance coupling between vibrating structures leads to anomalous dispersion of surface waves causing them to become evanescent in certain frequency bands. Such media are called `locally-resonant' seismic metamaterials, and the collective behavior when several structures are present inside one seismic wavelength corresponds to the physics observed at the lab-scale for elastic waves in a plate with a set of rods attached to it.

This doctoral thesis focuses on metamaterial physics at the geophysics scale (a few meters to a few kilometers) in the urban seismology context. We analyze ambient noise recordings inside a forest of pine trees and inside wind farms, which are ideal proxies for a city with tall buildings. From the META-FORET experiment dataset, we find that around the tree longitudinal resonance frequency, the energy radiated by the trees is evanescent inside the forest. We extend this hypothesis of coupled resonators to a forest of wind turbines with the META-WT experiment in the Nauen wind farm (Germany). The noise data from dense array deployments including DAS (Distributed Acoustic Sensing) fiber optic cable gives us interesting insights into the near-field radiation of the turbines. From the spectral analyses, as well as noise correlations of the wavefield, we conclude that the surface waves strongly attenuate in distinct frequency bands, suggesting a metamaterial-like effect inside the wind farm.

The experimental and numerical studies in this thesis directly contribute to the understanding of how seismic surface waves interact with specific features of the urban landscape from the novel perspective of metamaterial physics. The results will have important implications for seismic hazard in urban areas.

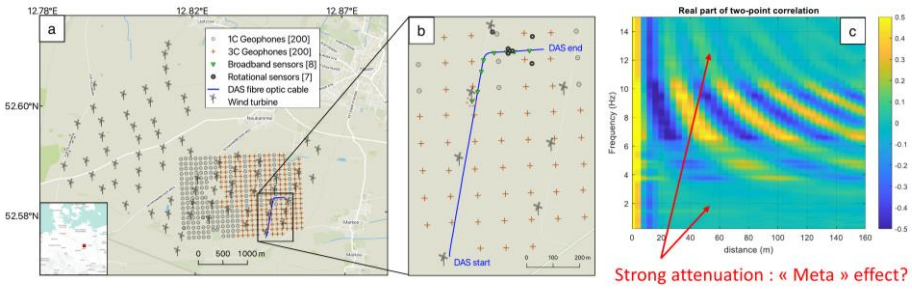

META-WT experiment array configuration (a) in the Nauen wind farm, Germany (see location in the inset) with a zoom on the DAS fiber optic cable (b). Real part of the normalized two-point correlation function plotted as a frequency-vs-distance representation (c). The surface waves exhibit strong attenuation in various frequency bands which can be attributed to the metamaterial-like behavior of the wind farm.

Tristan MONTAGNON

A new Deep-Learning approach for the sub-pixel correlation of optical images in the near-field of earthquake rupture

Year 3

Supervisors: James Hollingsworth, Sophie Giffard-Roisin, Erwan Pathier, Mauro Dalla Mura (GIPSA Lab)

Cycle sismiques et déformations transitoires / Seismic cycles and transient deformations

Precise estimation of ground displacement from correlation of optical satellite images is fundamental for the study of natural disasters. In the case of earthquakes, characterizing near-field displacements around surface ruptures provides valuable constraints on the physics of earthquake slip. Recently, image correlation has been used to investigate the degree of slip localization, and how it may vary as a function of geological parameters (such as fault structural maturity), raising the possibility that slip localization (vs distribution) may be predictable, with important implications for seismic hazard assessment.

Current sub-pixel correlation methods (frequency or spatial domain) all rely on the same general approach: they work at a local scale, with small sliding windows extracted from a pair of co-registered satellite images acquired at different times, and they assume a rigid uniform shift between the two correlation windows. However, in the near-field of fault ruptures, where the correlation window spans the fault discontinuity, this hypothesis breaks down, and may bias the displacements. Additional smoothing associated with the correlation window further complicates the interpretation of sharp features in the displacement field, artificially shifting displacement to the off-fault region.

We developed a U-net-based method to solve the sub-pixel displacement estimation problem at a global scale. Such architecture is able to retrieve full scale surface displacement maps, making use of both global and local features, and potentially tackling different noises of the input images. We trained our model with real satellite acquisitions, warped with ultra-realistic synthetic displacement maps representing realistic faults. The model exhibits promising preliminary results, showcasing its capability to retrieve full-scale surface displacement maps with high accuracy. While direct comparisons with other state-of-the-art approaches (COSI-Corr and MicMac) are pending, our findings suggest that our proposed U-net-based approach has the potential to compete or even outperform these correlators.

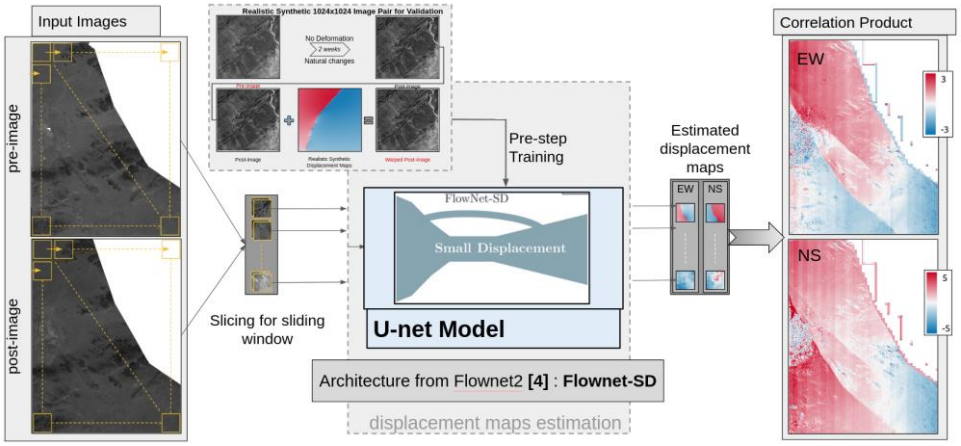

U-NET pipeline estimating full EW & NS ground displacement fields from optical satellite images

Sarah MOUAOUED

Exploration des données sismiques de Ridgecrest en 2019 à l'aide d'une méthode en apprentissage profond non supervisée

Year 3

Supervisors: **Michel Campillo**

Ondes & structures / Waves & structures

On analyse des données sismiques continues enregistrées à proximité du séisme de M_w 7.4 qui a eu lieu à Ridgerest en 2019. On utilise une méthode en apprentissage profond non supervisée proposée par Seydoux et al. (2020), à la recherche de signatures sismiques ou physiques de la phase préparatoire du séisme. On a téléchargé les données des 3 stations différentes B918, avec une fréquence d'échantillonnage de 1000 Hz, SRT et CLC avec une fréquence d'échantillonnage de 40 Hz. à l'aide d'un réseau de scattering combiné avec une Analyse en Composante Indépendantes (ICA), on définit des caractéristiques plus stables pour nos formes d'onde. Puis les signaux continus, extraits à l'aide d'une fenêtre glissante, sont groupés avant d'en proposer une interprétation en fonction de la famille à laquelle ils appartiennent. On discute également davantage les résultats de concert avec des données externes tel qu'un catalogue de sismicité locale obtenu indépendamment. Nous avons aussi analysé une représentation de nos coefficients de scattering basé sur une approche dite en manifold learning (UMAP). Selon nos premiers résultats fusionnés avec l'analyse du catalogue de sismicité on est capable de séparer les différents évènements du bruit et d'identifier différents types de bruit et de sismicité.

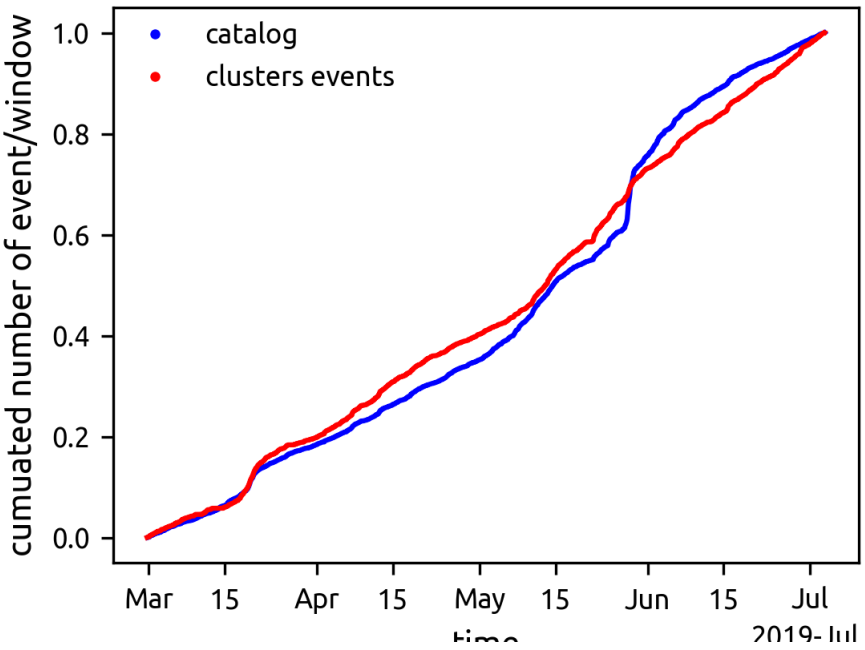

Le cumul de la détection des groupes contenant des évènements, correspond en partie à celui du cumul du nombre d'évènements du catalogue de sismicité.

Victoria MOWBRAY

Integrating geophysical, structural and tectonic data in a probabilistic seismic hazard assessment (PSHA) for the South-East of France

Year 1

Supervisors: Céline Beauval, Anne Lemoine (BRGM), Marguerite Mathey (IRSN)

Cycle sismiques et déformations transitoires / Seismic cycles and transient deformations

Identifying and studying active faults is crucial for assessing seismic hazards and implementing measures to mitigate earthquake risks in areas prone to seismic activity. The region of South-East France is found in a tectonic domain where seismic activity is low to moderate and crustal deformation is slow, nevertheless about one magnitude 6 earthquake is recorded per century (Bertrand et al., 2007). Social vulnerability to seismic hazard in South-East France is noticeble, specifically due to the presence of urban agglomerations, chemical industries and most importantly, nuclear facilities.

Today's seismic activity in this region is of transtensional behaviour and is dominated by the ongoing tectonics of the post-alpine orogen and gravitational isostatic adjustments (Sue et al., 2007). However, the near future location and magnitude of this activity is not well constrained due to the relatively small-time windows of seismic records and GPS data aquisition in respect to the seismic cycle of a slow deformation domain. The available knowledge on potentially active structures which determine the location of events is low, affirmed after the unexpected 4.9 M_w Teil earthquake in 2019 (Cornou et al., 2021).

My work aims to analyse all major tectonic structures in the South-East of France and re-evaluate their near future rupture probability in accordance to the instrumental and historical seismicity and the stress field. The characterisation of potentially active faults in a slow deformation domain is a complex task which requires the determination of uncertainty levels for the defined data. For this, a methodology of estimation of fault activity and information reliability is proposed. The resulting fault dataset from this study will then be applied for the construction of a multidisciplinary and complex source model which considers all possible ruptures for a PSHA study of the area.

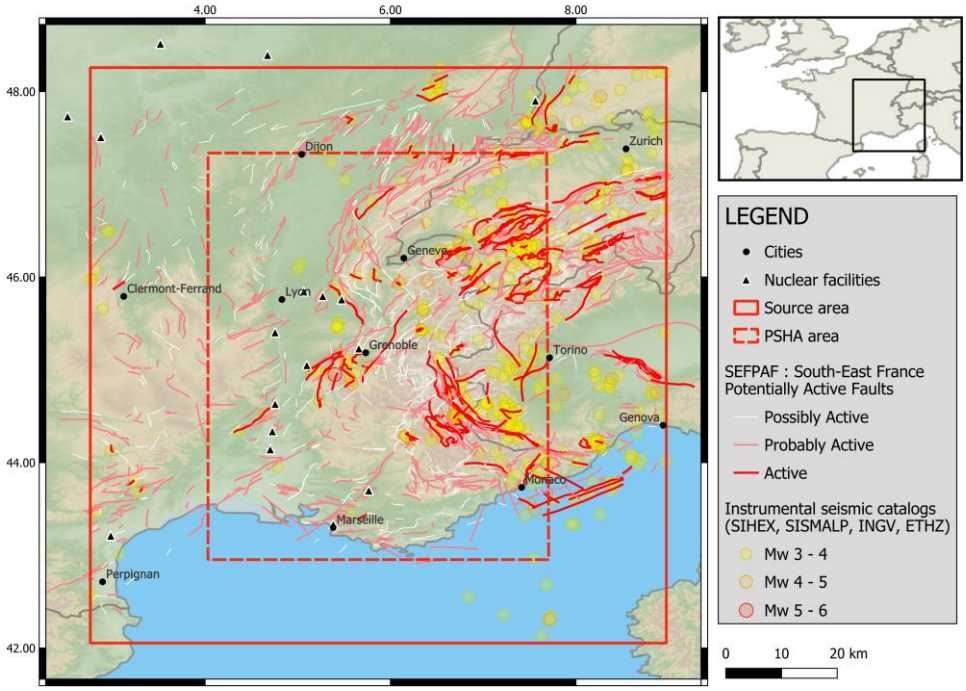

Fig.1 Study zone with the area comprised for a seismic source model and the area comprised for the PSHA results. The location of vulnerable sites is plotted (cities and nuclear facilities). The instrumental seismic catalogs represent the seismic activity from the last 60 years with moment magnitudes 3 to 6. The SEFPAF fault catalog (produced during this PhD) is plotted, distinguishing the faults by their activity index (1 - Possibly active, 2 - Probably active and 3 - Active).

Naomi NITSCHKE

Restoration of gold-mining sites in French Guiana : Stabilisation and fate of natural and anthropogenic Hg and Pb

Year 3

Supervisors: Stéphane Guédron, Jennifer Hellal (BRGM Orléans), Arnauld Heuret (Université Guyane)

Géochimie / Geochemistry

French Guiana is experiencing a new rush in artisanal and small-scale gold mining (ASGM). Unlike illegal ASGM, legal mines extract gold without mercury (Hg). However, both mining activities have an impact on Hg emissions to rivers as they involve deforestation and soil excavation, remobilising particles from naturally Hg-rich Amazonian soils. In French Guiana, legal mines are responsible for restoring their sites after exploitation, through landscaping and replanting. However, the impact of legal mines on particle and contaminant fluxes, and the efficiency of their restoration is not fully characterised, as their remote location makes continuous monitoring challenging.

In this study, we monitored particle and Hg fluxes during rain events, comparing two different sites on a small scale legal alluvial gold mine: one replanted site with trees and vegetation cover (>3 years), and a site with bare soil (< 6 month). Fluxes were monitored over three campaigns spanning one year, and indicators related to soil restoration were measured (i.e., root density, enzyme activity and DNA concentration).

Results showed that THg (dissolved + particulate) fluxes were reduced 3-fold over one year in the non-replanted site. Hg fluxes in the replanted site were 100 times below the non-replanted site at the beginning of the study (1.7 ng Hg/m^2/L rain), and close to zero after one year. These results are explained by the increase in root density due to spontaneous revegetation on both replanted and non-replanted sites (7 and 4.5 fold, respectively). Initial soil restoration with an increase in some enzyme activity (arylsulfatase) was also observed on both replanted (3-fold) and bare soil (4.5-fold) sites.

This indicates that spontaneous revegetation significantly decreases particle and Hg fluxes from the restored mining to the downstream watershed. To reduce completely fluxes and enable soil refunctionalisation, the relevance of assisted revegetation (replanting) is demonstrated here.

Temporal evolution of a gold mining flat in French Guiana after the restoration phase.

Piel PAWLOWSKI

Study of the mantle transition zone by combining earthquake data and seismic noise data: application to the Alps and Massif Central

Year 1

Supervisors: Helle Pedersen, Pierre Boué

Ondes & structures / Waves & structures

The mantle transition zone is a key element in the dynamics of the inner Earth. Knowledge of its geometry, i.e. the depth and detailed structure of its upper and lower boundaries (the so-called 410 and 660 km discontinuities), makes it possible to determine mantle temperatures and constrain its composition. The 410 and 660 km discontinuities are observed by seismic waves, mainly by P- and S-wave reflections. But each type of wave provides only partial information on the discontinuities. The aim of the thesis project is to combine classical and new observations to clarify the characteristics - thickness, discontinuity depths, velocity contrasts, etc. - of the mantle transition zone, with two main targets: the Alps and the Massif Central.

The opportunity to combine different body wave observations to study the mantle transition zone has only recently become apparent. The classical method relies on the conversion of P-waves from teleseismic waves to discontinuities (receiver function method). Today, we also need to be able to analyze P-waves generated by seismic noise and reflected by mantle discontinuities. Based on a set of mineralogical and mantle temperature models discussed with a group of experts, we will compare synthetic seismic signals and real data to better describe the mantle transition zone.

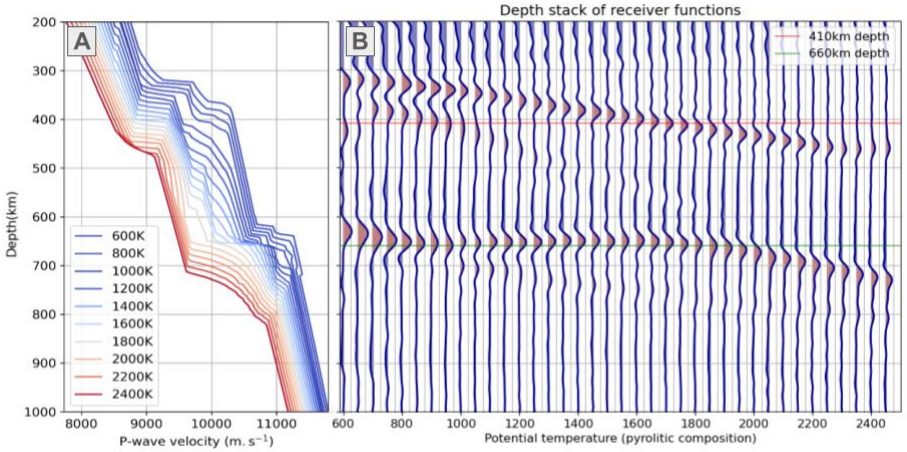

Panel A: P-wave velocity profiles for a pyrolitic composition between 200 and 1000 km depth. Colors represent potential temperature (i.e. surface temperature for an adiabatic temperature profile in the mantle). Panel B: Synthetic depth-migrated receiver functions calculated using AxiSEM in the corresponding 1D models on the left-hand side.

Pei PEI

New hydraulic profile along the IODP borehole by combining drilling and logging-while-drilling data: Application to Japan Trench

Year 1

<u>Supervisors:</u> Mai-Linh Doan

<u>Mécanique des failles/ Fault mechanics</u>

Subduction zones have an extremely rich spectrum of seismic activity, which may be controlled by fluids. Drilling is a technique to provide direct information of the hydraulic properties of these subduction zone. A new technique has been developed to determine a continuous profile of fluid flow to the borehole, to describe the extent of damage around a fault zone and identify the main hydraulic channels within subduction zones (Pwavodi and Doan, 2024).

The technique is extended to other subduction zones (Nankai, Tohoku, Hikurangi,…). Especially, we revisit the Japan Trench Fast Drilling Project (JFAST), an Integrated Ocean Discovery Program (IODP) expedition in 2012, which sampled the shallow plate boundary of the Japan trench, less than 1 year after the 2011 M_w 9.1 Tohoku earthquake. This area experienced an unexpected large slip at the shallow trench, which may have helped by fluid lubrication of this area.

The method of Pwavodi and Doan (2024) has been improved, to provide a continuous estimate of hydraulic flow to the J-FAST borehole. The result of re-analyzing the average annular pressure (APRS) during drilling at site C0019B clearly shows there is little fluid flow from the formation to the borehole, even within the damage zones around the plate boundary. This suggests that any fluid overpressure prior to the earthquake has been dissipated. This is consistent with stress measurements from J-FAST that shows that tectonic loading has been fully relaxed after the 2011 megathrust earthquake.

The J-TRACK expedition, scheduled in Autumn 2024, will revisit the same site. By reusing the same techniques, it will be possible to check any hydromechanical reloading and healing of the shallow plate boundary, 13 years after the earthquake.

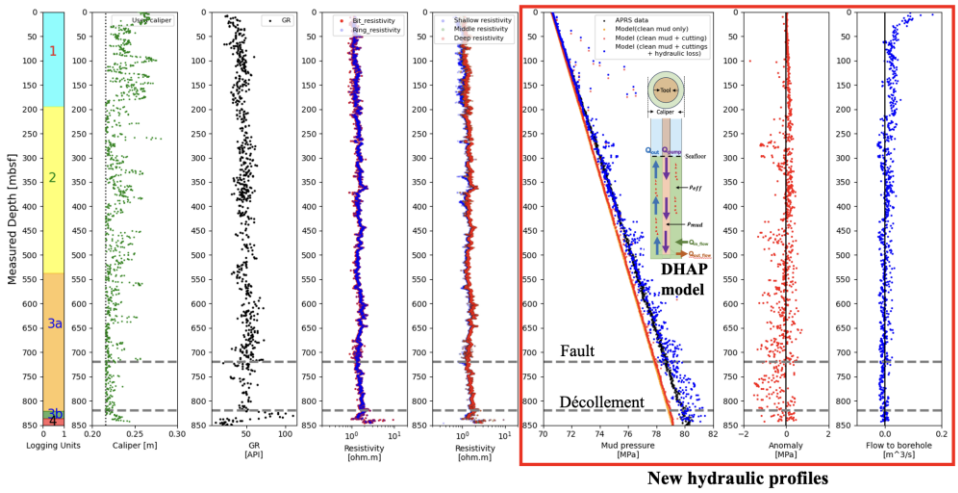

Contrary to cores, geophysical data provide continuous information about the formation crossed by the borehole. Our technique, based on additional drilling information, provide new high resolution hydraulic profile along C0019B, that crossed the Tohoku subduction interface.

Arpad PUSZTAI

Shedding new light on basaltic glass weathering by combining reactor and soil column experiments

Year 2

Supervisors: **Damien Daval, Bastien Wild**

Géochimie / Geochemistry

The weathering of calcium and magnesium silicates plays a significant role in the long-term carbon cycle, by initiating the formation of carbonate rock and providing important nutrients for surface ecosystems. Basaltic glass, one of the most reactive and abundant silicate phases, has been extensively studied in laboratories for its dissolution rates and kinetics under varying pH, temperature, and solution compositions. However, laboratory measurements made on freshly ground powders and surface area conversions relying mainly on BET surface area are not necessarily suitable for scaling with dissolution rates. Additionally, only considering surface alteration layers and potential biotic enhancements fails to explain weathering rates measured in natural settings.

To address this gap, this study examined the dissolution of basaltic glass using monoliths with controlled initial surface properties. An approach based on surface sensitive techniques, including vertical scanning interferometry (VSI) and atomic force microscopy (AFM), enabled accurate scaling of the weathering rates to geometric surface area. In-depth investigations of the resulting surfaces unraveled signatures of weathering processes associated with various dissolution conditions. In parallel, similar samples were introduced in soil columns cored from Réunion Island to shed light on factors controlling basaltic glass dissolution in more complex environment. Where overall surface retreats as well as specific retreats related to observed microorganisms were studied.

In addition, we are studying the surface alteration layers developing in both of these experiments to understand a potential reason for observed long term low weathering rates.

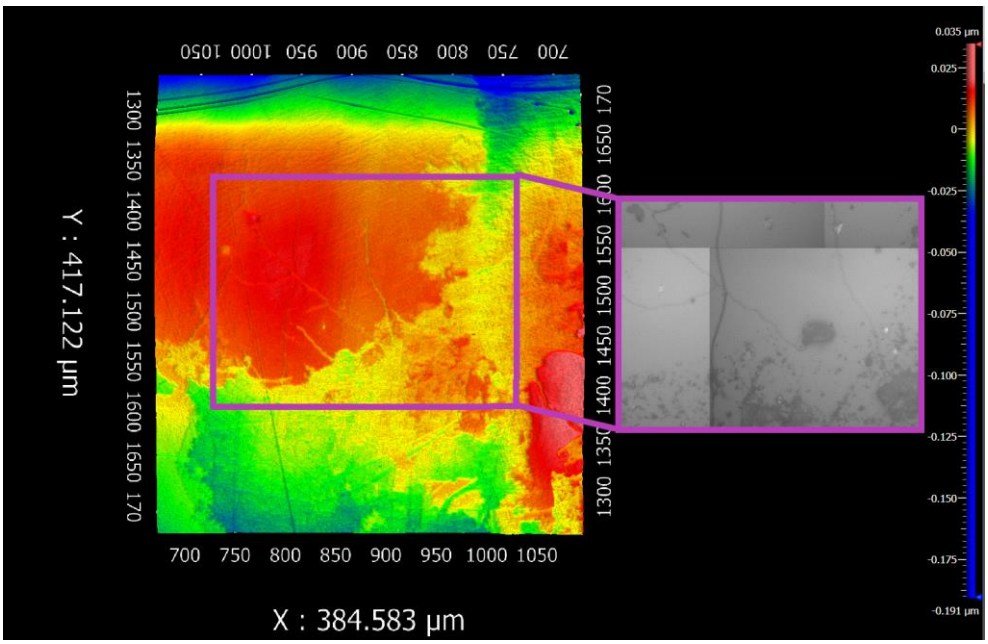

Correlating observations of filamentous organisms and surface features impacted by them.

Marcelline PÉAN

Ice cap fluctuations in East Antarctica (Terre Adélie): contributions from a geomorphological and geochronological approach

Year 1

Supervisors: **Yann Rolland (USMB, Edytem), Pierre Valla**

Tectonique, Reliefs, Bassins / Tectonics, Reliefs, Basins

The response of the East Antarctic Ice Sheet (EAIS) to long-term climate variations is still poorly understood, yet it is essential for modelling its future behaviour and its contribution to sea-level rise. The studies are based on offshore ocean sedimentary records, and not on all the EAIS interaction domains. The aim of our study is to obtain geochronological data on the coastal region of Terre Adélie in order to supplement that already acquired on the scale of the EAIS, and to reason about the interactions between ocean currents and the cap, in particular with the major glaciers along the coast of the sector - the Astrolabe and the Zélée. Our initial $^{26}Al/^{10}Be$ results on erratic boulders from the Lacroix moraine reveal a complex exposure history, suggesting a very ancient formation (Pliocene), or punctual and multiple episodes of deglaciation during the Plio-Pleistocene. These results should help to constrain the modelling of ice flows.

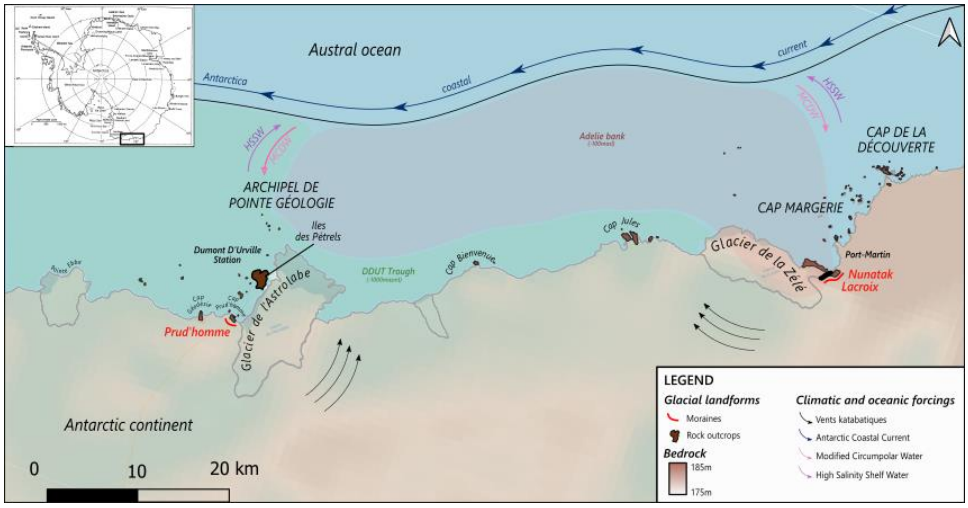

This map represents the main EAIS interaction domains : (1) oceaning forcings through different currents carrying warm waters (2) katabattic winds, both eroding the ice cap.
Rare rock outcrops and moraines are also represented as they are the main material to apply geochronology (cosmogenic nuclides datation) and document the last deglaciation (since 20ka). Results on moraine Lacroix are in treatment. And moraine of Cap Prud'homme is to be dated in the next Antarctic mission. These results serve as constraints for glaciological model reconstructing ice cap behaviors.

Camila Celeste RIBA PEREYRA

Magnetotellurics for investigating fractured geothermal reservoirs

Year 2

Supervisors: Jean-Luc Got, Anna Martí Castells (Universitat de Barcelona), Éric Benoit (USMB / LISTIC Laboratoire)

Géophysique des volcans & Géothermie / Geophysics of volcanoes & geothermal energy

Magnetotellurics (MT) faces two main challenges regarding the data quality when the recordings are acquired in urbanized areas: 1) The low signal-to-noise ratio if the noise sources are close to the measurement station and/or if the noise is correlated between channels and/or between stations and 2) The decrease in the spectral power of the natural signal due to the dead-bands.

To study a potential shallow geothermal reservoir located at 1.5-2km depth, range comprising the low frequency dead-band, one of the aims is to discern between the most appropriate rejection criteria during robust processing when dealing with data affected by anthropic correlated noise.

53 sites have been set up to record MT data close to an active strike-slip fault, at low and high frequency sampling rates. Various processing methods based on robust approaches have been used to reprocess 43 usable sites, comprising bivariate and multivariate approaches. Different rejection criteria are analyzed and selected, including statistical outlier's rejection and time-dependent window selection by the eigenvalue criteria from the FFMT software [1].

Preliminary results show a major improvement when using the FFMT aproach and criteria, as it is capable of detecting and rejecting time windows containing correlated noise for each target frequency at a given site. 1D inversion models at many sites are well-resolved down to ~2.5 km depth. This positive result encourages the research on this line.

After the analysis of the different processing approaches and rejection criteria, we are currently working on the characterization and quantification of the dimensionality of the geoelectrical structures and the hypothetical anisotropy on the MT data. We expect the Vuache fault damaged zone to be anisotropic due to its fracturing. The aim of our study is to characterize this eventual anisotropy by analyzing the MT resistivity tensor.

[1] Castro, C., Hering, P. & Junge, A. (2020), FFMT: a MATLAB-based toolbox for Magnetotellurics (MT). 10.13140/RG.2.2.12465.92007.

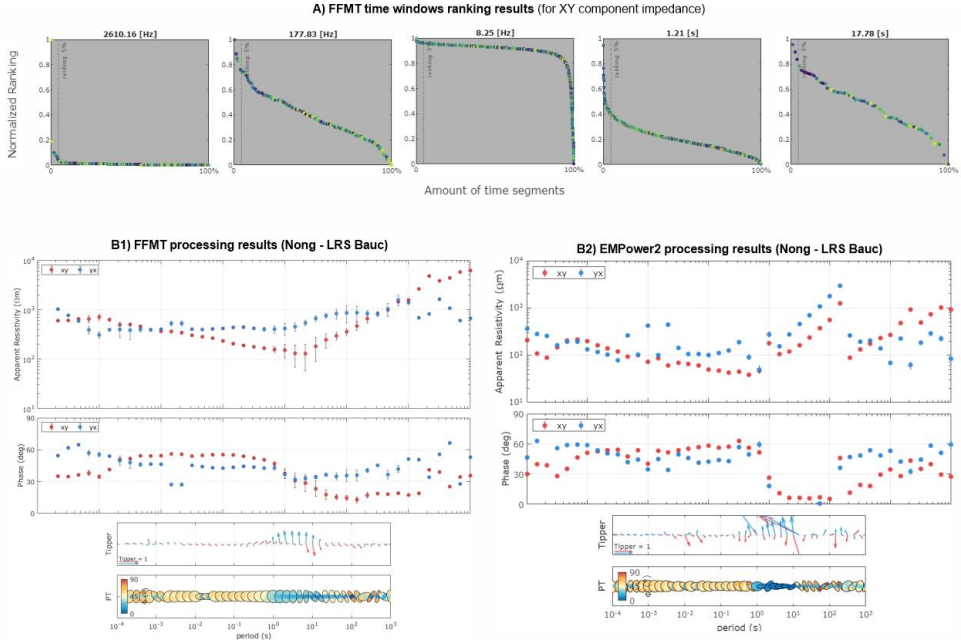

A) Ranking results for 5 target frequencies after applying the FFMT criteria. The HF and LF dead bands are visible at 2610Hz and 1.21s.
B) Processing results. B1) The FFMT multi variate approach gives stable results, especially visible for the tipper, and improves the smoothness on the LF dead band. The results are obtained by saving just the best 5% of the time segments ranking, as shown in figure A. B2) Results obtained by the bivariate approach of EMPower2 and applying a post-processing phase quadrant criterion.

Aurélien RIGOTTI

Investigating the rheology of the marginal ice zone trough DEM simulations of a dry frictional granular material

Year 2

Supervisors: **Jérôme Weiss**

Mécanique des failles/ Fault mechanics

In sea ice, the strain experienced at the local (micro) scale has a significant influence over the deformation patterns that emerge at much larger (macro) scales. With this idea in mind, this study aims at improving the current grid-scale (i.e., mesoscale) parameterisations of sea ice strength for continuum sea ice models used for short and long-term predictions of sea ice conditions in the Arctic and Antarctic, by formulating a constitutive law and coupling functions between its ice-strength parameters (apparent viscosity and elastic modulus) and the state (packing fraction, level of damage, floe size distribution) of the sea ice cover at the subgrid-scale, and in particular in the closed-packed limit. To do so, a molecular dynamics model (LAMMPS) is used to compute the apparent level of damage, viscosity and elastic modulii at the scale of an idealized, frictional, granular assembly of ice floes and to establish its dependence on the applied shear rate, friction coefficient and, eventually, its granular concentration.

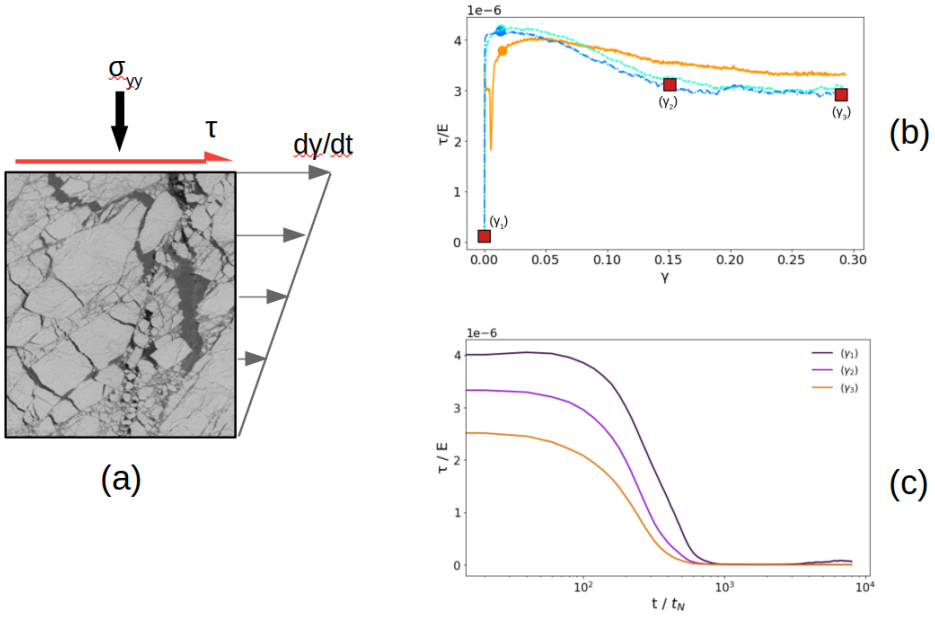

(a) Schematic representation of the experimental set up used to investigate the rheology of granular sea ice. A constant pressure and shear strain rate is applied to the system until great deformation is reached. (b) Shear stress versus shear strain evolution. An elasto-visco-plastic-like behavior is recovered. (c) Evolution of the shear stress under relaxation conditions. As the shear strain increases in the granular packing, relaxation time decrease and a constant residual value is obtained.

Pauline RISCHETTE

Optimization of seismic motions recordings in free field for a better estimation of the seismic hazard

Year 2

Supervisors: **Fabrice Hollender, Paola Traversa (EDF TEGG), Emeline Maufroy**

Géophysique des Risques sismiques et gravitaires / Geophysics of seismic and gravity risks

A proper and reliable measurement of ground motion is essential for an accurate estimate of the seismic hazard. Current ground motion databases used to develop Ground Motion Models (GMM) rarely provide information about the station housing and sensor installation conditions. Therefore, users often assume that these sensors are installed in free-field condition, i.e. at the natural surface of the ground without disturbances related to nearby buildings or structures. Nevertheless, the analysis of the information collected from seismological networks worldwide has highlighted a large variety of sensor installation modalities, including the housing typology, the coupling of the seismometers etc . Recent studies have shown that different installation conditions can have a significant impact at high frequencies on the recorded ground motion, in comparison with true free-field measurements.

My PhD focuses on the qualification of three types of installation effects on ground motion, through several experiments that have been set up in Greece (mainly in Kefalonia Island) . The first effect is addressed through the “ArgoScarp” experiment and concerns the influence of the topography at short wavelengths. Ground motions recorded at sensors installed along a profile going from the foot to the top of a cliff about twenty metres high are compared among them and with respect to a reference. Second, the effect of the soil-sensor coupling typology is studied in the framework of the “ArgoSlab” experiment, where about 30 seismometers have been installed (i) on concrete slabs of different size and shape, (ii) on seismic pillars, (iii) inside manholes, (iv) outdoor or sheltered, and compared to free-field recordings. Finally, the effect of the soil-structure interaction is studied by analysing the ground motion recorded by sets of sensors set up inside and very close to buildings that are hosting several greek key stations with respect to free-field measurements.

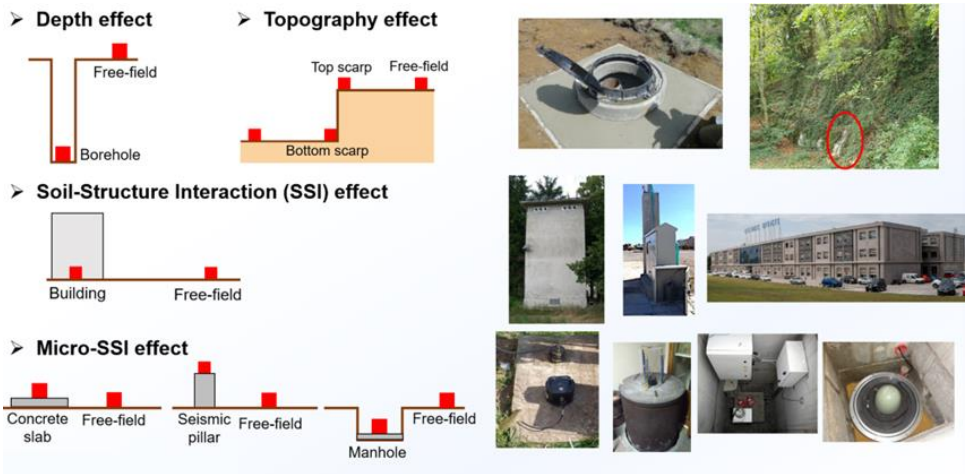

List of the installation effects to be investigate: depth effect, topography effect, SSI effects at the scale of buildings and the scale of slabs.

Georges SABBACK

High-resolution multi-scale multi-physics multi-dimensional seismic numerical twin based on massively parallel high-performance

Year 1

Supervisors: **Cécile Cornou**

Géophysique des Risques sismiques et gravitaires / Geophysics of seismic and gravity risks

My thesis focuses on developing a digital twin (EFISPEC3D) to predict ground movements in deep sedimentary valleys, with the Grenoble valley as a case study, with existing H/V data.

After reviewing relevant literature, I am currently conducting simulations based on sedimentary layer designs from Vallon 1999. These simulations utilise vertical plane waves in both 1D and 3D models.

I am comparing time and frequency series obtained from different methods to validate the EFISPEC3D approach. So far, simulations have been conducted on a model with a maximum meshing frequency of 2 Hz (that is the validity of the analyses). I am also in the process of post-processing and developing scripts to detect and analyse body waves and find their characteristics.

Future work includes:
- Continuing the analyses.
- Expanding the frequency range of meshing and reanalysing.
- Comparing different methods and calculating 3D/1D aggravation factors.

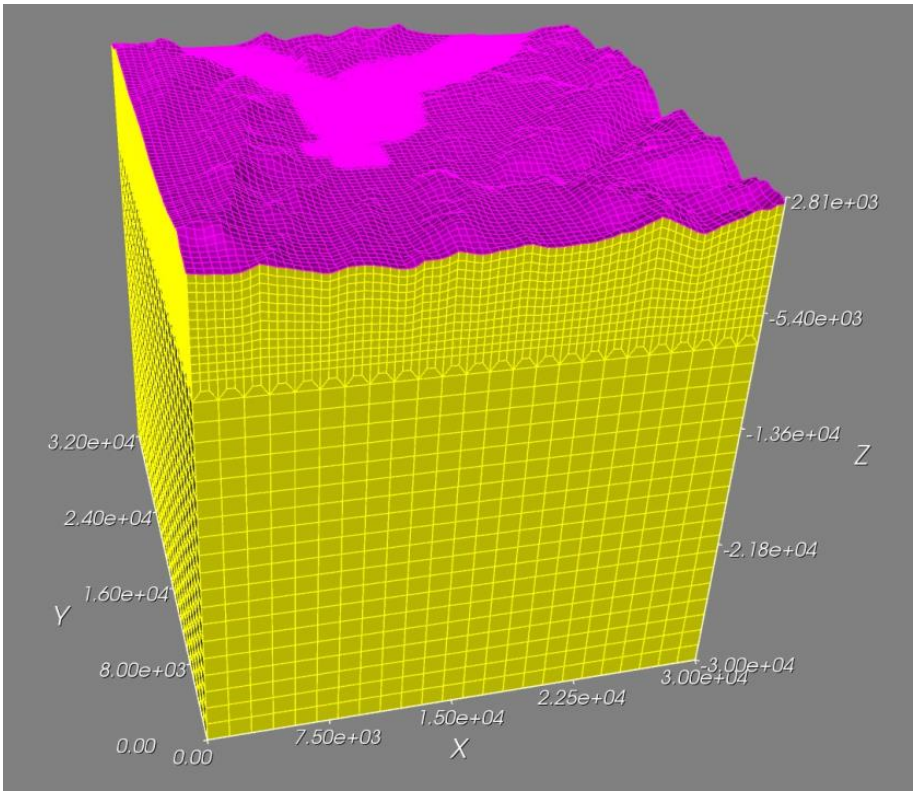

The Grenoble basin model mesh, valid to a frequency of 2 Hz. The dimensions are in km and the Y-axis in the positive direction is the North orientation.
The Y-shaped refinement is the sedimentary part of the basin.

Diksha SAINI

Redox reactivity of Selenium in environmental geomedia

Year 3

Supervisors: Alejandro Fernandez-Martinez

Géochimie / Geochemistry

Due to its long half-life of 3.27×10^5 a and high activity, ^{79}Se is an important radionuclide to monitor for a correct assessment of the safety of nuclear waste repositories. Selenium is present in five oxidation states in nature ranging from −II, −I, 0, +IV, and +VI. Selenium solubility is controlled by its oxidation state, hence depends on the redox conditions present in soils, sediments, rock and aquifers. The −II, −I and 0 oxidation states are commonly predominant in "reducing" anoxic environments, while the +IV and +VI states predominate in "oxidizing" environments . Selenate [Se(VI)], the most oxidized form of Se, is an anion with high mobility in the pore waters of the Callovo-Oxfordian (COx) clayey formations that could potentially host the French repository for high-activity and long-life nuclear wastes (HLW). It is therefore important to evaluate the possible redox reactions that could lead to a decrease of its mobility, with a change in its oxidation state, in the environmental conditions of the repository.

It is known that magnetite, a Fe(II)-containing solid phase present as a result of the corrosion of the steel canisters and in natural COx clayrock, can reduce selenate to elemental Se, a non-mobile solid species. Selenate is an oxyanion that is typically adsorbed via the formation of outer-sphere complexes, and for which kinetic barriers for electron transfer could be high. The interactions with Fe(II) and S(−II)-bearing redox active solids- mediate the oxido-reduction kinetics of selenium oxyanions, playing an important role in the control of Se speciation. Regarding Se(VI), it has been found to be metastable (far from thermodynamic equilibrium) and to co-exist in different oxidation states in the COx pore waters. The reduction of Se(VI) by magnetite, much slower than for Se(IV), has been described to include different steps: adsorption, reduction to Se(IV), and further reduction to less soluble Se phases, each of them imposing a kinetic barrier for the whole reduction process. At present it is not clear whether the Se(VI) initial adsorption or its reduction to Se(IV) are concomitant or not, and extra work needs to be done in this direction to establish the reduction pathway. Though it has been shown that Se(VI) can be reduced by Fe(II)-bearing solids [3,4] such as magnetite or pyrite, little is known about the potential competition with other aqueous ions present in the COx porewater such as carbonate or sulfate. These ions have been shown to adsorb forming both outer and inner-sphere complexes, therefore potentially limiting the contact of Se(VI) molecules with the Fe(II)-bearing solids, and therefore potentially inhibiting the electron transfer necessary for Se(VI) reduction. The aim of this work is to study the redox reactions of Se(VI) with magnetite and pyrite under neutral pH conditions at both macroscopic and molecular levels by combining batch sorption studies and advanced spectroscopic techniques. In addition, the influence of sulfate and carbonate ions present in the pore waters of the COx clay rock will be investigated. The presence of these ions could pose kinetic barrier for the reduction of selenate at the magnetite-water interface.

A series of batch experiments (sequential addition) were performed at pH 7 under anoxic conditions by pre-equilibrating (14 days) the magnetite suspension with sulfate and then introducing selenate. Another series was performed by simultaneous addition of sulfate and selenate. In both cases, a reduced uptake of selenate with increasing sulfate concentrations was noticed at the macroscopic level. As shown from XANES measurements (Figure 1), the competing effect of sulfate slows down the electron transfer from the magnetite to the aqueous selenate. Indeed, a higher degree of reduction of the selenate to elemental Se is observed in the absence of sulfate. This result points to a limited electron transfer under sulfate-rich conditions, probably due to specific interactions of the magnetite surface with the sulfate ions.

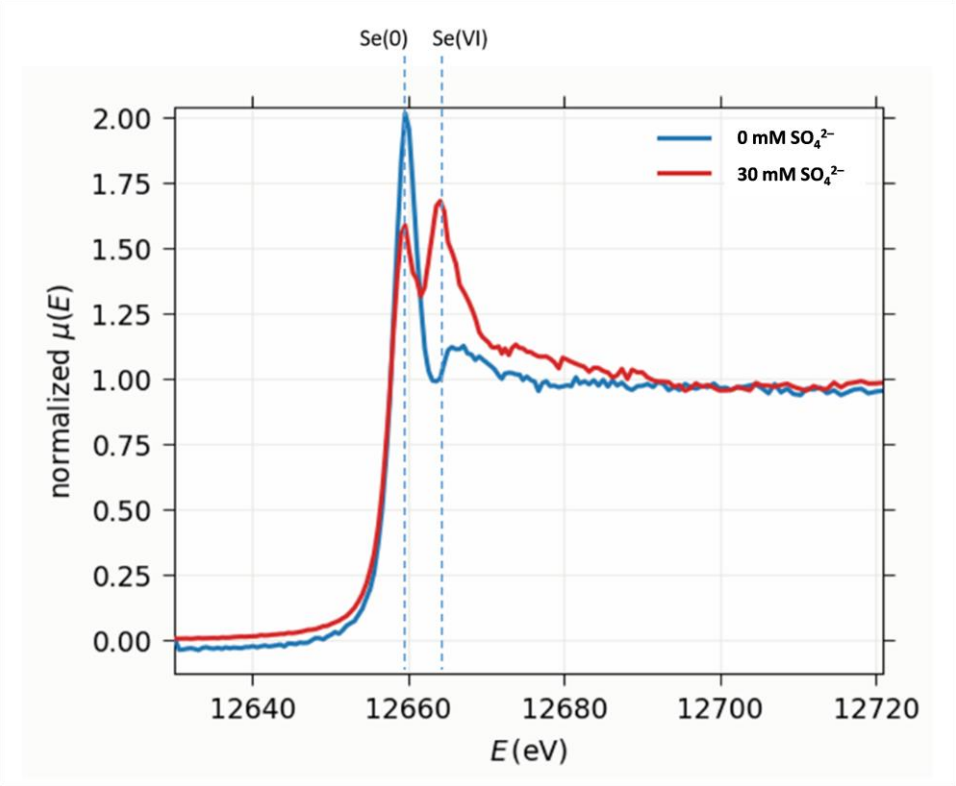

Figure 1. Se K-edge XANES spectra of two samples of magnetite reacted in the presence and absence of sulfate at pH 7 and equilibration time of 3h (sequential addition).

Nicolas SALERNO

Dynamics of stakeholder decision rules and their impact on subsoil resource needs assessment

Year 1

Supervisors: Olivier Vidal

Minéralogie et Environnements / Mineralogy and Environments

My PhD involves developing a serious game based on the DYMENDS model. My work ranges from introducing decisions into the model to designing the game. The game aims to interest different audiences in the systemic effects between the energy-matter nexus (with a focus on mineral resources) and multiple socio-economic processes.

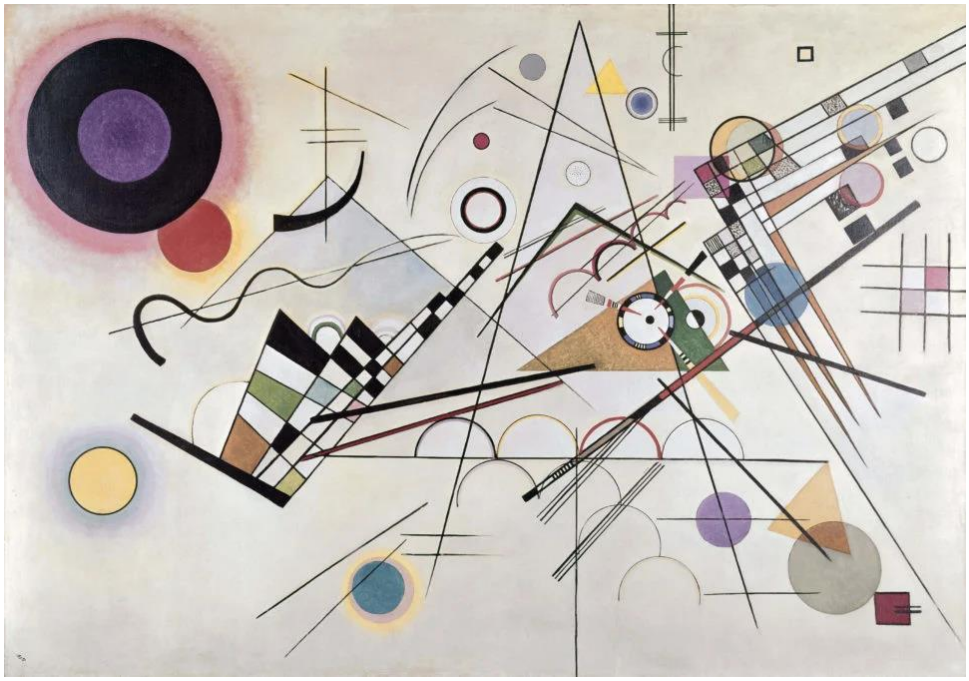

Composition 8, 1923 by Vasili Kandinsky. The abstract style of Kandinsky represent well the epistemological challenges of my thesis.

Valentin SCHINDELHOLZ

Satellite imagery strategies for earthquake strong-motion prediction and shakemap generation

Year 2

Supervisors: **Cécile Cornou, Emeline Maufroy**

Géophysique des Risques sismiques et gravitaires / Geophysics of seismic and gravity risks

The objective of this project is to develop an alternative and innovative method for accurate estimation of sediment thicknesses and prediction of sediment resonance periods (both being physical parameters to the seismic response of valleys) based on InSAR satellite images. Indeed, recent studies have shown the ability of the InSAR approach to map subsidence rate with millimeter accuracy, especially in urban areas. With the exception of anthropogenic causes (pumping, presence of heavy urban infrastructure, etc.), the subsidence rate can be related to sediment compaction. The compaction is large when the thickness of the stiff sediments is large, or when the sediments are composed of soft shallow deposits, which implies a correlation between subsidence rate and sediment resonance period. This simple idea has been tested in the Grenoble Basin and it shows that indeed sediment thickness and resonance periods can be predicted from subsidence rate measurements alone.

This project consists in exploiting the subsidence rate in different French valleys, urbanized and subject to seismic hazard. Correlations between subsidence rates and sediment thicknesses, as well as between subsidence rates and resonance periods in the different sedimentary contexts, will be calibrated using artificial intelligence methods via the spectral analysis of local earthquake recordings by the seismological networks of the Résif infrastructure. We also propose to analyze all the available additional data of geological, geophysical and geotechnical type, in particular to take into account the various sedimentary contexts. The correlations obtained will allow us to build a physical model of the aggravation of seismic motion at the surface of sedimentary valleys, valid at high resolution because the target scale is that of buildings, and applicable in different sedimentary contexts.

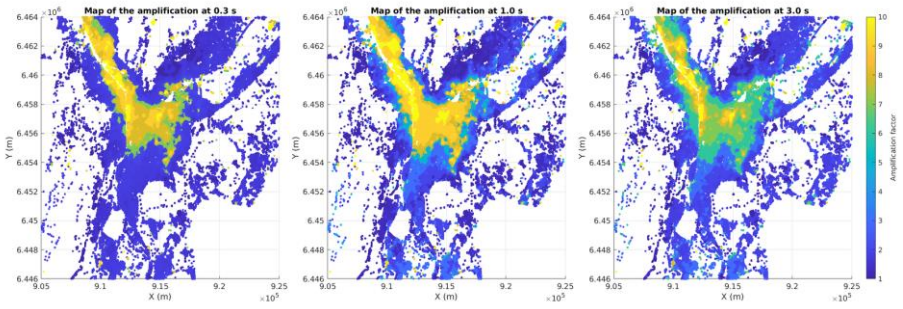

Map of the amplification factor at 0.3, 1 and 3Hz for the Grenoble Basin, derived from the subsidence rate.

Juliane STARKE

Acoustics and Seismics of natural cliffs, to better understand and monitor fracturation and erosion processes

Year 1

Supervisors: Éric Larose, Laurent Baillet

Mécanique des failles/ Fault mechanics

Rainfall, temperature variations, and chemical processes are well-known drivers of rock erosion. The impact of rainfall on rocks is not well-understood yet but may impact the mechanical properties (including damage, rigidity, deformation) of the rock. In this study, we exhibit the effect of rainfall events on the resonance frequency of a rock column.

Resonance frequencies of structures have been utilized to monitor rock columns due to their sensitivity to changes in the rock apparent rigidity (1). For instance, daily temperature changes induce stress variations in the rock column, resulting in a daily cycle of resonance frequency changes (thermal-acousto-elasticity, 2).

This research involves long-term monitoring of the first resonance frequency of a 50 m high limestone cliff covering the Chauvet cave in the Ardèche plateau, SW France, exposed to climatic solicitations including daily solar radiation, air temperature fluctuations, and rain events. The rock column was equipped with seismic and meteorologic stations and monitored continuously during three years.

To demonstrate the effect of rainfall events on the mechanical properties of the rock, we calculated the resonance frequency depending only on air temperature and solar radiation, using a simple bivariate linear regression. The regression provides well-fitting results for dry periods but shows larger deviations during most rainy periods. This indicates that rain has an effect on the changes in rock resonance frequency. Identifying and quantifying these changes would be a key factor in understanding the evolution of damage.

1) Bottelin, P., Baillet, L., Larose, E., Jongmans, D., Hantz, D., Brenguier, O., ... & Helmstetter, A. (2017). Monitoring rock reinforcement works with ambient vibrations: La Bourne case study (Vercors, France). Engineering Geology, 226, 136-145.
2) Guillemot, A., Baillet, L., Larose, E., & Bottelin, P. (2022). Changes in resonance frequency of rock columns due to thermoelastic effects on a daily scale: observations, modelling and insights to improve monitoring systems. Geophysical Journal International, 231(2), 894-906.

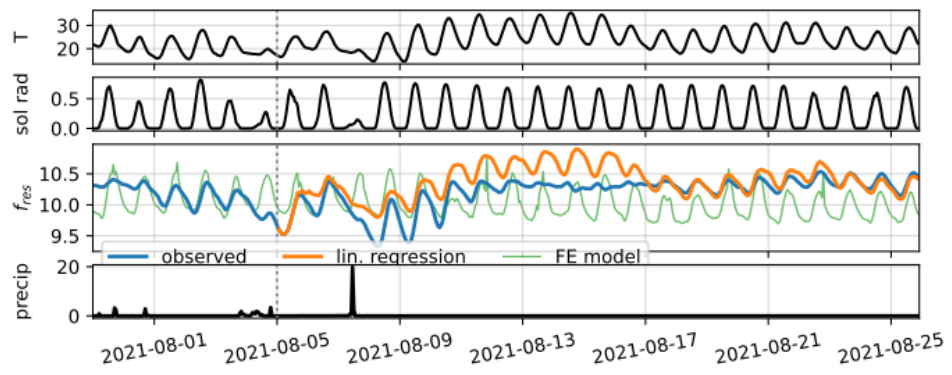

Inputs and results of the resonance frequency for a rainfall period in August 2021. The top two subplots illustrate the input parameters utilized for the modeling: air temperature and solar radiation. In the third subplot, the observed resonance frequency of the rock column is presented alongside the outcomes of finite element modeling (in green) and linear regression modeling (in orange). A vertical dotted line marks the training period of the linear regression model. The bottom subplot displays the observed precipitation throughout the specified time period.

Hongyi SU

Near-fault Ground Motion Prediction, Site Effects and Wave Propagation at Regional Scale for a Shallow Earthquake in SE France

Year 1

Supervisors: Cécile Cornou, Mathieu Causse, Sébastien Hok (IRSN), Céline Gélis (IRSN)

Géophysique des Risques sismiques et gravitaires / Geophysics of seismic and gravity risks

This thesis aims to improve seismic hazard assessment in south-eastern France by modelling near-fault ground motions for the 2019 M_w 4.9 Le Teil earthquake, the most damaging seismic event in France since 1967. The earthquake occurred near two nuclear power plants (NPP) in the Rhone Valley (Cruas and Tricastin) and resulted in significant damage at the epicentre despite its moderate magnitude. However, this event was only recorded from considerable distance. Generally, the absence of near-fault observations poses challenges in comprehending and calibrating ground motion prediction equations (GMPEs), especially in moderately seismic regions like Le Teil. Hence, the primary goal of this thesis is to develop a numerical simulation method that integrates fault rupture models, wave propagation, and the impacts of near-surface geology (site effects) to accurately simulate the seismic wavefield in the epicentral region. Furthermore, ground motions recorded at large distances reveal distinctive characteristics, such as rapid attenuation of high-frequency content (Laurendeau et al., submitted), which may be linked to the shallow source and regional geology. Our goal is to validate this hypothesis through our earthquake modelling efforts. To address these scientific questions, we calculate synthetic ground motions using a virtual sensor array positioned both near the fault and further away. We will utilize both kinematic and dynamic modelling of fault rupture. Both approaches consider wave propagation and site effects by incorporating seismic properties of the medium. The combined modelling approach addresses uncertainties in fault rupture, site effects, and wave propagation, important for accurately simulating the level of ground motion. Validation of our approach will involve comparing simulated seismic waveforms, evaluating displaced objects in the epicentral area, and analysing seismic recordings from remote locations.

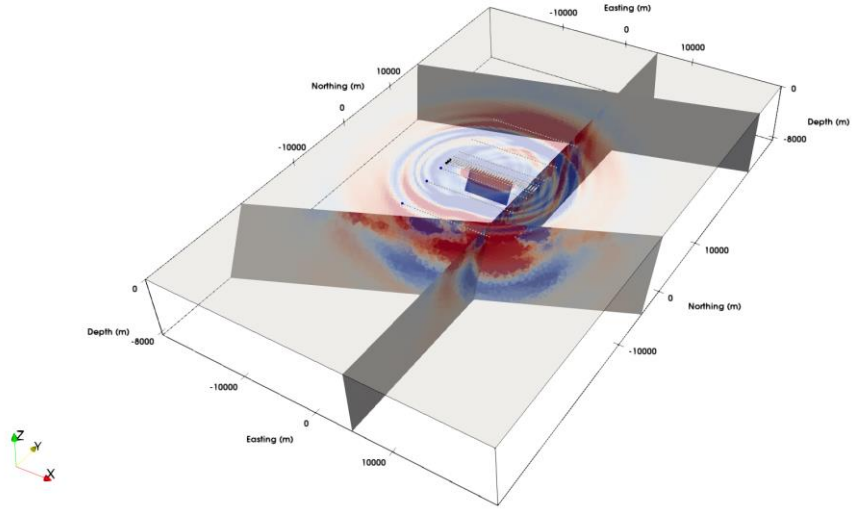

Snapshot of the synthetic seismic wavefield propagating in 3D media coupled with dynamic fault slip at 6.5 seconds. The dots on the surface represent virtual receivers (VR). The mesh domain covers 8.5 km in depth, 70 km in the north-south direction, and 45 km in the east-west direction.

Anna THEUREL

Effect of crystallization on eruptive dynamics for silicic magmas

Year 3

Supervisors: Alain Burgisser, Marielle Collombet, Caroline Martel (ISTO)

Géophysique des volcans & Géothermie / Geophysics of volcanoes & geothermal energy

Most active volcanoes show outgassing through their vent even during inter-eruptive phases, i.e., without magma ascent in the volcanic column. This implies that gas can move towards the surface within an immobile magma. However, in the case of silica-rich magma such as those found in Indonesia's Merapi or Santiaguito in Guatemala, gas bubbles are unable to move by gravity due to the high viscosity of surrounding magma. Understanding how gas does or does not outgas from the volcano is essential, as it is a parameter that seems to control the transition from effusive to explosive regime. The paradox between theoretically immobile gas trapped in immobile magma and visible and measurable gas losses at the volcano's surface during inter-eruptive periods is the key focus of my research.

To shed some light on this, I'm making synthetic lava in high-pressure, high-temperature autoclaves. I'm mainly interested in the relationship between magma crystals and gas bubbles. We observe that the bubbles connect to each other thanks to capillary forces exacerbated by the constraint of the surrounding crystals. If these connections are sufficiently stable and well-developed, chains of bubbles can allow percolation through the sample, the permeability of which can be calculated by Lattice Boltzman calculations. We also evidence that this channeling is time-dependent, and it is already possible to some extent to estimate the time required for coalescence and channeling to reach a permeable state, as well as the time required for such a chain to rupture if the flow decreases or ceases.
The next phase of my research is to translate these initial findings into practical applications for real volcanoes, proposing estimates that align with volcanic time scales. In a broader sense, my work in fundamental volcanology holds the promise of a novel approach to assess volcanic hazards.

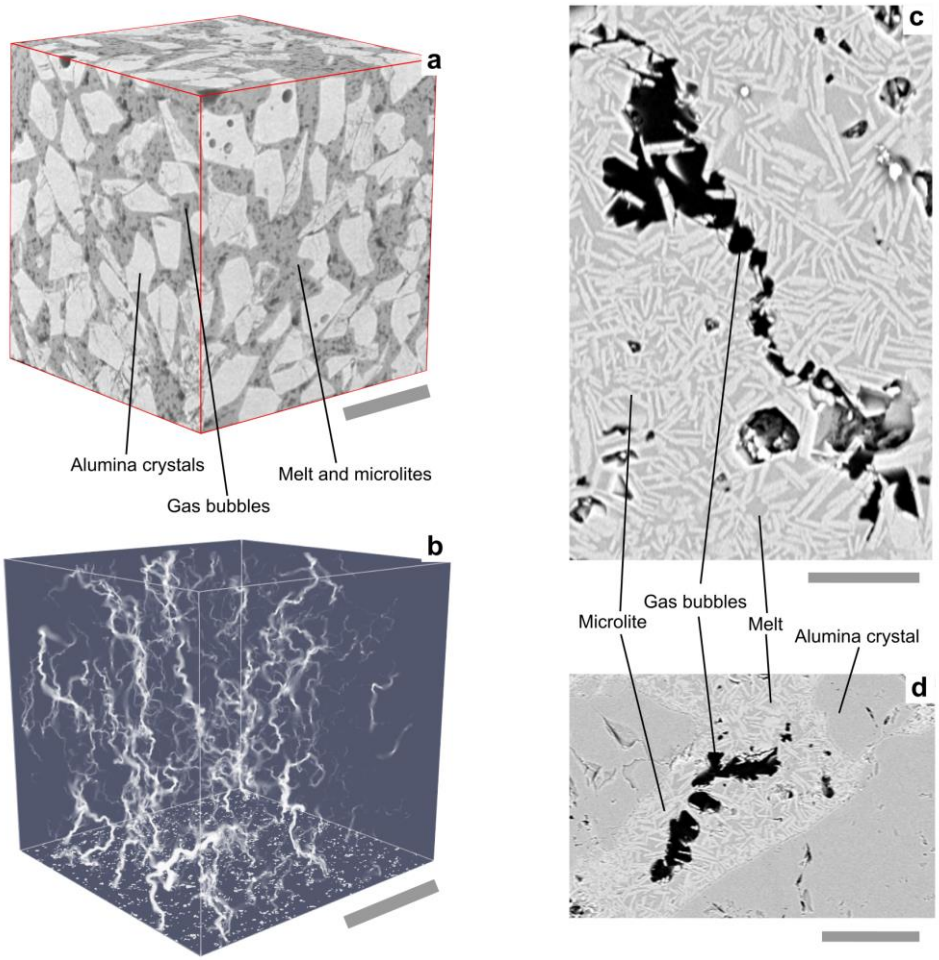

Vizualisation of the samples. (a) Reconstructed volume of a sample via µ-tomographic images (scale bar is 200 µm) (b) Rendering of gas flow (white gradient is velocity magnitude) in a permeable sample obtained from numerical simulation (scale bar is 200 µm) (c) SEM image showing percolating bubble chain when coalescence just happened (scale bar is 20 µm) (d) SEM image showing multiple bubble clusters (already resulting from coalescence) close to coalesce with each other (scale bar is 50 µm).

Anuar TOGAIBEKOV

Observing and modeling short-term changes in basal friction during rain-induced speed-ups on an Alpine glacier

Year 4

Supervisors: Andréa Walpersdorf

Cycle sismiques et déformations transitoires / Seismic cycles and transient deformations

Basal shear stress on hard-bedded glaciers results from normal stress against bed roughness, which depends on basal water pressure and cavity size. These quantities are related in a steady state but are expected to behave differently under rapid changes in water input, which may lead to a transient frictional response not captured by existing friction laws. Here, we investigate transient friction using GPS vertical displacement and horizontal velocity observations, basal water pressure measurements, and cavitation model predictions during rain-induced speed-up events at Glacier d'Argentière, French Alps. We observe up to a threefold increase in horizontal surface velocity, spatially migrating at rates consistent with subglacial flow drainage, and associated with surface uplift and increased water pressure. We show that frictional changes are mainly driven by changes in water pressure at nearly constant cavity size. We propose a generalized friction law capable of capturing observations in both the transient and steady-state regimes.

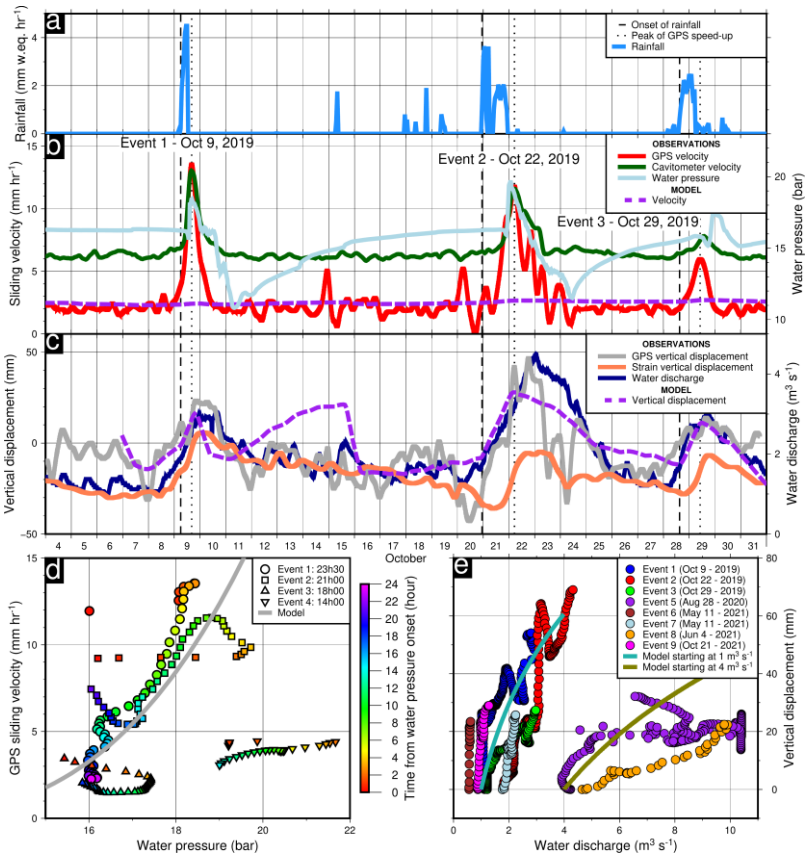

Relationship between GPS-derived sliding velocity measurements averaged over the five stations and other observations. Temporal variations in October 2019 in (a) liquid precipitation; (b) GPS, cavitometer, and modeled sliding velocity; (c) GPS, strain-induced, and modeled vertical displacement and observed water discharge. The plot for events 4-9 is available in Supporting Information S2 (Figure S3). The vertical dashed lines in (a, b, c) mark the onset of the rainfall events, and the dotted lines mark the peak of horizontal velocity associated with each event. Panels (d-e) show the observed and modeled relationship between (d) water pressure and GPS-derived sliding velocity, and (e) water discharge and vertical displacement. In (d), water pressure is shown only when it exceeds the background level.

Lisa TOMASETTO

Microseism correlation functions as a new dataset for Deep Earth imaging

Year 3

Supervisors: **Laurent Stehly, Pierre Boué**

Ondes & structures / Waves & structures

Ambient noise recorded globally is usually dominated by natural sources below 1 Hz. In particular, ocean wave interactions with the seafloor generate acoustic waves transmitted to the crust in the 3-30s period band. If we zoom in, the 3-10s period band, called the secondary microseismic peak, results from non-linear interactions of oceanic waves traveling in opposite directions.

Seismographs globally record the emitted waves. If surface waves are dominant in amplitude, body waves can also be retrieved. The latter presents an interest in extracting properties of the Deep Earth since they are traveling within media and are less scattered.

Recent improvements in global oceanographic hindcast, such as the WAVEWATCH III model, have allowed seismologists to track the spatiotemporal behavior of such sources. Also, seismic interferometry methods can be used to extract signals from continuous records.

My subject consists of integrating both hindcast information and interferometry methods to select time windows and station pairs to retrieve body waves at the global scale. By comparing travel times to global 3D models this might add new measures to the earthquake travel times datasets with unconventional coverage.

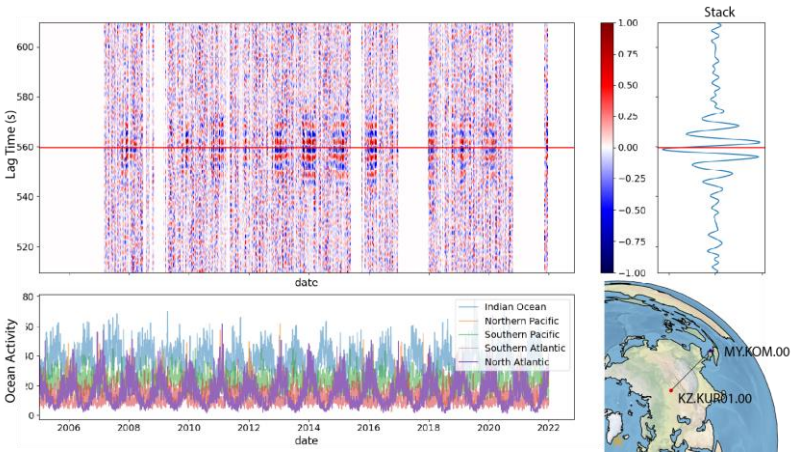

(top left) Weekly cross-correlation functions for station pair KZ.KUR01.00-MY.KOM.00 from 2007 to 2022 windowed around the PP-P interference arrival time (red line). (top right) Stack.
(bottom left) Oceanic activity given by the WAVEWATCHIII hindcast in different areas; focus on Northern Atlantic.
(bottom right) Station's location.

Ena TOPALOVIĆ

Tracing the genesis of bauxite material in Croatian karst deposits: Insights from mineralogical and geochemical Analyses

Year 3 (Visiting PhD researcher)

Supervisors: Andrea Čobić (University of Zagreb, Croatia), Nenad Tomašić (University of Zagreb, Croatia); ISTerre Referent: Stanislas Jelavić

Croatia boasts a wealth of karst bauxite deposits that played a significant role in fueling the aluminum industry throughout the 20th century, yielding an estimated 27.5 million tons of bauxite material [1]. With the escalating demand for rare earth elements (REE), bauxite emerges as a promising reservoir, often harboring concentrations exceeding 1000 mg/kg of REE [2].

This study focuses on bauxite samples sourced from seven sites in Lika and the Dalmatian inland of Croatia. These deposits comprise three Triassic-age sites (Grgin brijeg, Rudopolje, and Vrace) and four Eocene-age sites (Tošići-Dujići, Jukići-Đidare, Stari Gaj, and Gljev). While prior investigations have conducted comprehensive bulk mineralogical and geochemical analyses [3, 4], a detailed understanding of their genesis and provenance remains elusive.

It is proposed that Triassic bauxites originated in situ through bauxitic processes during the onset of the Alpine orogeny, coinciding with emersion in the Ladinian to Carnian age [3]. The parent material comprises Ladinian clasts and pyroclasts [3]. Eocene bauxite formation aligns with the Pyrenean orogenic phase in the Middle Eocene, resulting in emersion and bauxite accumulation over Upper Cretaceous and Lower Paleogene limestones [3].

Our study aims to delve into bauxite mineralogy, with a specific focus on REE minerals and their distribution within the deposits. Furthermore, we endeavor to pinpoint the origin of bauxite material and its correlation with regional geological events. To achieve these goals, a suite of advanced analytical techniques will be deployed, including qualitative and quantitative X-ray diffraction analyses, scanning electron microscopy (SEM), and geochemical assessments employing inductively coupled plasma mass spectrometry (ICP-MS). Additionally, geochronological investigations will be undertaken on select minerals to establish the age of the bauxite material, thereby contextualizing it within the broader geological framework.

This research endeavors to illuminate the genesis, mineralogy, and geological significance of Croatian karst bauxite deposits, providing valuable insights into their potential as REE sources and their role within the regional geological context.

Références :

[1] Vujec S. (1994) Rudarstvo u Hrvatskoj. Rudarsko-geološko-naftni zbornik, 8, 11-17.
[2] Maksimović Z. & Pantó G (1996) Authigenic Rare Earth Minerals in Karst-Bauxites and Karstic Nickel Deposits. In : Rare Earth Minerals, Chemistry, Origin and Ore Deposits. London, UK : Chapman & Hall.
[3] Marković S. (2002) Hrvatske Mineralne Sirovine. Zagreb, Croatia: Hrvatski geološki institute.
[4] Tomašić N., Čobić A., Bedeković M., Miko S., Ilijanić N., Gizdavec N. & Matošević M. (2021) Rare earth elements enrichment in the Upper Eocene Tošići-Dujići bauxite deposit, Croatia, and relation to REE mineralogy, parent material and weathering pattern. Minerals, 11, 1260.

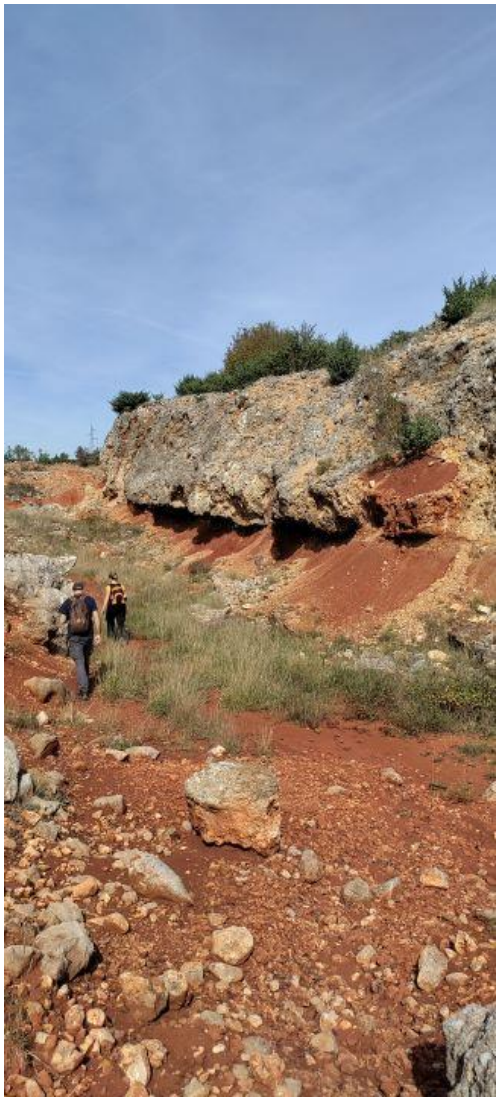

Field trip to the Vrace bauxite deposit in Croatia

Juan Carlos VERANO ESPITIA

Statistical physics of creep rupture of heterogeneous materials

Year 2

Supervisors: **Jérôme Weiss**

Mécanique des failles/ Fault mechanics

Understanding how materials deform, damage and approach failure is relevant for engineering. Nevertheless, in classical mechanics and engineering literature, creep failure is described by empirical approaches. Therefore, this project aims to track the progressive damage in different heterogeneous materials, such as paper and concrete, during creep loading using various monitoring tools and to introduce statistical physics theory to interpret this damage evolution and subsequently predict failure.

Preliminary works studied the effect of heterogeneity on the creep lifetime using Fiber Bundle Models (mean-field), showing that the heterogeneity amplifies the damage, i.e. shortens creep lifetimes. In the present work, using a more complex model to simulate non-mean-field elastic redistribution kernels as present in brittle materials such as rocks or concrete, we show that additionally to the heterogeneity, the nature of the elastic interaction kernel (friction coefficient) plays an additional effect on the creep lifetime.

Furthermore, from creep experiments at room temperature on sheets of paper under different loads, acoustic emission was recorded, and we studied the relationship between the time when an acoustic emission event (over a predefined threshold) occurred and the creep lifetime. We observed a power law relationship between these times. Interestingly, such correlation is observed from the first event, meaning that some information about the failure time can be obtained early in this heterogeneous material.

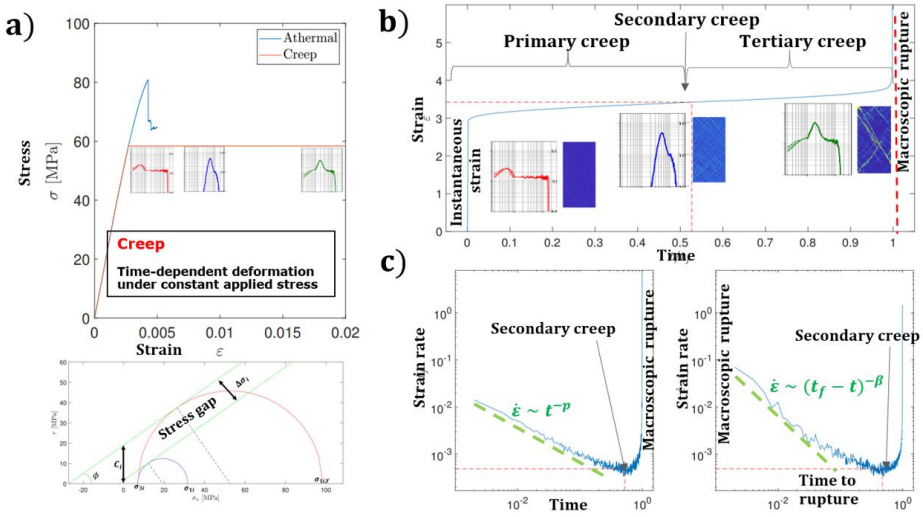

a) Strain-Stress curves representing creep behaviour and rupture without any thermal activation. Evolution of the stress gap for different strain values according to the Mohr-Coulomb criterion. b) Time - Strain curve and representation of the different stages during the creep behaviour and the evolution of the stress gap. c) Time-Strain rate and Time to rupture-Strain rate curves.

François VERZIER

Multiregional assessment of technologies, energy and resources

Year 3

Supervisors: Olivier Vidal

Minéralogie et Environnements / Mineralogy and Environments

I am working on a numerical model named "MATER" (Multi-integrative Approach Towards socio-Ecosystemic scenaRios) that tests the energy transition scenarios through biophysical indicators such as energy consumption, material consumption and impact emission.

The following sections elucidate the model framework and equations.

3.1. The model was designed to have flexible disciplinary, geographical, temporal, and sectoral scopes. The framework and equations are generalized so that most users would only need to input their data to fully integrate their specific scopes with the existing framework.

3.2 The general framework in question is based on stock and flow dynamics. Each element's stock changes according to the activities that affect it. For instance, the number of cars changes over time based on the cars reaching the end of their life and the new cars being built and introduced to the market. The old cars are scrapped and can be recycled to produce newelements like recycled steel or aluminum. This stock dynamic can be applied to almost all known infrastructures, resources, energy vectors, services, or living organisms.

3.3. Some of these activities are autonomous, like reaching the end of life. However, the conceptof "nothing comes for free" introduced in the previous section, means that most activities affecting an element actually involve other activities (processes) and require a functioning element to be produced (in-use stock). For example, building a new car inevitably involves the consumption of steel, aluminum, water, or energy. This car manufacturing process cannot occur without human labor or the operation of a factory, which itself had to be built at some point. The activities of a process are determined by the type of element to produce or recycle and the technology of the element used to execute the process. Thus, all sectors are interconnected through one or more processes, leading to numerous feedback loops in the model.

3.4. This final part models a socio-economic system driven by the final demand and based on the constant endogenous adaptation of the industrial sectors to potentially meet societal needs. The system described so far is an autonomous system that can evolve on its own from the initial conditions. However, humans are capable of adjusting certain activities to maintain a stock of elements at the desired level. For example, the number of cars decreases because some reach the end of their life, but we can adjust the production in factories to meet the demand. However, a car factory has a maximum production capacity that it cannot exceed and can also reach the end of its life. In addition to the number of cars, the number of car factories is also controlled. However, the reference is not exogenous as it is for cars but rather endogenous. Therefore, we have a cascade control phenomenon that allows for the endogenous calculation of industrial activity and the modeling of certain blocking constraints along the entire production chain of a good. Finally, natural resources are not controlled by humans and thus have a stock that evolves freely over the course of the simulation.

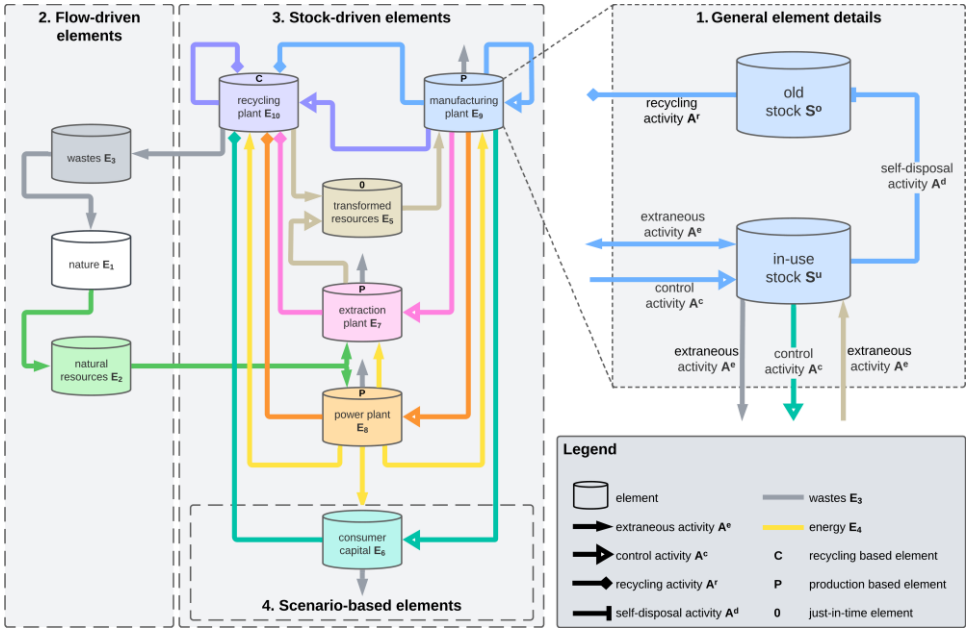

Simplified explanatory diagram of the MATER model focusing on industry and resources. Horizontal activities influence the stocks of elements by either replenishing or depleting them. Vertical activities are employed by an element to facilitate one of its processes. The diagram's legend elucidates the main components of the model's structure. Each element consists of two types of stocks that are modified by various activities. The "in-use" stock of an element can generate activities via process recipes, while the "old" stock accumulates elements that have reached the end of their operational life, pending recycling. There are four main types of activities: extraneous activities Ae, which are either consumed or co-produced by other elements; control activities Ac, representing the primary production activity of an element; recycling activities Ar , which convert old scrap stocks into new distinct elements; and self-disposal activities Ad, illustrating the end-of-life phase of an element.

The legend specifies the colors for "wastes" and "energy" elements because arrows may not directly connect to their respective element blocks, though all activities are color-coordinated with their related elements. The legend's final three entries C, P, and 0 denote the control strategy type for each element within the model.

Ivan VUJEVIĆ

Modelling and laboratory studies of fluid-solid interaction during H_2 transport along fractures

Year 1

Supervisors: **Laurent Truche**

Minéralogie et Environnements / Mineralogy and Environments

Hydrogen's role as a reducing agent in geological settings, and its interactions with oxidized minerals such as pyrite, hematite, and sulfate, present significant challenges and opportunities for environmental science. This PhD project systematically investigates hydrogen reactivity, which may occur via abiotic processes on catalytic mineral surfaces or through microbial mediation. The research is structured around three primary objectives: First, to quantify hydrogen adsorption under elevated hydrogen pressures with temperatures ranging from 25°C to 80°C. Second, to elucidate the underlying mechanisms of hydrogen reactivity within core samples of both reservoir and cap rocks. Third, to develop a comprehensive model for hydrogen migration and fluid-rock interactions, focusing on reservoir rocks and fracture networks in cap rocks. Expected results include detailed volumetric adsorption isotherms, insights into hydrogen's migration and reactivity at the core scale under ultra-high saline conditions using parametric experiments in a tri-axial cell, and a calibrated reactive transport model based on the obtained experimental data. This study aims to advance our understanding of hydrogen dynamics in geological contexts, thereby enhancing resource management and reducing the environmental risks associated with the production of toxic by-products such as hydrogen sulfide.

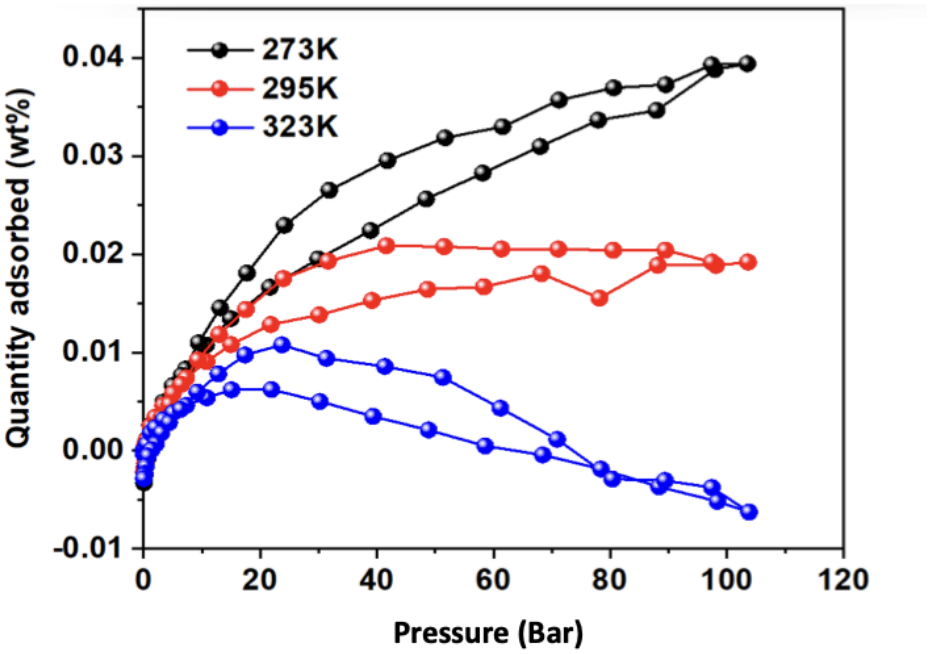

H_2 adsorption isotherms recorded at elevated H_2 pressure (up to 110 bar) and at 3 different temperature: 0°C (blue dots), 25°C (red dots), and 90°C (black dots) on COx sample. The adsorption and desorption paths are shown.

Heming WANG

Seismic properties of serpentinites under increasing pressure and temperature conditions

Year 4

Supervisors: Mai-Linh Doan, Anne-Line Auzende, Stéphane Schwartz, Xiao-Ming Tang (China University of Petroleum)

Mécanique des failles/ Fault mechanics

The lizardite/antigorite transition depends on the increasing pressure and temperature, playing a crucial role in various tectonic activities and seismicity. The seismic Vp/Vs ratio is a useful parameter for identifying serpentinites from other mantle rocks. To understand the effects of the increasing metamorphic degree and microstructure variation on the serpentinite velocity, we collected several natural serpentinite rocks with different metamorphic degrees in the western Alps and measured the ultrasonic velocity of the samples at confining pressures up to 90 MPa. The measured velocity increases and the Vp/Vs ratio decreases with the metamorphic degree increasing. The velocity anisotropy increases from lizardite to antigorite. The pressure dependency of the serpentinite velocity is insignificant. The petrological results are used to explain the velocity anisotropy and the pressure dependency. The new results expanded the widely-used Vp/Vs crossplot for discriminating serpentinite, providing new laboratory constraints for tracking the lizardite/antigorite transition from field seismic data.

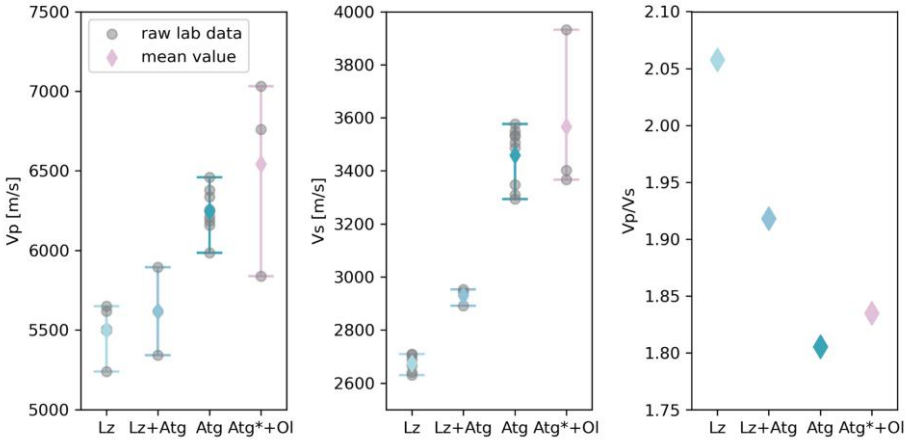

Serpentinite:	Lz	Lz+Atg	Atg	Atg*+Ol
Temperature (°C):	300-340	340-390	390-480	>480
Pressure (*kbar*):	8-10	10-12	12-15	>20

The measured ultrasonic Vp, Vs, and Vp/Vs of the cube serpentinite samples in the ambient environment, where the velocities of each sample are measured in three orthogonal directions.

Louise XIANG

Analysis of the 2016 Central Italy earthquake sequence using a refined earthquake catalog

Year 3

Supervisors: **David Marsan**

Cycle sismiques et déformations transitoires / Seismic cycles and transient deformations

The 2016 Central Italy seismic sequence occurred within an area dominated by normal-fault systems present along the Apennines. The sequence began with the M_w 6.0 Amatrice event on 24 August 2016, followed by the M_w 5.9 Visso event on 26 October 2016 and then, four days later, the M_w 6.5 Norcia event. In this study, we aim at modeling the seismicity of this complex earthquake sequence in order to determine the location of highly-pressurized fluids under the studied area through swarms occurring during the sequence. To do so, we take advantage of a high-resolution earthquake catalog based on arrival times derived using a deep-neural-network-based picker. As a first step, we apply a density-based clustering approach to group earthquakes into dense clusters. The majority of the resulting clusters highlight distinct fault planes which indicates an activation of a complex fault network. We further define a 4-dimensional seismicity model based on the ETAS model, in which we introduced an earthquake detection probability to accommodate observed rapid fluctuations in earthquake detection throughout the sequence. By computing the ratio between the observed and ETAS-modeled rates of high-density clusters, we can identify candidate seismic swarms. To evaluate their consistency, we compute the weighted index of the largest seismic event and the magnitude difference between the largest and the 4^{th}-largest earthquakes occurring within a target candidate. Furthermore, to analyze their migration behavior, eigenvectors are computed to identify primary and secondary directions, and swarm earthquakes are projected onto these directions, in which we fit a linear regression model. Observed slope values are compared to those from a distribution of simulated slopes generated by 1000 random shuffling, and statistical significance is assessed. The results reveal among the 40 seismic swarms, 29 of them show significant migration with a significance level of 95%. Migration velocity is determined by components representing velocities along primary and secondary directions, measured in kilometers per day based on slope and earthquake count. Our swarms exhibiting significant migration suggest the implications of variations in pore fluid pressure influenced by structural complexity and intense faulting in the region.

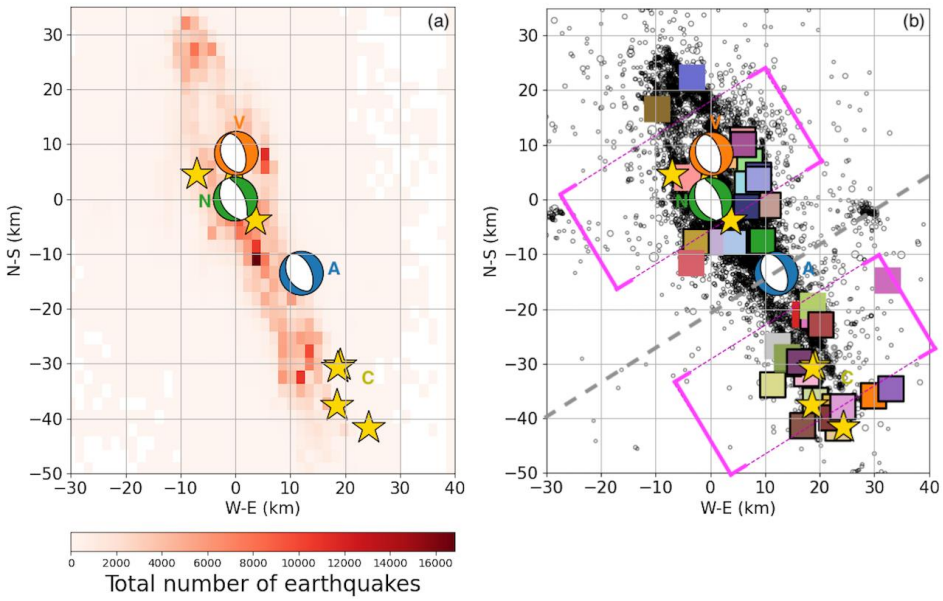

(a) Earthquakes per 2 kmx2 km. (b) Location of 40 seismic swarms. mL ≥ 2 earthquakes are dark circles. The Amatrice (A), Visso (V), and Norcia (N) earthquakes are marked with blue, orange, and green focal mechanisms, respectively. mL ≥ 5 earthquakes are golden stars, with a burst near Campotosto (C). Each swarm is colored, with bold squares showing migrating swarms. Gray-dashed line separates central and southern swarms groups. Purple-dashed-line rectangles are cross-sectional profiles.

Yan YAO

Characterising and evaluating permeability in fault zones for underground hydrogen storage in geological reservoirs

Year 1

Supervisors: **Frédéric Donzé**

Mécanique des failles/ Fault mechanics

Fault zones traversing caprocks present a critical consideration for effective hydrogen (H_2) storage in porous geological formations. Recent studies have indicated that subcritical mechanical responses within these zones might substantially influence permeability changes under minimal increases in fluid pressure. Specifically, fluid injection experiments in a clay-rich fault zone at the Tournemire IRSN underground laboratory have shown permeability enhancements by several magnitudes with only slight fluid pressure adjustments, despite minimal plastic deformation being observed. This phenomenon is particularly significant given the high mobility characteristics of hydrogen—attributable to its high diffusivity, low viscosity, and low density—which increases the risk of H_2 leakage along these zones. Therefore, a re-evaluation of permeability laws is necessary to better model these effects.

The primary aim of this project is to develop a new formulation of permeability evolution within fault zones specifically for H_2 flow, integrating this model into numerical simulations to assess the integrity of large-scale geological H_2 storage sites. Our approach involves deriving these formulations from laboratory experiments and field monitoring data, incorporating scaling effects and in situ stress conditions into numerical models of H_2 reservoirs. These models will utilize advanced computational techniques requiring high-level coding skills in environments such as MATLAB or C++, with the implementation of state equations for multiple phase components. Validation of our proposed models will be achieved by aligning simulation outputs with established experimental results and additional numerical analyses. Furthermore, parametric studies will be conducted to evaluate the influence of various parameters within the model, enhancing the predictive capabilities of our simulations. Ultimately, this research will facilitate a deeper understanding of the geomechanical dynamics associated with cyclic loading in faulted caprock scenarios, enabling more reliable designs for H_2 storage infrastructure.

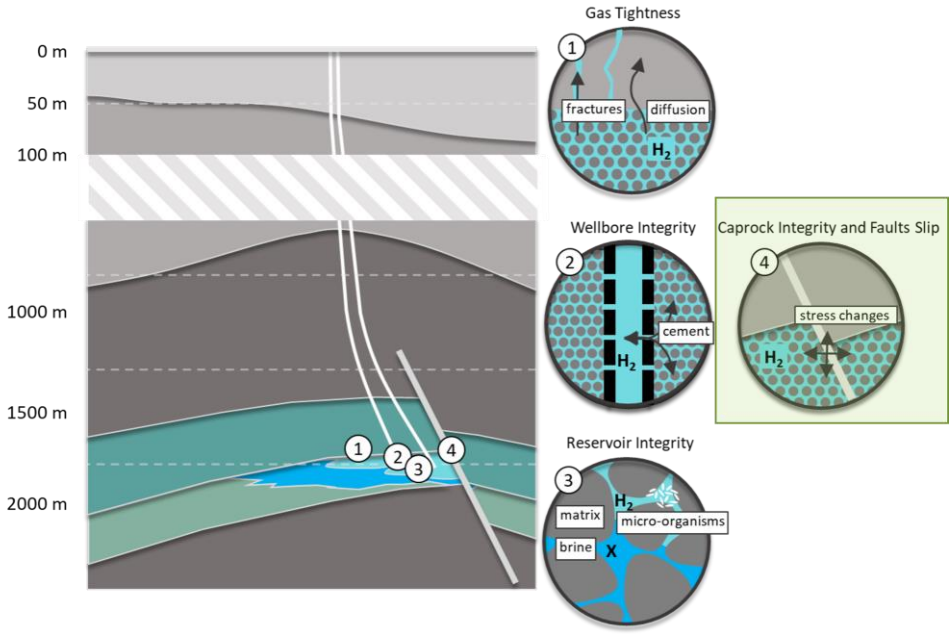

Schematic diagram about the key areas of storage integrity during UHS in subsurface porous media

Hooshmand ZANDI

Seismic wave inversion for sea ice characterization

Year 2

Supervisors: **Ludovic Moreau, Ludovic Métivier, Romain Brossier**

Ondes & structures / Waves & structures

The decline in Arctic sea ice has triggered both local impacts, such as Arctic warming and changes in ecosystems, and global consequences, including changes in climate. Understanding this dynamic system is crucial for addressing safety concerns and refining climate models. Seismology has been a foundational tool for decades for deriving ice properties, relying on the propagation of seismic guided waves within sea ice.
In the range of frequencies excited by natural seismic sources, the wavefield comprises three primary guided waves: longitudinal waves, shear-horizontal waves, and flexural waves. To derive elastic constants, ice thickness, and icequake locations, an inversion process is employed, based on minimizing the difference between synthetic and observed data.

In our study, we utilize the spectral element method (SEM) to model seismic wave propagation in sea ice, simulating wave propagation in a floating ice layer. Using SEM, a comprehensive database of simulations encompassing various ice models is created (given the elastic constants and density of ice), to be used as synthetic data in the inversion process.

In Step 1 of the inversion process, Particle Swarm Optimization (PSO), an efficient method with easy tuning, is employed to estimate ice thickness and icequake locations using a limited number of stations. For this step, five records of the flexural wave are utilized. Subsequently, in Step 2, utilizing the icequake locations identified previously, we refine ice thickness estimates between the source and receiver locations for all stations (248 stations) in the network using a grid search approach. This two-step process yields ice thickness along each path connecting icequake locations and receiver positions, ultimately contributing to the construction of a 2D map of ice thickness.

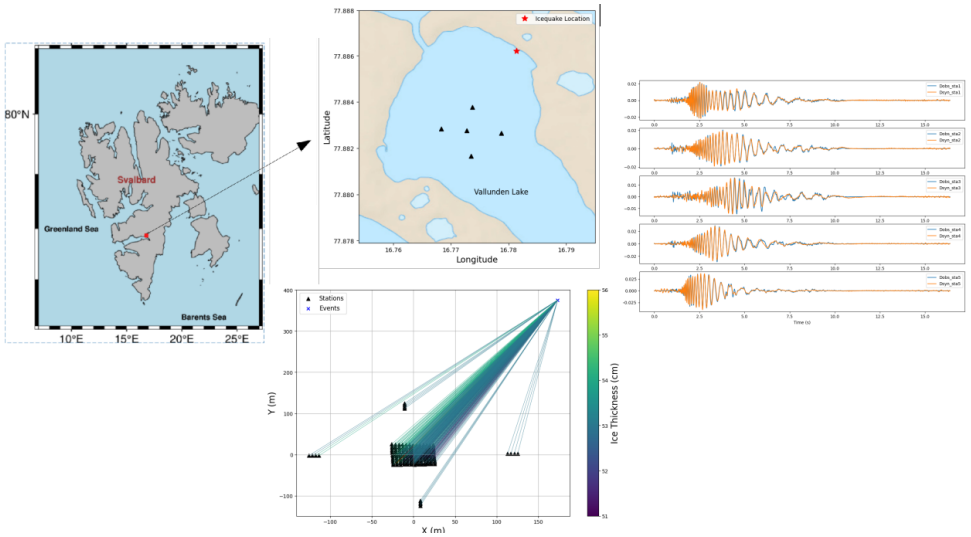

Illustration of Icequake Localization and Ice Thickness Estimation: A recorded icequake on the vertical channels of five stations (depicted by black triangles) serves as the basis. Using Particle Swarm Optimization (PSO) in Step 1, the location of the icequake (indicated by a red star) and the ice thickness are estimated. The figure on the upper right shows the fitting between observed and synthetic data. In Step 2 of the inversion process, the estimated ice thickness along paths connecting the source to all 248 stations is refined, utilizing the icequake location determined in Step 1.

Léa ZUCCALI

Assimilation of geodetic data for volcanic hazard assessment in near-real time by means of a particle filter

Year 2

Supervisors: Virginie Pinel

Géophysique des volcans & Géothermie / Geophysics of volcanoes & geothermal energy

In a perspective of volcanic hazard assessment, it is fundamental to be able to determine as early as possible whether, where and when the magma that has started to propagate from the storage zone will reach the surface. The propagation phase is generally rapid, lasting from a few hours to a few months, but it induces seismicity and deformation signals recorded by continuous sensors and InSAR data. Furthermore, dynamic numerical models can be used to calculate the trajectory and the velocity of magma propagation as a function of the physical properties of the magma and the crust, and the initial conditions (local stress field and magma reservoir location).

Data assimilation is a method that combines a dynamic model with current and past observations based on error statistics and predicts the future state of the observed system. This method therefore appears to be an appropriate tool for addressing the need to predict the position and timing of a volcanic eruption based on available models and observations.

The particle filter is particularly noteworthy for its ability to handle nonlinear models and non-Gaussian error statistics. This method is based on a representation of the probability density of the dynamic model by a discrete set of model states (particles) and relies on Bayes' theorem.

In order to assess the potential of the particle filter for tracking magma propagation at depth, we implemented this assimilation strategy by considering, in two dimensions, the case of magma propagating beneath a caldera in an extensional stress field. The input parameters of the propagation model are the initial position of the magma at depth, its viscosity and driving pressure, the volume of magma injected, the crustal rigidity, and the local stress field characterized by the balance between tectonic extension and caldera unloading. Surface displacements induced by magma propagation are estimated using an Okada dislocation model. We first validate our assimilation strategy with synthetic data in order to take into account geodetic data recorded on volcanic systems in the future.

Initial situation. Particles are drawn randomly and propagate during 3600s.

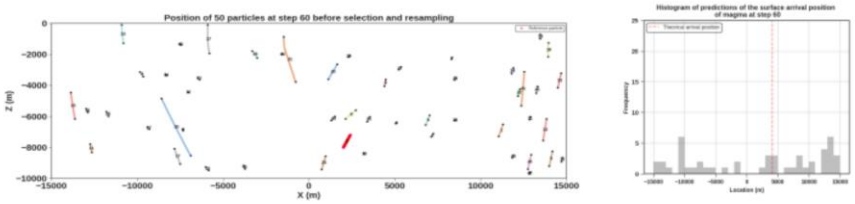

Particles after 51 assimilation steps.

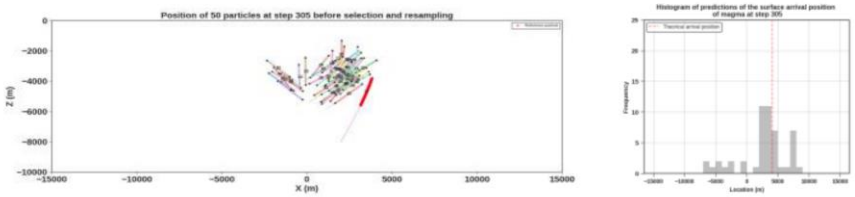

Particles after the final assimilation step.

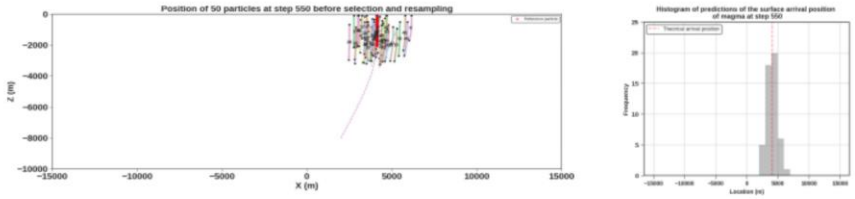

We consider 50 particles and 100 assimilation steps. The model integration step is 60s. From the initial condition, the particles propagate freely during 3600s, then assimilation is performed every 300s.


seismic
earthquake
multi
data
mantle
fault
approach
tectonic
dynamics
assessment
Impact
site
Wave
modelling
zone
sequence
Imaging
near
scale
Motion Prediction
Characterization
natural
rupture
evolution
optical
hazard
Ground Motion
ice
volcano
interaction
response
Earth
resource
deformation
hydraulic
mining
seismicity
Données
Laboratory
Alpine
Effect
correlation
environmental
glacier
Modélisation
time
drilling
application
geodetic
strategies
geophysical
reactivity
Monitoring
Central
High resolution
Deep
Reservoirs
Shallow
analysis
Alps
activity
serpentinites
hydrogen
understand
inversion
South
Exploration
New
methods
crustal
geochemical
associated
monitor
Diversity
Cretaceous
populations
material
combining
InSAR
France
source
Acoustic
active
their
better
imagery
geothermal
Fractures
conditions
heterogeneous
FWI
Regional
Water
structure
intraslab
subduction
integrating
East
large
Characteristics
Ridgecrest
volcanic
Abiotic
Parameters
sensor
radar
physics
field
cycle
Propagation
tracing
under
sea
Archean
Mineral
transition
gold
How
along
Investigating
fluid
plate
Antarctica
H2
CO2
Trench
Indian
Experimental
Dataset
energy
convection
Detailed
image
crystallization
Krafla
MODELS
Multiscale
Chamrousse
Prediction
Insights
cliffs
logging
speed
increasing
vestige
Observing
Ecuador
footprint
affect
through
apprentissage
multiphysics